Resonant nonlinear magneto-optical effects in atoms*

D. Budker[†]

*Department of Physics, University of California, Berkeley, California 94720-7300
and Nuclear Science Division, Lawrence Berkeley National Laboratory, Berkeley,
California 94720*

W. Gawlik[‡]

*Instytut Fizyki im. M. Smoluchowskiego, Uniwersytet Jagielloński, Reymonta 4,
30-059 Kraków, Poland*

D. F. Kimball,[§] S. M. Rochester,[‖] and V. V. Yashchuk[¶]

Department of Physics, University of California, Berkeley, California 94720-7300

A. Weis[**]

*Département de Physique, Université de Fribourg, Chemin du Musée 3,
CH-1700 Fribourg, Switzerland*

(Published 20 November 2002)

The authors review the history, current status, physical mechanisms, experimental methods, and
applications of nonlinear magneto-optical effects in atomic vapors. They begin by describing the
pioneering work of Macaluso and Corbino over a century ago on linear magneto-optical effects (in
which the properties of the medium do not depend on the light power) in the vicinity of atomic
resonances. These effects are then contrasted with various nonlinear magneto-optical phenomena that
have been studied both theoretically and experimentally since the late 1960s. In recent years, the field
of nonlinear magneto-optics has experienced a revival of interest that has led to a number of
developments, including the observation of ultranarrow (1-Hz) magneto-optical resonances,
applications in sensitive magnetometry, nonlinear magneto-optical tomography, and the possibility of
a search for parity- and time-reversal-invariance violation in atoms.

CONTENTS

I. INTRODUCTION

Magneto-optical effects arise when light interacts with a medium in the presence of a magnetic field. These effects have been studied and used since the dawn of modern physics and have had a profound impact on its development.[1] Most prominent among the magneto-optical effects are the *Faraday* (1846a, 1846b, 1855) and the *Voigt* (1901) *effects*, i.e., rotation of light's polarization plane as it propagates through a medium placed in a longitudinal or transverse magnetic field, respectively

---

[1] Magneto-optics were listed among the most important topics in physics at the World Congress of Physics in Paris in 1900 (Guillaume and Poincaré, 1900).

(Fig. 1). The linear (Secs. II and III) near-resonance Faraday effect is also known as the Macaluso-Corbino (1898a, 1898b, 1899) effect. The Voigt effect is sometimes called the Cotton-Mouton (1907, 1911) effect, particularly in condensed-matter physics.

The remarkable properties of resonant (and, particularly, nonlinear) magneto-optical systems—as compared to the well-known transparent condensed-matter magneto-optical materials such as glasses and liquids—can be illustrated with the Faraday effect. The magnitude of optical rotation per unit magnetic field and unit length is characterized by the *Verdet constant V*. For typical dense flint glasses that are used in commercial Faraday polarization rotators and optical isolators, $V \simeq 3 \times 10^{-5}$ rad G^{-1} cm^{-1}. In subsequent sections, we shall describe experiments in which nonlinear magneto-optical rotation corresponding to $V \simeq 10^{4}$ rad G^{-1} cm^{-1} is observed in resonant rubidium vapor (whose density, $\sim 3 \times 10^{9}$ cm^{-3}, satisfies the definition of very high vacuum). Taking into account the difference in density between glass and the rarified atomic vapor, the latter can be thought of as a magneto-optical material with some 10^{20} greater rotation "per atom" than heavy flint.

In this paper, we briefly review the physics and applications of resonant linear magneto-optical effects and
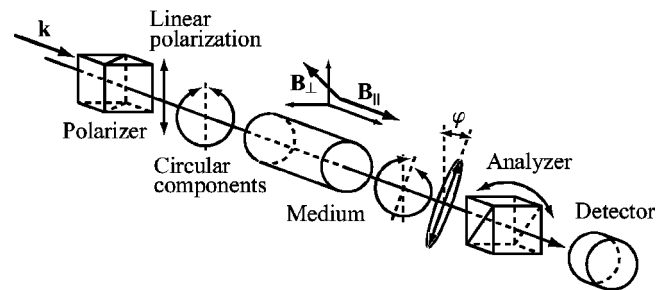
FIG. 1. The Faraday and Voigt effects. In the Faraday effect, light, after passing through a linear polarizer, enters a medium subjected to a longitudinal magnetic field $\mathbf{B}_{\parallel}$ ($\mathbf{B}_{\perp}=0$). Left- and right-circularly polarized components of the light (equal in amplitude for linearly polarized light) acquire different phase shifts, leading to optical rotation. A difference in absorption between the two components induces ellipticity in the output light. The intensity of the transmitted light with a particular polarization is detected depending on the orientation of the analyzer relative to the polarizer. Analyzer orientation varies with the type of experiment being performed. In forward-scattering experiments (Sec. II.B), the analyzer is crossed with the input polarizer, so that only light of the orthogonal polarization is detected. In the "balanced polarimeter" arrangement (Sec. XI.B), a polarizing beam splitter oriented at $\pi/4$ to the input polarizer is used as an analyzer. In this case, the normalized differential signal between the two channels of the analyzer depends on the rotation of light polarization while being insensitive to induced ellipticity. The Voigt effect is similar except that instead of a longitudinal magnetic field, a transverse field $\mathbf{B}_{\perp}$ ($\mathbf{B}_{\parallel}=0$) is applied. Here optical rotation and induced ellipticity are due to differential absorption and phase shifts of orthogonal linearly polarized components of the input light (Sec. VI).
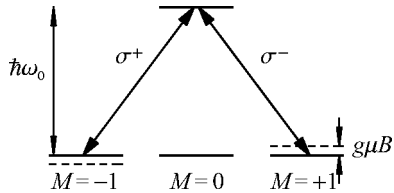
FIG. 2. An $F=1 \to F'=0$ atomic transition. In the presence of a longitudinal magnetic field, the Zeeman sublevels of the ground state are shifted in energy by $g\mu BM$. This leads to a difference in resonance frequencies for left- (σ^+) and right- (σ^-) circularly polarized light.

then turn to our main focus—the nonlinear effects (i.e., effects in which optical properties of the medium are modified by interaction with light). We also discuss various applications of nonlinear magneto-optics in atomic vapors, and the relation between nonlinear magneto-optics and a variety of other phenomena and techniques, such as coherent population trapping, electromagnetically induced transparency, nonlinear electro-optics effects, and self-rotation.

II. LINEAR MAGNETO-OPTICS

In order to provide essential background for understanding nonlinear magneto-optical effects (NMOE), we first review *linear* near-resonant magneto-optics of atoms and molecules. (See Sec. III for a discussion of the difference between the linear and nonlinear magneto-optical effects.)

A. Mechanisms of the linear magneto-optical effects

At the conclusion of the 19th century, Macaluso and Corbino (1898a, 1898b, 1899), studying absorption spectra of the alkali atoms in the presence of magnetic fields, discovered that the Faraday effect (magneto-optical activity) in the vicinity of resonance absorption lines had a distinct resonant character (see also work by Fork and Bradley, 1964).

The principal mechanism of the linear Macaluso-Corbino effect can be illustrated by the case of an $F=1 \to F'=0$ transition (Fig. 2), where F, F' are the total angular momenta.[2] Linearly polarized light incident on the sample can be decomposed into two counter-rotating circular components $\sigma^\pm$. In the absence of a magnetic field, the $M=\pm 1$ sublevels are degenerate and the optical resonance frequencies for σ^+ and σ^- coincide. The real part of the refractive index n associated with the atomic medium is shown in Fig. 3 as a function of the
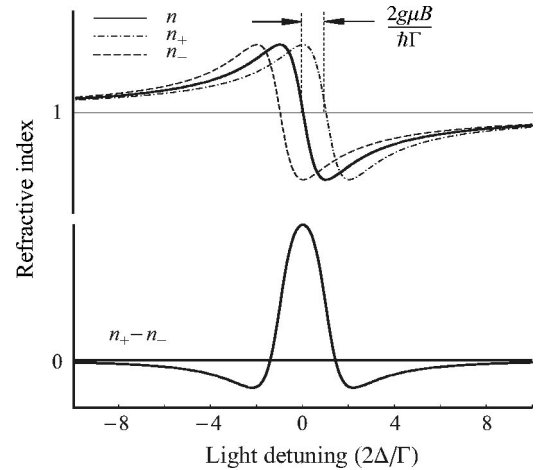
FIG. 3. The dependence of the refractive index on light frequency detuning Δ in the absence (n) and in the presence ($n_\pm$) of a magnetic field. Shown is the case of $2g\mu B = \hbar\Gamma$ and a Lorentzian model for line broadening. The lower curve shows the difference of refractive indices for the two circular polarization components. The spectral dependence of this difference gives the characteristic spectral shape of the linear magneto-optical rotation (the Macaluso-Corbino effect).

light frequency detuning Δ (the solid dispersion curve). The refractive index is the same for the two circular components.

When a magnetic field is applied, however, the Zeeman shifts[3] lead to a difference between the resonance frequencies for the two circular polarizations. This displaces the dispersion curves for the two polarizations as shown in Fig. 3. A characteristic width of these dispersion curves, Γ, corresponds to the spectral width (full width at half maximum, or FWHM) of an absorption line. Under typical experimental conditions in a vapor cell this width is dominated by the Doppler width and is on the order of 1 GHz for optical transitions. The difference between n_+ and n_- (Fig. 3) signifies a difference in phase velocities of the two circular components of light and, as a result, the plane of polarization rotates through an angle

$$\varphi = \pi(n_+ - n_-)\frac{l}{\lambda}. \tag{1}$$

Here l is the length of the sample, and λ is the wavelength of light. In addition to the difference in refraction for the two circular polarizations (circular birefringence), there also arises a difference in absorption (circular dichroism). Thus linear light polarization before the sample generally evolves into elliptical polarization after the sample. For nearly monochromatic light (i.e., light with spectral width much smaller than the transition width), and for zero frequency detuning from the

---

[2]Throughout this article, we designate as F, F' total angular momenta of the lower and upper states of the transition, respectively. For atoms with zero nuclear spin, F, F' coincide with the total electronic angular momenta J, J'.

[3]The connection between the Faraday and the Zeeman effects was first established by Voigt (1898b), who also explained the observations of Macaluso and Corbino (Voigt, 1898a).

resonance, the optical rotation in the sample as a function of magnetic field B can be estimated from Eq. (1) as[4]

$$\varphi \simeq \frac{2g\mu B/\hbar\Gamma}{1+(2g\mu B/\hbar\Gamma)^2} \frac{l}{l_0}. \qquad (2)$$

Here g is the Landé factor, μ is the Bohr magneton, and l_0 is the absorption length. This estimate uses for the amplitude of each dispersion curve (Fig. 3) the resonance value of the imaginary part of the refractive index (responsible for absorption). The Lorentzian model for line broadening is assumed. The Voigt model (discussed by, for example, Demtröder, 1996), which most accurately describes a Doppler- and pressure-broadened line, and the Gaussian model both lead to qualitatively similar results. The dependence of the optical rotation on the magnitude of the magnetic field [Eq. (2)] has a characteristic dispersionlike shape: φ is linear with B at small values of the field, peaks at $2g\mu B \simeq \hbar\Gamma$, and falls off in the limit of large fields.

For atoms with nonzero nuclear spin, mixing of different hyperfine components (states of the same M but different F) by a magnetic field also leads to linear magneto-optical effects (Novikova *et al.*, 1977; Roberts *et al.*, 1980; Khriplovich, 1991; Papageorgiou *et al.*, 1994). The contribution of this mechanism is comparable to that of the level-shift effect discussed above in many practical situations, e.g., linear magneto-optical rotation in the vicinity of the alkali D lines (Chen *et al.*, 1987). For the Faraday geometry and when $g\mu B \ll \hbar\Gamma \ll \Delta_{hfs}$, the amplitude of the rotation can be estimated as

$$\varphi \simeq \frac{g\mu B}{\Delta_{hfs}} \frac{l}{l_0}, \qquad (3)$$

where Δ_{hfs} is the separation between hyperfine levels. Since hyperfine mixing leads to a difference in the magnitude of n_+ and n_- (and not the difference in resonance frequencies as in the level-shift effect), the spectral profile of the rotation for the hyperfine mixing effect corresponds to dispersion-shaped curves centered on the hyperfine components of the transition.

There exists yet another mechanism in linear magneto-optics called the *paramagnetic effect*. The populations of the ground-state Zeeman sublevels that are split by a magnetic field are generally different according to the Boltzmann distribution. This leads to a difference in refractive indices for the corresponding light polarization components. For gaseous media, this effect is usually relatively small compared to the other mechanisms. However, it can be dramatically enhanced by creating a nonequilibrium population distribution between Zeeman sublevels. This can be accomplished by *optical pumping*, a nonlinear effect that will be discussed in detail in Sec. IV.A.

_____

[4]Explicit formulas for $n_\pm$ are given, for example, by Mitchell and Zemansky (1971, Appendix VII); analogous expressions can also be obtained for induced ellipticity.

B. Forward scattering and line crossing

Magneto-optics plays an important role in the study of resonant light scattering in the direction of the incident light (*forward scattering*), whose detection is normally hindered experimentally by the presence of a strong incident-light beam that has identical properties (frequency, polarization, direction of propagation) to the forward-scattered light. In order to investigate this effect, Corney, Kibble, and Series (1996) used two crossed polarizers (Fig. 1). In this arrangement, both the direct unscattered beam and the scattered light of unchanged polarization are blocked by the analyzer. Only the light that undergoes some change in polarization during scattering is detected. If the medium is isotropic and homogeneous and there is no additional external perturbation or magnetic field, the forward-scattered light has the same polarization as the primary light and cannot be detected. The situation changes, however, when an external magnetic field **B** is applied. Such a field breaks the symmetry of the σ^+ and σ^- components of the propagating light in the case of $\mathbf{B}\|\mathbf{k}$ (and π and σ components when $\mathbf{B}\perp\mathbf{k}$) and results in a nonzero component of light with opposite polarization that is transmitted by the analyzer.

In the late 1950s, it was determined (Colegrove *et al.*, 1959; Franken, 1961) that coherence between atomic sublevels (represented by off-diagonal elements of the density matrix; see Sec. VII.B) affects lateral light scattering. For example, in the Hanle (1924) or level-crossing effects (Colegrove *et al.*, 1959; Franken, 1961), the polarization or spatial distribution of fluorescent light changes as a function of relative energies of coherently excited atomic states. Another example is that of *resonance narrowing* in lateral scattering (Guichon *et al.*, 1957; Barrat, 1959). In this striking phenomenon, the width of resonance features (observed in the dependence of the intensity of scattered light on an applied dc magnetic field or the frequency of an rf field) was seen to decrease with the increase of the density of the sample; this appeared as an effective increase in the upper state lifetime despite collisional broadening that usually results from elevated density. This effect is due to multiple light scattering (radiation trapping), which transfers excitation from atom to atom, each of the atoms experiencing identical evolution in the magnetic field (a more detailed discussion is given by, for example, Corney, 1988).

In lateral scattering, the resonance features of interest are usually signatures of interference between various sublevels in each individual atom. In forward scattering, the amplitudes of individual scatterers add in the scattered light (Corney *et al.*, 1966; Durrant, 1972). Thus forward scattering is coherent, and interference can be observed between sublevels belonging to different atoms. The forward-scattered light has the same frequency as the incident light. However, the phase of the scattered light depends on the relative detuning between the incident light and the atom's effective resonance frequency. This leads to inhomogeneous broadening of the

forward-scattering resonance features; at low optical density, their width (in the magnetic-field domain) is determined by the Doppler width of the spectral line.[5] For this reason, the corresponding forward-scattering signals associated with linear magneto-optical effects can be regarded as Doppler-broadened, multiatom Hanle resonances. Here the Hanle effect is regarded as a manifestation either of quantum-mechanical interference or of atomic coherence, depending on whether it appears in emissive or dispersive properties of the medium (see Sec. II.D.1). If the optical density of the sample increases to the extent that multiple scattering becomes important, substantial narrowing of the observed signals results, interpreted by Corney *et al.* (1966) as coherence narrowing. Forward-scattering signal narrowing was observed in Hg by Corney *et al.* (1966) and in Na by Królas and Winiarczyk (1972). Further exploring the relation between manifestations of single-atom and multiatom coherence, Corney *et al.* analyzed the phenomenon of *double resonance* in the context of forward-scattering. This is a two-step process in which, first, optical excitation by appropriately polarized resonant light populates atomic states. Subsequently, transitions are induced among the excited states by a resonant rf field. Corney *et al.* also studied double resonance in the limiting case in which the upper states have the same energy, so that the second resonance occurs at zero frequency. Such a zero-frequency resonant field is simply a constant transverse magnetic field. Thus the double-resonance approach is applied to the interpretation of the Voigt effect in an unorthodox manner.

The fact that in forward scattering light scattered by different atoms is coherent makes it possible to study the phenomenon of *line crossing*. Whereas, in level crossing (Colegrove *et al.*, 1959; Franken, 1961), signals in lateral light scattering are observed when different sublevels of single atoms cross (for example, in an external magnetic field), in a line-crossing experiment interference occurs due to crossing of sublevels of different atoms. This effect was first demonstrated by Hackett and Series (1970), who observed interference in the forward-scattering signals due to crossing of Zeeman sublevels of different Hg isotopes contained in one cell. Church and Hadeishi (1973) showed that line crossing occurs even when atoms of different kinds are contained in separate cells. Hackett and Series (1970), Church and Hadeishi (1973), Stanzel (1974a), and Siegmund and Scharmann (1976) investigated the possibility of applying the line-crossing effect to precise measurements of isotope shifts. This idea is based on the fact that line crossings occur when the applied magnetic field is such that the Zeeman shifts compensate for the initial field-free isotope shifts. It was hoped that strong coherence narrowing of the line-crossing resonance would significantly increase the precision of such measurements. However, these authors found that various complica-

---

[5]Obviously, homogeneous broadening (e.g., pressure broadening) also affects these widths.
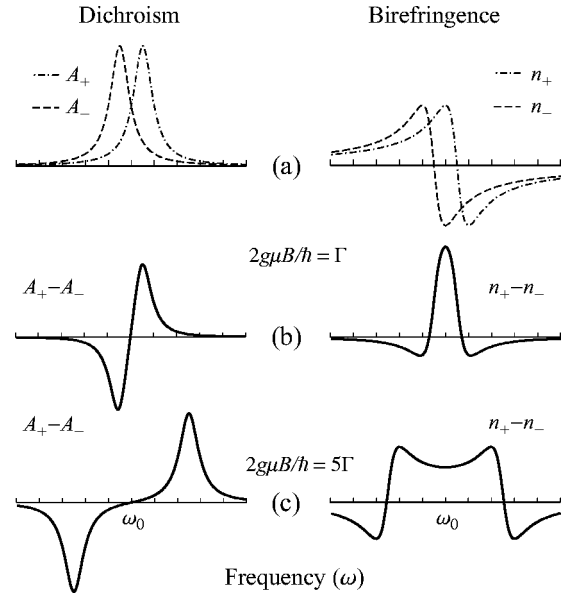
FIG. 4. Spectral dependences of the circular dichroic ($A_+ - A_-$) and birefringent ($n_+ - n_-$) anisotropies that determine the forward-scattering signal for a $F=0 \rightarrow F'=1$ transition. The σ^+ and σ^- resonance frequencies are split by a longitudinal magnetic field B. For curves (a) and (b), the magnitude of the splitting is equal to the resonance width Γ. For the curves (c), it is five times larger.

tions (arising, for example, from pressure broadening of the signals), rendered this method impractical for isotope shift measurements.

Forward-scattering signals for weak-intensity light can be written as

$$I_{FS} = \frac{1}{4} \int \xi(\omega)[e^{-A_+\omega l/c} - e^{-A_-\omega l/c}]^2 d\omega$$

$$+ \int \xi(\omega)\sin^2\left\{(n_+ - n_-)\frac{\omega l}{2c}\right\}e^{-(A_+ + A_-)\omega l/c}d\omega,$$

$$(4)$$

where $\xi(\omega)$ is the spectral density of the incident light, $A_\pm$ characterizes absorption and $n_\pm$ are the refractive indices for the $\sigma^\pm$ components of the incident-light beam, respectively, and l is the sample length. We assume ideal polarizers here.

In general, the two terms in Eq. (4) give comparable contributions to the forward-scattering signal. The first term is due to differential absorption of the σ^+ and σ^- components of the incident light (circular dichroism), and the second term is due to differential dispersion (circular birefringence). The two contributions have different frequency dependences. This can be illustrated with the simple case of the $F=0 \rightarrow F'=1$ transition, for which the $\sigma^\pm$ resonance frequencies are split by a longitudinal magnetic field (Fig. 4). While the function in the first integral goes through zero at $\omega = \omega_0$ (since the function in the square brackets is antisymmetric with respect to detuning), the second (birefringence) term is maximal at zero detuning (for small magnetic fields). For a narrow-band light source, it is possible to eliminate the dichroic
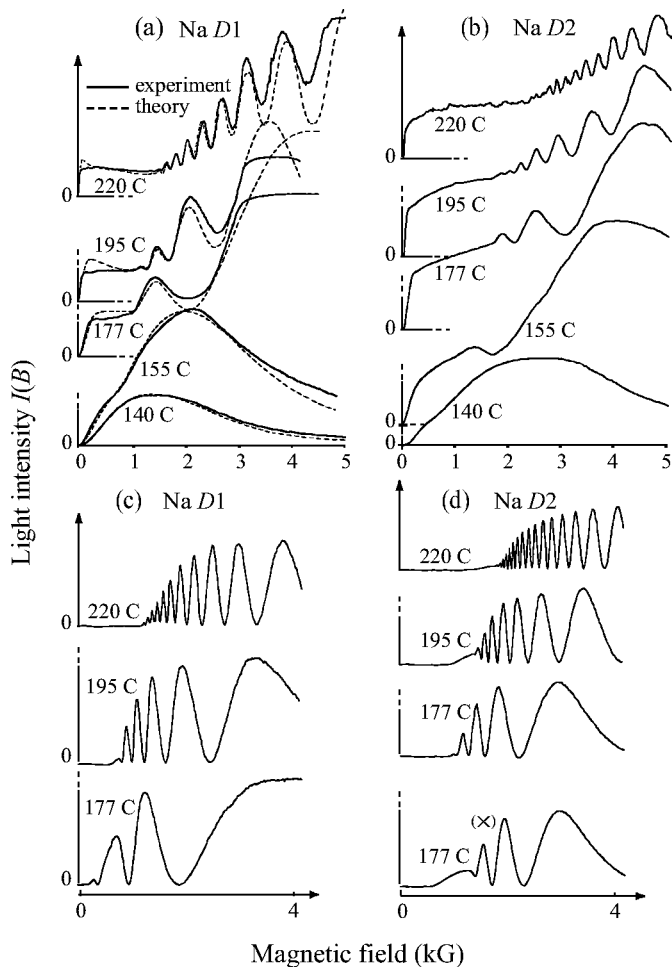
FIG. 5. Forward-scattering signals $I(B)$ observed on the sodium $D1$ [(a) and (c)] and $D2$ [(b) and (d)] lines by Gawlik (1975). Curves (a) and (b) are signals obtained with a conventional spectral lamp (single D line selected by a Lyot filter). Curves (c) and (d) are signals obtained with single-mode cw dye-laser excitation. The laser is tuned to the atomic transition in all cases except the one marked ($\times$). Curve ($\times$) was recorded with the laser detuned by about 600 MHz to demonstrate the influence of residual dichroism. In plot (a), flattening of some curves at high fields is due to detector saturation—the dashed lines represent calculated signals. From Gawlik, 1975.

contribution by tuning to the center of the resonance. One is then left with only the second integral, representing Malus's law, where $\varphi = (n_+ - n_-)\omega l/(2c)$ is the Faraday rotation angle [Eq. (1)].

When the density-length product for the medium is sufficiently high, the range of variation of φ can easily exceed π, and intensity transmitted through the apparatus shown in Fig. 1 oscillates as a function of the magnetic field (Fig. 5), see also Durrant and Landheer (1971). These oscillations are clearly seen despite the proximity of the absorption line because the refractive indices drop with detuning slower than the absorption coefficients. When $\xi(\omega)$ represents a narrow spectral profile, the modulation contrast can be high, particularly when the magnetic field is strong enough to split the $A_\pm$ profiles completely. Such a case is shown schematically in Fig. 4(c).

At the center of a Zeeman-split resonance, absorption drops off with the magnitude of the splitting much faster than optical rotation does. Thus, using a dense atomic vapor in a magnetic field and a pair of polarizers, it is possible to construct a transmission filter for resonant radiation, which can be turned into an intensity modulator by modulating the magnetic field (Fork and Bradley 1964; Aleksandrov 1965).

C. Applications in spectroscopy

Magneto-optical effects can provide useful spectroscopic information. For example, given a known atomic density and sample length, a measurement of Faraday rotation for a given transition can be used to determine the oscillator strength f for that transition. Conversely, when f is known, Faraday rotation may be used to determine vapor density. Vliegen *et al.* (2001) found that Faraday rotation measurements with high alkali-metal densities ($\sim 10^{15}$–10^{16} cm^{-3}) are free from certain systematic effects associated with measurement of absorption. An earlier review of applications of magneto-optical rotation was that of Stephens (1989).

1. Analytical spectroscopy and trace analysis, investigation of weak transitions

An example of an application of magneto-optical rotation to molecular spectroscopy is the work of Aubel and Hause (1966), who, using a multipass cell, demonstrated that the magneto-optical rotation spectrum of NO is easier to interpret than the absorption spectrum. Molecular magneto-optical spectra are in general much simpler than the absorption spectra (see discussion by Herzberg, 1989, Chap. V.5). This is because significant magneto-optical effects are present only for transitions between molecular states of which at least one has nonzero electronic angular momentum. In addition, since molecular g values decrease rapidly with the increase of the rotational quantum number J (see discussion by Khriplovich, 1991, Chap. 7.2), only a small part of the rotational band produces magneto-optical effects. Magneto-optical rotation has been used to identify atomic resonance lines in Bi against a complex background of molecular transitions (Barkov and Zolotorev, 1980; Roberts *et al.*, 1980).

Magneto-optical rotation, in particular, the concept of forward scattering, was also applied in analytical spectroscopy for trace element detection. This was first done by Church and Hadeishi (1974), who, using forward-scattering signals, showed sensitivity an order of magnitude higher than could be obtained with absorption measurements. The improved sensitivity of magneto-optical rotation over absorption is due to almost complete elimination of background light and a corresponding reduction of its influence on the signal noise. Such noise is the main limitation of the absorption techniques. Following this work, Ito *et al.* (1977) also employed both Faraday and Voigt effects for trace analysis of various elements.

The detection of weak transitions by magneto-optical rotation (with applications to molecular and analytical

spectroscopy) was spectacularly advanced by the employment of lasers. Using tunable color-center lasers, Litfin *et al.* (1980) demonstrated 50 times better sensitivity in detection of NO transitions in the vicinity of 2.7 μm with magneto-optical rotation than with absorption spectroscopy. Similar results were obtained by Yamamoto *et al.* (1986), who obtained 200-fold enhancement in sensitivity over absorption spectroscopy in their work with a pulsed dye laser and the sodium $D2$ line. Another interesting result was reported by Hinz *et al.* (1982), who worked in the mid-infrared range with NO molecules and a CO laser. These authors also demonstrated that magneto-optical rotation improves sensitivity in either of the basic configurations, i.e., in the Faraday as well as the Voigt geometry.

The advent of high-sensitivity laser spectropolarimeters, allowing measurement of optical rotation at the level of 10^{-8} rad and smaller (Sec. XI.B), made possible the sensitive detection of species with low concentration. Detection of on the order of hundreds of particles per cubic centimeter was reported by Vasilenko *et al.* (1978). It is important to note that, while it is beneficial from the point of view of the photon shot noise of the polarimeter to operate at a high light power, great care should be taken to make sure that the atoms of interest are not bleached by nonlinear saturation effects (Sec. III.B). As a practical way to optimize a trace analysis setup, we suggest the use of a buffer gas to pressure-broaden the homogenous width of the transition up to the point when this width becomes comparable to the Doppler width. This way, the linear absorption and Faraday rotation are not compromised, but the light intensity constraints due to nonlinearities are relaxed by many orders of magnitude.

Due to its high sensitivity, the magneto-optical rotation method can also be applied to the study of weak transitions, such as magnetic dipole transitions with small transition magnetic moments (Barkov *et al.*, 1989b).

2. Measurement of oscillator strengths

Fork and Bradley (1964) performed some of the earliest work in which resonant magneto-optical rotation was used to measure oscillator strengths.[6] They measured light dispersion in Hg vapor at about five Doppler widths from the center of the 253.7-nm line. They used an electrodeless discharge ^{198}Hg lamp, placed in a solenoid as a light source tunable over eight Doppler widths, and measured the dispersion using a Mach-Zehnder interferometer. In addition to the observation of Faraday rotation in excess of 7 rad, they also demonstrated the inversion of the sign of the dispersion in a vapor with inverted population, and the feasibility of using Faraday rotation for narrow-band modulatable optical filters.

---

[6]Early measurements of oscillator strength are described in a monograph by Mitchell and Zemansky (1971).
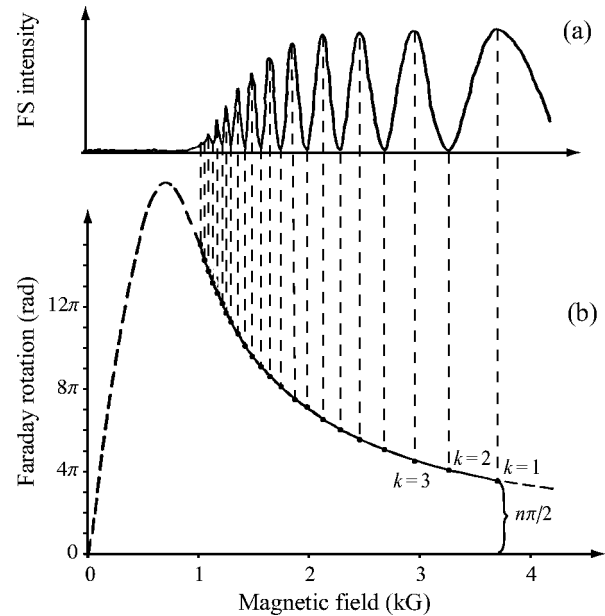
FIG. 6. Forward scattering signal and Faraday rotation as a function of magnetic field. (a) Signals obtained by Gawlik *et al.* (1979) from forward scattering of single-mode cw laser light tuned to the Na $D1$ line. (b) Magnetic-field dependence of the Faraday rotation angle φ obtained from the extrema of the $I(B)$ curve of figure (a). From Gawlik *et al.*, 1979.

The advent of tunable lasers has enabled significant improvement of magneto-optical-rotation methods for measuring absolute and relative oscillator strengths. This is illustrated by the results, shown in Fig. 5, of an experiment performed by Gawlik (1975). Here curves (a) and (b) refer to a forward-scattering experiment performed with a sodium spectral lamp and a Lyot filter that selected one of the Na D lines. The light from the lamp had an asymmetric spectral profile with some *self-reversal* (a line-profile perturbation due to reabsorption of resonance light at the line center) and FWHM of about 8 GHz. From the results for the $D1$ and $D2$ lines, one can see how the modulation period depends on the product of atomic density and oscillator strength of the investigated transitions and how the oscillatory birefringent contribution (see also Fig. 6) becomes overwhelmed by the structureless dichroic one, particularly at small magnetic fields. Figures 5(c) and (d) represent results from the same experiment, but with, in place of a lamp, a narrow-band cw dye laser tuned to the centers of gravity of the Na $D1$ and $D2$ lines, respectively (see also Gawlik, 1977; Gawlik *et al.*, 1979). Several important changes are seen: first, the modulation depth is now 100%—this allows accurate determination of $\varphi(nl,\omega,B)$, where ω is the light frequency (Fig. 6); second, the dichroic contribution can be fully eliminated by appropriately tuning the laser (this is because the dichroic effect has a nearly dispersive spectral dependence which goes through zero when the Faraday rotation contribution is nearly maximal); third, as seen by the envelope of the oscillatory pattern, total absorption $\exp[-(A_+ + A_-)\omega l/c]$ plays a role only for small B, in agreement with the above considerations [see Figs. 5(c)

and (d)]. Fast oscillation in the region of low total absorption makes it possible to determine the absorption profile (envelope) simultaneously with the measurement of φ. This technique allows one to determine simultaneously the real and imaginary parts of the complex index of refraction, which is useful for measuring collisional parameters, for example.

A number of experiments have measured oscillator strengths by scanning the light frequency (at a fixed magnetic field). For example, employing synchrotron radiation and superconducting magnets, oscillator strengths of ultraviolet lines of Rydberg series of several elements were determined by Garton *et al.* (1983), Connerade (1983), and Ahmad *et al.* (1996). An interesting experimental method employing pulsed magnets and UV lasers was developed by Connerade and co-workers for studies of Faraday rotation in autoionizing resonances and transitions to Rydberg states (Connerade and Lane, 1988; Connerade *et al.*, 1992) and of collisional broadening (Warry *et al.*, 1994).

It should be remembered that most methods based on light dispersion measure not just the oscillator strength f but the product of f and the optical density.[7] Knowledge of the optical density is hence a central issue in absolute measurements. On the other hand, these methods can be very useful for high-precision relative measurements.

3. Investigation of interatomic collisions

The effect of pressure broadening on the magneto-optical rotation spectra of resonant gaseous media was theoretically analyzed within the impact approximation by Giraud-Cotton *et al.* (1975). Later, collisional effects in magneto-optical rotation in a $F=0 \rightarrow F=1$ atomic transition were treated with the density-matrix formalism by Schuller *et al.* (1987). This work considered atomic motion and light fields of arbitrary intensity (and thus included nonlinear effects), but was limited to optically thin samples. The case of high optical density appears to be particularly difficult. This is because for high atomic densities the impact approximation is not appropriate—the effect of quasimolecular behavior of the perturbed atoms becomes significant. Consequently, optical transitions contributing to the rotation spectra can no longer be regarded as isolated. Faraday rotation produced under such circumstances was studied in an

experiment of Kristensen *et al.* (1994) with the $D2$ line of Rb atoms that were highly diluted in Xe buffer gas at densities of $\sim 10^{20}$ cm^{-3}. It was found necessary to include the effect of Born-Oppenheimer coupling of Rb-Xe long-range-collision pairs in order to explain the magnitude of the observed rotation. Born-Oppenheimer coupling is the locking of the total electronic angular momentum to the collision axis at densities for which the mean free path falls below about 1 nm. Such angular momentum locking hinders the Larmor precession and hence reduces Faraday rotation.

Faraday rotation spectroscopy is now widely used for measuring collisional broadening and shift of spectral lines. For example, Bogdanov *et al.* (1986, 1988; Bogdanov and Kanorskii, 1987) used this method to study broadening and shift of the 648-nm magnetic dipole transition in Bi and self-broadening, foreign-gas broadening and shift, and electron-impact broadening of transitions between excited states in Cs. Barkov *et al.* (1988b, 1989b) studied buffer-gas broadening of transitions in atomic Sm. One of the important advantages of this method is that it provides the ability to modulate the signal by changing the magnetic field, thus distinguishing the signal from the background.

For measuring line broadening, e.g., collisional broadening, it is important that the characteristic spectral profile of the Macaluso-Corbino effect for an isolated line have two zero crossings (Fig. 3). The separation between zeros is linearly dependent on the Lorentzian width of the transition even when this width is much smaller than the Doppler width of the transition.

An experimental study of collisional broadening of Rydberg spectra with the use of Faraday rotation was performed by Warry *et al.* (1994). This work demonstrated that the resonant Faraday effect and the forward-scattering technique can be used for studies of collisional perturbations of Rydberg states with much greater precision than that of earlier photoabsorption experiments.

4. Gas lasers

Magneto-optical rotation of a weak probe light passing through a gas discharge is a useful tool for studying amplifying media in gas lasers. Early examples of this are the papers by Aleksandrov and Kulyasov (1972), who observed large rotations in a ^{136}Xe discharge, and Menzies (1973), who determined population and polarization relaxation rates of the Ne levels making up the 3.39-μm laser transition. The technique is applicable to transitions that exhibit light absorption as well as amplification depending on particular population ratios. Since the Faraday angle is proportional to the population difference for the two levels of a transition and changes sign when population inversion is achieved, such studies allow precise determination of population differences and their dependences on parameters such as gas pressure and discharge current. An example is the work of Winiarczyk (1977), who studied the 632.8-nm Ne line.

---

[7]One interesting exception is the early work of Weingeroff (1931), who devised a method of measuring the Lorentzian linewidth independently of the optical density. The method relies on using a white-light source and recording the intensity of light transmitted through an optically dense medium placed between two crossed polarizers in a longitudinal magnetic field B. When $B \neq 0$, the spectrum of the transmitted light has the form of a bright line on a dark background (the Macaluso-Corbino effect), but when the polarizers are uncrossed by appropriate angles, the line merges with the background. For a given atomic transition and magnetic field, the values of the uncrossing angles allow determination of the Lorentzian width without prior knowledge of density.

The method's sensitivity makes it useful for optimizing the efficiency of gas lasers, particularly those utilizing weak transitions.

5. Line identification in complex spectra and the search for "new" energy levels

We have already mentioned the utility of magneto-optical rotation for identification of molecular spectra and for distinguishing atomic resonances from molecular ones. Another, more unusual, application of Faraday rotation spectroscopy was implemented by Barkov *et al.* (1987, 1988b, 1989b). They were looking for optical magnetic dipole transitions from the ground term of atomic samarium to the levels of the first excited term of the same configuration whose energies were not known. A study of the spectrum revealed hundreds of transitions that could not be identified with the known energy levels (most of these were due to transitions originating from thermally populated high-lying levels). Drawing an analogy with infrared transitions between the ground-term levels for which unusually small pressure broadening had been observed[8] by Vedenin *et al.* (1986, 1987). Barkov *et al.* predicted small pressure broadening for the sought-after transitions as well. They further noticed that in the limit of $\gamma \gg \Gamma_D$ (where γ and Γ_D are the Lorentzian and Doppler widths, respectively), the peak Faraday rotation is $\propto \gamma^{-2}$ (in contrast to absorption, for which the amplitude is $\propto \gamma^{-1}$). In fact, at high buffer-gas pressures (up to 20 atm), the magneto-optical rotation spectra showed that almost all transitions in the spectrum were so broadened and reduced in amplitude that they were practically unobservable. The spectrum consisted only of the sought-after transitions, which had unusually small pressure broadening.

6. Applications in parity violation experiments

Magneto-optical effects have played a crucial role in experiments measuring weak-interaction-induced, parity-violating optical activity of atomic vapors.[9] Parity-violating optical activity is usually observed in the absence of external static fields near magnetic dipole ($M1$) transitions with transition amplitudes on the order of a Bohr magneton. The magnitude of the rotation is typically 10^{-7} rad per absorption length for the heavy atoms (Bi, Tl, Pb) in which the effect has been observed.

The Macaluso-Corbino effect allows calibration of the optical rotation apparatus by applying a magnetic field to the vapor. On the other hand, because the parity-violating optical rotation angles are so small, great care must be taken to eliminate spurious magnetic fields, since sub-milligauss magnetic fields produce Macaluso-Corbino rotation comparable in magnitude to the parity-violating rotation, albeit with a different line shape. The lack of proper control over spurious magnetic fields apparently was a problem with some of the early measurements of parity-violating optical activity in the late 1970s, whose results were inconsistent with subsequent, more accurate measurements.[10]

The origin of the parity-violating optical rotation lies in the mixing, due to the weak interaction, of atomic states of opposite parity,[11] which leads to an admixture of an electric dipole ($E1$) component to the dominant $M1$ amplitude of the transition. The observed effect is the result of the interference of the two components of the amplitude. In general, there is also an electric quadrupole ($E2$) component of the transition amplitude. However, there is no net contribution from $E1-E2$ interference to the parity-violating optical rotation, since the effect averages to zero for an unpolarized atomic sample. Nevertheless, knowledge of the $E2$ contribution is crucial for accurate determination of the parity-violating amplitude, as it affects the sample absorption and the Macaluso-Corbino rotation used for calibration. In addition, this contribution is important for interpretation of the parity-violation experiments, since the $E2/M1$ ratio can serve as an independent check of atomic theory. Fortunately, investigation of Macaluso-Corbino line shapes allows direct determination of the $E2/M1$ ratio (Roberts *et al.*, 1980; Bogdanov *et al.*, 1986; Tregidgo *et al.*, 1986; Majumder and Tsai, 1999). These measurements exploit the difference in the selection rules for these two types of transitions, and, more generally, the difference between line strengths for different hyperfine components of a transition.

7. Investigations with synchrotron radiation sources

Synchrotron radiation has been used for a number of years as a source of ultraviolet radiation to study magneto-optical effects in transitions to high-lying Rydberg and autoionization states [as in work by, for example, Connerade (1983), Garton *et al.* (1983), and Ahmad *et al.* (1986)].

In recent years, with the advent of synchrotron sources of intense radiation in the extreme ultraviolet ($\hbar\omega = 30$–250 eV) and soft-x-ray ($\hbar\omega = 250$ eV to several keV) ranges (Attwood, 2000), the studies and applications of resonant magneto-optical effects have been extended to atomic transitions involving excitation of core electrons.

---

[8]This was attributed to shielding of the valence $4f$ electrons by other atomic shells. Note that the same mechanism is responsible for appearance of ultranarrow lines in the optical spectra of rare-earth-doped crystals (for example, Thiel *et al.*, 2001).

[9]See, for example, a review of early experiments by Khriplovich (1991) and more recent reviews by Bouchiat and Bouchiat (1997) and Budker (1999).

[10]The most accurate optical rotation measurements to date (Meekhof *et al.*, 1995; Vetter *et al.*, 1995) have reached the level of uncertainty of ~1% of the magnitude of the effect.

[11]Parity-violating interactions mix states of the same total angular momentum and projection. As a consequence of time-reversal invariance, the mixing coefficient is purely imaginary, which is the origin of the chirality that leads to optical rotation.
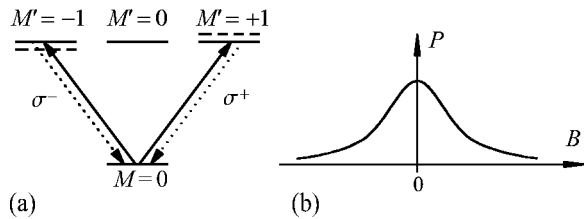
FIG. 7. The Hanle effect. (a) An $F=0 \to F'=1$ atomic transition. In the presence of a longitudinal magnetic field, the Zeeman sublevels of the exited state become nondegenerate. This leads to a magnetic-field-dependent phase difference for σ^+ and σ^- circular-polarization components of the reemitted light and to the alteration of the net reemitted light polarization. (b) Dependence of the reemitted light degree of polarization P on the applied longitudinal magnetic field B.

Linear polarizers in this photon energy range are based on polarization-selective reflection at near-Brewster angles from multilayer coatings (see discussion by Attwood, 2000, Sec. 4.5.5), while additional polarization control (for example, conversion of linear polarization to circular) can be achieved using magneto-optical effects themselves (Kortright *et al.*, 1997, 1999).

Resonant magneto-optical effects, due to their element-specific character (Kortright and Rice, 1995), are proving to be a useful tool for the study of heterogeneous magnetic materials (Hellwig *et al.*, 2000; Kortright and Kim, 2000).

D. Related phenomena

1. Magnetic depolarization of fluorescence: Hanle effect and level crossing

Apart from magneto-optical rotation, much attention has been devoted to studies of polarization properties of resonance fluorescence and its magnetic-field dependence. In particular, Wood (1922) and Wood and Ellett (1923, 1924) noted strong magnetic-field dependence of polarization of the 253.7-nm resonance fluorescence of Hg. These studies were continued and analyzed by Hanle (1924),[12] who interpreted his observations in terms of the induced dipole moments precessing in an external magnetic field. A weak field causes slow Larmor precession, so the dipoles have no time to change their orientation before they spontaneously decay. Consequently, reemitted fluorescence preserves the polarization of the incident excitation light. On the other hand, in a high field, fast precession causes rapid averaging of the dipoles' orientation, i.e., there is efficient depolarization of the reemitted light. The degree of polarization depends on the rates of spontaneous decay of the induced dipoles and Larmor precession. Hence the product of the excited-state lifetime τ and the Landé factor g can be determined by measuring the magnetic-field dependence of the degree of polarization.

Figure 7(a) shows the energy-level scheme of the Hg 253.7-nm transition between the ground state with $F=0$ and the excited state with $F'=1$ (and Zeeman components $M'=0,\pm1$). Light linearly polarized along a direction perpendicular to the quantization axis (solid arrows) excites the $M'=\pm1$ sublevels; spontaneous emission of σ^+ and σ^- light (dashed arrows) follows. When $B=0$ and the excited state is degenerate, the relative phases of the σ^+ and σ^- components are the same and the reemitted light has a high degree of polarization P [Fig. 7(b)]. When $B\neq0$, the $M'=\pm1$ sublevels are split and the $\sigma^\pm$ components acquire a B-dependent phase difference which alters the net polarization of the reemitted light and reduces P. The width of the $P(B)$ dependence is inversely proportional to the product τg.

The interpretation of the Hanle effect in terms of a classical Lorentz oscillator was far from satisfactory as it did not explain, for example, why $D2$ lines in atoms with one electron above closed shells exhibited the Hanle effect while $D1$ lines did not. (The modern explanation is that the upper state of $D1$ lines has $J=1/2$ and thus, neglecting hyperfine interactions, polarization moments higher than orientation do not occur, while $D2$ lines have $J=3/2$ in the upper states and alignment is possible; see Appendix B.1 for a discussion of atomic polarization moments.) This and other difficulties inspired many eminent theoreticians to analyze the Hanle experiment. Bohr (1924) discussed the role of quantum-state degeneracy and Heisenberg (1925) formulated the principle of spectroscopic stability. Other important contributions were made by Oppenheimer (1927), Weisskopf (1931), Kroff and Breit (1932), and Breit (1932, 1933).

The Hanle effect can be viewed as a generic example of quantum interference. In the basis in which the quantization axis is along the magnetic field, the two circular components of the incident light coherently excite atoms to different Zeeman sublevels of the upper level. Due to the Zeeman splitting, light spontaneously emitted from different sublevels acquires different phase shifts, leading to magnetic-field-dependent interference effects in the polarization of the emitted light. The time dependence of the fluorescence polarization is referred to as quantum beats (Haroche, 1976; Dodd and Series, 1978; Alexandrov *et al.*, 1993).

The Hanle method was also extended to degeneracies occurring at $B\neq0$, which is the basis of *level-crossing spectroscopy* (Colegrove *et al.*, 1959). Level-crossing spectroscopy has been widely used for determination of fine- and hyperfine-structure intervals, lifetimes, g factors, and electric polarizabilities of atomic levels (Moruzzi and Strumia, 1991; Alexandrov *et al.*, 1993). An advantage of the level-crossing method is that its spectral resolution is not limited by Doppler broadening because it measures the frequency difference between two optical transitions for each atom.

---

[12]An English translation of Hanle's paper as well as interesting historical remarks can be found in a book edited by Moruzzi and Strumia (1991). Hanle (1926) also observed the influence of an electric field on the polarization of resonance fluorescence.

2. Magnetic deflection of light

A uniaxial crystal generally splits a light beam into two distinct light beams with orthogonal linear polarizations. This effect (linear birefringence) vanishes when the **k** vector of the incident beam is either parallel or perpendicular to the crystal axis.

If, instead of a preferred axis, an axial vector **a** (also called a gyrotropic axis) determines the symmetry of the medium, another type of birefringence occurs. Here, a light beam is split into linearly polarized beams propagating in the $(\hat{k},\hat{a})$ and $(\hat{k},\hat{k}\times\hat{a})$ planes, respectively. The birefringent splitting in this case is maximal when **k** is perpendicular to **a**. Examples of media with such a gyrotropic axial symmetry are isotropic media in an external magnetic field or samples with net spin orientation (magnetization).

The dielectric tensor of a medium in a magnetic field **B** is given by (Landau *et al.*, 1995)

$$\varepsilon_{ij}(\mathbf{B}) = \tilde{n}^2 \delta_{ij} + i\tilde{\gamma}\epsilon_{ijk}B_k, \tag{5}$$

where $\tilde{n}$ is the complex index of refraction in the absence of the magnetic field. The real and imaginary parts of $\tilde{\gamma}$ are responsible for the circular birefringence and circular dichroism of the medium, respectively. A straightforward calculation yields the direction of the Poynting vector **P** of a linearly polarized plane wave in the case of a weakly absorbing medium ($\text{Im}\,\tilde{n}^2, |\text{Im}\,\tilde{\gamma}B| \ll \text{Re}\,\tilde{n}^2 \simeq 1$):

$$\mathbf{P} \propto \hat{k} + \text{Im}\,\tilde{\gamma}\sin\beta(\mathbf{B}\cos\beta + \hat{k}\times\mathbf{B}\sin\beta), \tag{6}$$

where β is the angle between the polarization and the field. A transversely polarized beam ($\beta = \pi/2$) will thus be deflected by an angle $\alpha \simeq \text{Im}\,\tilde{\gamma}B$. This results in a parallel beam displacement upon traversal of a sample with parallel boundary surfaces.[13] The effect was first observed in resonantly excited Cs vapor in fields up to 40 G (Schlesser and Weis, 1992). The small size of the effect (maximal displacements were a few tens of nanometers) impeded the use of low light intensities, and the experimental recordings show a strong nonlinear component, presumably due to optical pumping. These nonlinearities manifest themselves as dispersively shaped resonances in the magnetic-field dependence of the displacement, which are similar to those observed in the nonlinear Faraday effect (see Sec. V). Unpublished results obtained by A. Weis at high laser intensities have revealed additional resonances—not observed in magneto-optical rotation experiments—whose origin may be coherences of order higher than $\Delta M = 2$. A theoretical analysis of the results of Schlesser and Weis based on the Poynting-vector picture and the density-matrix method described in Sec. VII.B was attempted by Rochester and Budker (2001b). It was found that, while the theory reproduces the magnitude and spectral de-pendence of deflection at low light power reasonably well, it completely fails to reproduce the saturation behavior. This suggests existence of some additional nonlinear mechanism for deflection, perhaps at the interface between the vapor and the glass.

As mentioned above, a spin-polarized medium has the same symmetry properties as a medium subjected to an external magnetic field; beam deflection was observed in a spin-polarized alkali vapor by Blasberg and Suter (1992).

The magnetic-field-induced displacement of light bears a certain resemblance to the Hall effect—the deflection of a current **j** of electrons (holes) by a field **B** in the direction $\mathbf{j}\times\mathbf{B}$—and might thus be called the "photonic Hall effect." However, this term was actually used to designate a related observation of a magnetic-field-induced asymmetry in the lateral diffusion of light from condensed-matter samples in tesla-sized fields (Rikken and van Tiggelen, 1996). Recently, the description of the propagation of light in anisotropic media in terms of a Poynting-vector model was questioned following a null result in a magneto-deflection experiment on an aqueous solution of Nd^{3+} (Rikken and van Tiggelen, 1997). More experimental and theoretical work is needed to clarify these issues.

3. The mechanical Faraday effect

Since the effect of applying a magnetic field to a sample can be interpreted, by Larmor's theorem, as a rotation of the atomic wave function, a question can be raised: can optical rotation be induced by macroscopic rotation of the whole sample? If the electrons bound in the sample "feel" the macroscopic rotation, a *mechanical Faraday effect* results. This rotation can only be felt if strong coupling exists between atomic electrons and their environment. The mechanical Faraday effect has been demonstrated in a rotating solid-state sample by Jones (1976; see also Baranova and Zel'dovich, 1979 for a theoretical discussion), but there is still the question of whether one can rotate atoms in the gas phase. Woerdman *et al.* (1992), Nienhuis *et al.* (1992), and Nienhuis and Kryszewski (1994) found that an isolated atom cannot be rotated but if diatomic complexes are formed during its interaction with the environment (collisions), mechanical Faraday rotation may be possible. Such binary complexes in high-density atomic vapor were observed in the experiment of Kristensen *et al.* (1994) described in Sec. II.C.3. These authors observed rotational locking of the electronic wave function to the instantaneous interatomic collision axes that could possibly be used for a demonstration of the mechanical Faraday effect. Estimates by Nienhuis and Kryszewski (1994) show that the ratio of the rotation due to the mechanical and magnetic effects, when the angular velocity equals the Larmor precession frequency, is of the order of the collision frequency multiplied by the duration of the collision. As far as the authors of this review are aware, such an effect has not yet been observed in the gas phase.

---

[13]The order of magnitude of the displacement for sufficiently weak magnetic field can be estimated as $(g\mu B/\Gamma)(l/l_0)\lambda$ (with the usual notations).

III. LINEAR VS NONLINEAR LIGHT-ATOM INTERACTIONS

In its broadest definition, a nonlinear optical process is one in which the optical properties of the medium depend on the light field itself. The light field can consist either of a single beam that both modifies the medium and probes its properties, or of multiple beams (e.g., a pump-probe arrangement). In certain situations, light-induced modifications of the optical properties of the medium can persist for a long time after the perturbing light is turned off (these are sometimes referred to as *slow nonlinearities*). In such cases, the pump and probe interactions can be separated in time, with the effect of the pump interaction accumulating over a time limited by the relaxation rate of the slow nonlinearity. This is the situation in optical pumping (Sec. IV.A) and in much of the nonlinear magneto-optical work discussed in this review. In this section, we provide a classification of optical properties based on the perturbative approach and introduce saturation parameters that are ubiquitous in the description of nonlinear optical processes near resonance.

A. Perturbative approach

The classification of atom-light interactions in terms of linear and nonlinear processes can be done using a description of the atomic ensemble by its density matrix ρ. The knowledge of ρ allows one to calculate the induced polarization **P** (the macroscopic electric dipole moment) using the relation

$$\mathbf{P} = \mathrm{Tr}\rho(\mathcal{E})\mathbf{d}, \tag{7}$$

which is the response of the medium to the optical field $\mathcal{E}$, where **d** is the electric dipole operator. The evolution of ρ is described by the Liouville equation (see, for example, Corney, 1988), which is linear in the Hamiltonian describing the interaction of the ensemble with the external magnetic field and the optical field. As discussed, for example, by Stenholm (1984) and Boyd (1992), the solutions ρ of the Liouville equation can be expanded in powers of the optical-field amplitude

$$\rho = \sum_{n=0}^{\infty} \rho^{(n)} \mathcal{E}^n. \tag{8}$$

Figure 8 is a diagramatic representation of this perturbative expansion for light interacting with a two-level atom, in which each level consists of a number of degenerate Zeeman sublevels. In the absence of light and in thermodynamic equilibrium, the density matrix contains only lower-level populations ρ_{aa}. The lowest-order interaction of the light field with the atomic ensemble creates a linear polarization characterized by the off-diagonal matrix element $\rho_{ab}^{(1)}$. This polarization is responsible for linear absorption and dispersion effects, such as the linear Faraday effect. In the next order of perturbation, excited-state populations $\rho_{bb}^{(2)}$ and coherences $\rho_{aa'}^{(2)}$ and $\rho_{bb'}^{(2)}$ in the ground and excited states appear. They are needed to describe fluorescence and quantum interference effects (e.g., quantum beats),
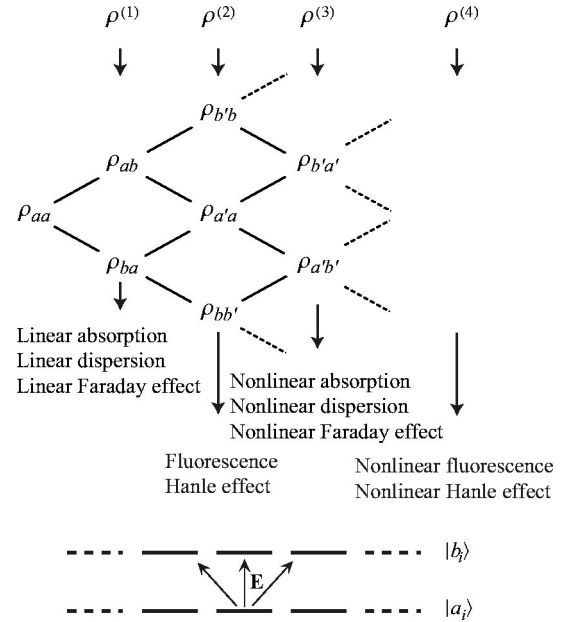
FIG. 8. Perturbative evolution of the density matrix of two-level atoms interacting with an optical field. Note that for any given order, the primed quantities label any of the magnetic sublevels or coherent superpositions thereof that may be reached from the previous order by a single interaction respecting the angular momentum selection rules.

excited-state level crossings, and the Hanle effect (Sec. II.D.1). Generally, even-order terms of ρ are stationary or slowly oscillating, while odd-order terms oscillate with frequencies in the optical range. In particular, the next order $\rho_{ab}^{(3)}$ is the lowest order in which a nonlinear polarization at the optical frequency appears. It is responsible for the onset of nonlinear (saturated) absorption and dispersion effects, such as the nonlinear Faraday and Voigt effects. The appearance of $\rho^{(4)}$ marks the onset of nonlinear (saturated) fluorescence and the nonlinear Hanle effect. In terms of quantum interference (Sec. II.D.1), these effects can be associated with opening of additional interference channels (in analogy to a multislit Young's experiment).

The Liouville equation shows how subsequent orders of ρ are coupled (see discussion by Boyd, 1992):

$$\dot{\rho}_{ab}^{(n)} = -(i\omega_{ab} + \gamma_{ab})\rho_{ab}^{(n)} - \frac{i}{\hbar}[-\mathbf{d}\cdot\mathcal{E}, \rho^{(n-1)}]_{ab}, \tag{9}$$

where $\hbar\omega_{ab}$ is the energy difference between levels a and b. The density matrix ρ to a given order $\rho^{(n)}$ can thus be expressed in terms of the elements $\rho^{(n-1)}$ of the next-lowest order. Odd orders of ρ describe optical coherences and even orders describe level populations and Zeeman coherences [according to Eq. (9) the latter are the source terms for the former and vice versa]. The magnitude of the linear absorption coefficient, governed by $\rho_{ab}^{(1)}$, can be expressed in terms of the populations $\rho_{aa}^{(0)}$. Similarly, $\rho_{ab}^{(3)}$, which determines the lowest-order saturated absorption and the lowest-order nonlinear Faraday effect, is driven by $\rho_{aa}^{(2)}$ and $\rho_{bb}^{(2)}$ (excited- and

ground-state populations), $\rho_{bb'}^{(2)}$, (excited-state coherences), and $\rho_{aa'}^{(2)}$, (ground-state coherences).

In the language of nonlinear optics, the induced polarization can be expanded into powers of $\mathcal{E}$:

$$\mathbf{P} = \sum_{n=1}^{\infty} \mathbf{P}^{(n)} = \sum_{n=1}^{\infty} \chi^{(n)} \cdot \mathcal{E}^n, \tag{10}$$

where the $\chi^{(n)}$ are the nth-order electric susceptibilities. Expression (10) is a particular case of the general expansion used in nonlinear optics in which n optical fields $\mathcal{E}_i$ oscillating at frequencies ω_i generate nth-order polarizations oscillating at all possible combinations of ω_i. In the present article, we focus on the case of a single optical field oscillating at frequency ω. Here the only polarizations oscillating at the same frequency are of odd orders in P. Coherent forward scattering is governed by P and is thus directly sensitive only to odd orders of ρ or χ. Even orders can be directly probed by observing (incoherently emitted) fluorescence light. Linear dispersion and absorption effects such as the linear Faraday effect are $\chi^{(1)}$ processes, while the nonlinear Faraday effect arises first as a $\chi^{(3)}$ process.

In forward-scattering experiments, the absorbed power is proportional to $\langle \dot{\mathbf{P}} \cdot \mathcal{E} \rangle$, which is given in (odd) order l by $(\chi^{(l)} \cdot \mathcal{E}^l) \cdot \mathcal{E} \propto \chi^{(l)} I^{(l+1)/2}$, where I is the light intensity.[14] Forward scattering in lowest order ($l=1$) involves $\chi^{(1)}$ and is a linear process in the sense that the experimental signal is proportional to I. In light-induced fluorescence experiments, the scattered power is proportional to the excited-state population, which, to lowest order $[\rho_{bb}^{(2)}]$ is also proportional to I. We adopt the following classification (which is consistent with the commonly used notions): Processes that involve $\rho^{(1)}$ and $\rho^{(2)}$ will be called *linear processes*, while all higher-order processes will be referred to as *nonlinear processes*.[15]

This perturbative approach is useful for understanding the onset of a given effect with increasing light power. It works well in most cases involving nonresonant light fields. In the case of resonant laser excitation, however, caution must be used, since there is no way to make meaningful distinctions between different perturbative orders once the transition is saturated [the series (9) and (10) are nonconverging and all orders of these expansions are coupled.]

This discussion is generalized in a straightforward manner to the case of pump-probe experiments (i.e., in which separate light beams are used for pumping and probing the medium). Here the signals that depend on both beams are, to lowest order, proportional to the product of the intensities of these beams and thus correspond to a $\chi^{(3)}$ nonlinear process.

B. Saturation parameters

Nonlinear optical processes are usually associated with high light intensities. However, nonlinear effects can show up even with weak illumination—conventional spectral lamps were used in early optical pumping experiments with resonant vapors to demonstrate nonlinear effects (Sec. IV.A). It is important to realize that the degree of nonlinearity strongly depends on the specific mechanism of atomic saturation by the light field as well as the relaxation rate of atomic polarization.

A standard discussion of optical nonlinearity and saturation for a two-level atom is given by Allen and Eberly (1987). The degree of saturation of a transition is frequently characterized by a *saturation parameter* of the general form

$$\kappa = \frac{\text{excitation rate}}{\text{relaxation rate}}. \tag{11}$$

The saturation parameter is the ratio of the rates of coherent light-atom interactions (responsible for Rabi oscillations) and incoherent relaxation processes (e.g., spontaneous decay).

Consider a two-level system in which the upper state decays back to the lower state and light is tuned to resonance. The saturation parameter is given by

$$\kappa_1 = \frac{d^2 \mathcal{E}_0^2}{\hbar^2 \gamma_0^2}. \tag{12}$$

Here d is the transition dipole moment, $\mathcal{E}_0$ is the amplitude of the electric field of the light, and γ_0 is the homogeneous width of the transition. (For simplicity, we assume that γ_0 is determined by the upper state's decay.) The excitation rate is $d^2 \mathcal{E}_0^2/(\hbar^2 \gamma_0)$, and the relaxation rate is γ_0.

When $\kappa_1 \ll 1$, the spontaneous rate dominates. Atoms mostly reside in the lower state. Occasionally, at random time intervals, an atom undergoes an excitation/decay cycle; the average fraction of atoms in the upper state is $\sim \kappa_1$. On the other hand, when $\kappa_1 \gg 1$, atoms undergo regular Rabi oscillations (at a rate much greater than that of spontaneous emission), and the average populations of the upper and the lower states equalize.

If the upper state predominantly decays to states other than the lower state of the transition, the character of saturation is quite different. If there is no relaxation of the lower level of the transition, light of any intensity will eventually pump all atoms out of the lower and up-

---

[14]This follows directly from Maxwell's equations in a medium (see discussion by, for example, Shen, 1984).

[15]The formalism of *nonlinear wave mixing* (see discussion by Boyd, 1992; Shen, 1984) allows one to describe *linear* electro- and magneto-optical effects as three- or four-wave-mixing processes, in which at least one of the mixing waves is at zero frequency. For example, linear Faraday rotation is seen in this picture as mixing of the incident linearly polarized optical field with a zero-frequency magnetic field to produce an optical field of orthogonal polarization. While this is a perfectly consistent view, we prefer to adhere to a more common practice of calling these processes linear. In fact, for the purpose of the present review, the term *nonlinear* will only refer to the dependence of the process on *optical* fields. Thus we also consider as linear a broad class of optical-rf and optical-microwave double-resonance phenomena.

per states into other states. When there is lower-state relaxation at rate γ in the absence of light, the saturation parameter is

$$\kappa_2 = \frac{d^2 \mathcal{E}_0^2}{\hbar^2 \gamma_0 \gamma}. \tag{13}$$

Here the excitation rate is the same as for κ_1, but the relaxation rate is now γ. In many experiments, γ is much smaller than γ_0, so that nonlinear effects can appear at lower light intensities than for systems characterized by κ_1. Note that the parameter κ_1 is also significant for open systems as it gives the ratio of the populations of the upper and lower states.

When the upper and lower levels of the transition are composed of Zeeman sublevels, the relevant saturation parameter for nonlinear effects depends on the specifics of the transition structure and the external (optical and other) fields. For example, if a "dark" state is present in the lower level, the system is effectively open (atoms are pumped into the dark state in a process known as *coherent population trapping*; see Sec. XIII.A), and the optical pumping saturation parameter κ_2 applies. For an $F=1/2 \rightarrow F'=1/2$ transition pumped with linearly polarized light, on the other hand, there is no dark state and the saturation parameter κ_1 applies. If circularly polarized light is used for optical pumping, however, or if a magnetic field is used to break the degeneracy between transitions for right- and left-circularly polarized light, the transition becomes effectively open and the parameter κ_2 applies.

The parameters κ_1 and κ_2 are also of use in the characterization of the magnitude of power broadening and of light shifts of the transition.

IV. EARLY STUDIES OF NONLINEAR MAGNETO-OPTICAL EFFECTS

In this section, we trace the development of the study of nonlinear magneto-optical effects (NMOE) from the early optical pumping work of the 1950s to the experiments with tunable lasers carried out in the 1980s and early 1990s that led to the formulation of quantitative theories of magneto-optics in simple systems and in the alkalis (Kanorsky *et al.*, 1993).

A. Optical pumping

Research on polarized light-atom interactions (Sec. II.D.1) initiated by Wood (1922), Wood and Ellett (1923, 1924), and Hanle (1924), was not pursued much further at the time. Twenty-odd years later, Kastler (1950) had the idea to make use of angular momentum conservation in light-matter interaction (Rubinowicz, 1918), to create spatially oriented atomic angular momenta by absorption of circularly polarized light (optical pumping). Anisotropy created by optical pumping can be detected by monitoring of the intensity and/or polarization of the transmitted light, monitoring of the fluorescence intensity and/or polarization, or state selection in atomic beams. For transmission monitoring, transmission of ei-

ther the pump beam or a probe beam can be recorded. The latter method has been most often applied with resonant probe beams for absorption monitoring (Dehmelt, 1957). In particular, Bell and Bloom (1957, 1961) employed Dehmelt's method for detection of the ground-state coherence induced by an rf field and by an intensity-modulated pump beam.

It was soon realized that probe transition monitoring could be used with off-resonant light for dispersion detection. Gozzini (1962) suggested observing the rotation of the polarization plane of a weak probe beam to detect the population imbalance in atomic sublevels created by optical pumping. This rotation (which occurs in zero magnetic field) is caused by amplitude asymmetry between the σ^+ and σ^- refractive indices, analogous to that occurring in paramagnetic samples (Sec. II.A); hence it is sometimes called the *paramagnetic Faraday effect*.[16] Many experiments were performed using this idea (reviewed by Happer, 1971). For optical pumping studies, off-resonance detection of dispersive properties has the advantage over absorption monitoring that the probe beam interacts only weakly with the pumped atoms. Thus high probe-beam intensities can be used, enhancing the signal-to-noise ratio of the detection, without loss of sensitivity due to power broadening. On the other hand, a probe beam detuned from exact resonance could induce light shifts[17] of the atomic energy levels, which may not be acceptable in high-precision work.

Because the optical properties of the atomic vapor are altered by the pump beam, and these changes are detected by optical means, optical pumping is classified as a nonlinear process. However, it should be realized that, in most of the pre-laser cases, the effect was due to the cumulative action of several optical-pumping cycles, i.e., sequences of absorption and spontaneous emission, occurring on a time scale shorter than the lower-state relaxation time but longer than the upper-state lifetime. Thus no appreciable upper-state population was produced.

Nonlinear effects related to upper-state saturation can arise even with lamps as light sources, provided that the light intensity is strong enough. An example of this can be found in the work of Schmieder *et al.* (1970), who investigated level-crossing signals in the fluorescence of Rb and Cs vapors. At high light intensities, narrow fea-

---

[16]Strictly speaking, the paramagnetic Faraday effect is not a magneto-optical effect, since it occurs even when there is no magnetic field present. Still, it affects atomic dispersion and so can play a role in magneto-optical effects.

[17]The quantum theory of light shifts in the context of optical pumping was developed by Barrat and Cohen-Tannoudji (1961; also see discussion by Cohen-Tannoudji, 1968). A simple classical derivation by Pancharatnam (1966) indicated a relation to atomic dispersion by showing that the light shift is given by a convolution of the spectral profile of the light field with the real part of the atomic susceptibility (refractive index). Since the real part of the refractive index is an antisymmetric function of the light detuning from atomic resonance, the light shift vanishes for resonant light beams.

tures appeared in the magnetic-field dependence near $B=0$. They were ascribed to the appearance of the ground-state Hanle signal in the excited-state fluorescence due to nonlinear coupling of the ground- and excited-state coherences. As with the Hanle experiment (Sec. II.D.1), the width of the resonance depended on the relaxation time of the atomic state; however, in contrast to the original Hanle effect, here it was the ground-state relaxation, rather than the upper-state relaxation, that was relevant. Very narrow widths (on the order of 1 μG) were seen by Dupont-Roc *et al.* (1969), who observed the ground-state Hanle effect in transmission. In this work, rubidium atoms contained in a paraffin-coated vapor cell (see Sec. VIII.E) were optically pumped by a circularly polarized beam from a Rb lamp, and thus acquired macroscopic orientation (magnetization) in their ground state. In the transverse-magnetic-field dependence of the pump-beam transmission, there was a Lorentzian resonance due to the ground-state Hanle effect. In order to get a dispersive resonance whose steep slope near the zero crossing could be used to detect small magnetic-field changes, Dupont-Roc *et al.* applied modulation to the magnetic field and performed lock-in detection of the transmitted light intensity at the modulation frequency. The ground-state Hanle effect studied was applied to ultrasensitive magnetometry by Cohen-Tannoudji *et al.* (1969) and Dupont-Roc (1970), providing sensitivity $\sim 10^{-9}$ G Hz$^{-1/2}$.

Bouchiat and Grossetete (1966) performed experiments that were an important precursor to later NMOE work with lasers (particularly that which utilized separated pump and probe light fields). They illuminated an alkali-vapor cell subject to a magnetic field with pump and probe lamplight sources in order to carry out detailed studies of spin-relaxation and spin-exchange processes. An interesting feature of this setup is that the pump and probe light fields could be resonant with different transitions of the same atom, or even with transitions in different isotopes or species. In the latter cases, atomic polarization induced by the pump light in one isotope or species is transferred to the other via spin-exchange collisions.

B. Nonlinear magneto-optical effects in gas lasers

When a magnetic field is applied to a gas laser medium, several nonlinear magneto-optical effects can be observed by monitoring laser intensity or the fluorescence light laterally emitted from the laser tube.[18] These effects include nonlinear Hanle and level-crossing effects (Sec. II.B) as well as a specific coherence effect

—————

[18]Such effects were extensively studied in the early days of laser physics, both experimentally (Culshaw and Kannelaud, 1964a, 1964b, 1964c; Dumont and Durand, 1964; Fork *et al.*, 1964; Krupennikova and Chaika, 1966; Schlossberg and Javan, 1966; Tomlinson and Fork, 1967) and theoretically (Dyakonov and Perel, 1966; Sargent *et al.*, 1967; van Haeringen, 1967).

known as *mode crossing*. Mode crossing occurs when the frequency separation between two laser modes matches the Zeeman splitting of a pair of magnetic sublevels. The two sublevels are then coherently driven by the two laser modes, resulting in a resonance feature in the magnetic dependence of the output power (Schlossberg and Javan, 1966; Dumont, 1972; Hermann and Scharmann, 1972; Hermann *et al.*, 1977). Mode crossing is an example of a three-level coherence resonance, related to various effects described in Sec. XIII.A.

Most gas lasers have tubes with Brewster windows and so possess high polarization anisotropy. Such lasers are sensitive to magneto-optical effects since the influence of light polarization on the laser output intensity is strongly enhanced by the cavity. Thus even minute changes in polarization are transformed into easily detected intensity variations. Early experimental demonstrations of such effects were described by Hermann and Scharmann (1967, 1968, 1972), Le Floch and Le Naour (1971), and Le Floch and Stephan (1972).[19]

It is possible to use a gas laser as a magnetometer by minimizing anisotropy in the cavity and applying a longitudinal magnetic field. The eigenmodes generated by the laser are two oppositely circularly polarized components with different frequencies (dependent on the magnetic field). If the two components have the same intensity, the resultant output of the laser is linearly polarized, with the direction of polarization rotating at half the difference frequency between the modes. The time dependence of the intensity transmitted through a linear analyzer gives a measurement of the magnetic field (Bretenaker *et al.*, 1992, 1995). Bretenaker *et al.* demonstrated a magnetometric sensitivity of a few μG Hz$^{-1/2}$ for fields on the order of 1 G.

C. Nonlinear effects in forward scattering

Forward scattering in the linear regime was discussed in Sec. II.B. At high light intensity, nonlinear effects appear in forward scattering [the quantities A and n in Eq. (4) become intensity dependent]. There are two principal mechanisms for the nonlinearity. One is velocity-selective modifications of the atomic population distributions by narrow-band light (see Sec. V.A); the other is related to light-induced coherences between Zeeman sublevels. Often, both of these mechanisms operate simultaneously.

In the early 1970s came the advent of the tunable laser, an ideal tool for optical pumping and generation of atomic coherences. The creation of atomic coherences by a strong light field was extensively analyzed, and is reviewed by several authors (e.g., Cohen-Tannoudji, 1975; Decomps *et al.*, 1976; Gawlik, 1994).

—————

[19]Additional information on magneto-optical effects coupled to intracavity anisotropy can be found in a book by Voytovich (1984) and in a topical issue of J. Opt. B (Semiclassical and Quantum Optics) **3** (2001).
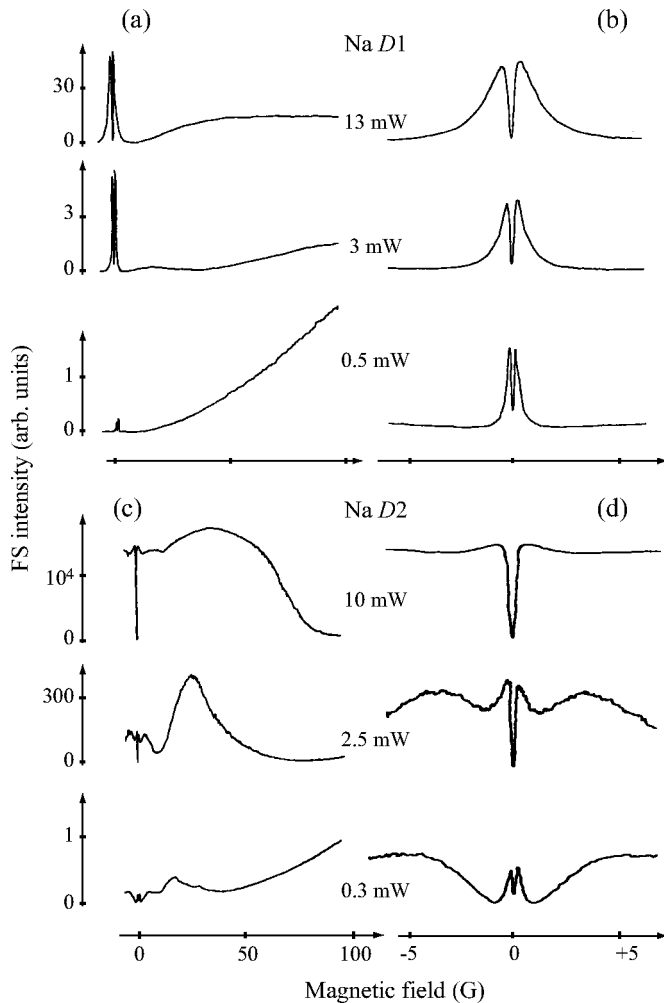
FIG. 9. Forward-scattering signals (FS intensity versus magnetic field) from the sodium (a) $D1$ and (c) $D2$ lines (note the additional broad structure arising from excited-state coherence) obtained for various laser intensities by Gawlik *et al.* (1974a). Plots (b) and (d) show signals near zero magnetic field. From Gawlik *et al.*, 1974a.

The first observations of laser-induced coherences in forward scattering (as well as the first observations of the nonlinear Faraday effect with lasers) were made by Gawlik *et al.* (1974a, 1974b), who used both cw and pulsed lasers. Very strong dependence of the forward-scattering signal intensity on the magnetic-field dependence was observed (Gawlik *et al.*, 1974a), in contrast to the prediction of the linear theory and earlier observations with spectral lamps (Corney *et al.*, 1966; Durrant and Landheer, 1971; Krolas and Winiarczyk, 1972). The observed curves, reproduced in Fig. 9, are measures of $\varphi^2(B)$ if the optical density is not too high.

The structures reported by Gawlik *et al.* (1974a) were *subnatural*, i.e., they were narrower than would be expected if they were due to the natural width of the optical transition (Sec. II.D.1). They were also not subject to Doppler broadening. This indicates that these structures were associated with ground-state coherences whose effective relaxation rate was determined by the finite atomic transit time across the light beam.

The amplitude of the signals depended nonlinearly on the light intensity, and the signals were easily power broadened. They were also quite sensitive to small buffer-gas admixtures, which indicated that optical coherences played a role in their creation [collisions destroy optical coherences faster than they do populations and ground-state coherences (Gawlik *et al.*, 1974a)]. The observed forward-scattering signals exhibited a complex structure that was similar to that seen by Ducloy (1973) in fluorescence. Ducloy attributed this structure to hexadecapole moments (associated with the coherence between the $M=\pm2$ sublevels of the $F=2$ ground-state component; see Appendix B.1 for a discussion of atomic multipoles). The experiment of Gawlik *et al.* (1974a) was initially interpreted in terms of such multipoles. This interpretation raised some controversy since, as pointed out by Giraud-Cotton *et al.* (1982a, 1985a),[20] signals like those observed by Gawlik *et al.* (1974a) could be explained by third-order perturbation theory (see Sec. III.A) in which quadrupoles are the highest-rank multipoles, i.e., without invoking the hexadecapole moment. On the other hand, under the conditions of the experiment of Gawlik *et al.* (1974a), perturbation theory was clearly invalid (Gawlik, 1982). Moreover, hexadecapole moments were unambiguously observed in several other experiments with fluorescence detection (Ducloy, 1973; Fischer and Hertel, 1982; McLean *et al.*, 1986) performed under similar conditions to those of Gawlik *et al.* (1974a). An intriguing question arose: do the higher-order multipoles affect the forward-scattering signals, and if so, why are simple perturbative calculations so successful in reproducing the experimental results? Answering this question was not straightforward, because higher-order multipoles exist in systems with high angular momenta and thus a large number of coupled sublevels. Hence it took quite some time until the above controversy was resolved. Łobodziński and Gawlik (1996) performed detailed nonperturbative calculations for the Na $D1$ line, taking all possible Zeeman coherences into account. They found that hexadecapoles can indeed affect forward-scattering signals but only when a single hyperfine structure (hfs) component is selected ($F=2 \rightarrow F'=2$ in the case of the Na $D1$ transition). Other hfs components of the Na $D1$ line are largely insensitive to the hexadecapole coherence. In later work by Łobodziński and Gawlik (1997), this result was interpreted in terms of two competing trap states (Sec. XIII.A) contributing to the forward-scattered signal.

Apart from the above-mentioned nonlinear magneto-optical effects at near-zero magnetic fields, some attention was also devoted to high magnetic fields. Gibbs *et al.* (1974) investigated Faraday rotation in the vicinity of the Na $D1$ transition under the conditions of saturation with cw light and, in a separate set of measurements, under the conditions of *self-induced transparency* (McCall and Hahn, 1969). These experiments were done

_____

[20]This was also discussed by Jungner *et al.* (1989), Stahlberg *et al.* (1990), and Holmes and Griffith (1995).

at magnetic fields in the range 1–10 kG. Gibbs *et al.* found that Faraday rotation in these nonlinear regimes is actually similar to the rotation in the linear regime. The utility of the nonlinear regimes is that they afford a significant reduction in absorption of the light, making it possible to achieve large rotation angles [in excess of $3\pi/2$ rad in the work of Gibbs *et al.* (1974)]. Agarwal *et al.* (1997) studied the influence of propagation effects (high optical density) and high light intensity on the forward-scattering spectra taken at high magnetic fields. This analysis is important for precision measurements of oscillator strengths (Sec. II.C.2).

D. "Rediscoveries" of the nonlinear magneto-optical effects

Some ten years after the first investigations of nonlinear magneto-optical effects in forward scattering (Gawlik *et al.*, 1974a, 1974b), similar effects were independently "rediscovered" by several groups, in certain instances in a somewhat dramatic manner.[21] For example, Davies *et al.* (1987) passed a linearly polarized laser beam tuned near an atomic resonance through a samarium vapor cell placed in a longitudinal magnetic field. After the light had passed through the cell, the direction of its polarization was analyzed. Normally, a small amount of buffer gas was present in the cell; the resulting magnitude and frequency dependence of the Faraday rotation were well understood. However, rather accidentally, it was discovered that, if the buffer gas was removed from the cell, the magnitude of the peak rotation changed sign and its size increased by some three orders of magnitude! The frequency and magnetic-field dependences of the rotation also changed radically. Similar observations were made by other groups, but a consistent explanation of the phenomenon was lacking. In order to clarify the situation, Barkov *et al.* (1989a) performed an experiment on several low-angular-momentum transitions of atomic Sm and identified two mechanisms (Fig. 10) responsible for the enhanced rotation: Bennett-structure formation in the atomic velocity distribution (Sec. V.A) and Zeeman coherences (Sec. V.B). The latter effect produces a larger enhancement of rotation in small magnetic fields; Barkov *et al.* (1989a) observed rotation $\sim 10^4$ times larger than that due to the linear Macaluso-Corbino effect. These experimental results were subsequently compared to theoretical predictions, showing good agreement (Kozlov, 1989; Zetie *et al.*, 1992). At about the same time, precision measurements and detailed calculations of the nonlinear Faraday

---

[21]These "rediscoveries" prompted systematic investigations of nonlinear magneto-optical effects. The experimental work included that of Badalyan *et al.*, 1984; Stahlberg *et al.*, 1985, 1990; Drake, 1986; Lange *et al.*, 1986; Buevich *et al.*, 1987; Davies *et al.*, 1987; Drake *et al.*, 1988; Baird *et al.*, 1989; Barkov *et al.*, 1989b; Chen *et al.*, 1990; and Weis, Wurster, and Kanorsky, 1993. Theoretical investigations include those of Giraud-Cotton *et al.*, 1985a, 1985b; Fomichev, 1987; Schuller *et al.*, 1987; Jungner *et al.*, 1989; and Kanorsky *et al.*, 1993.
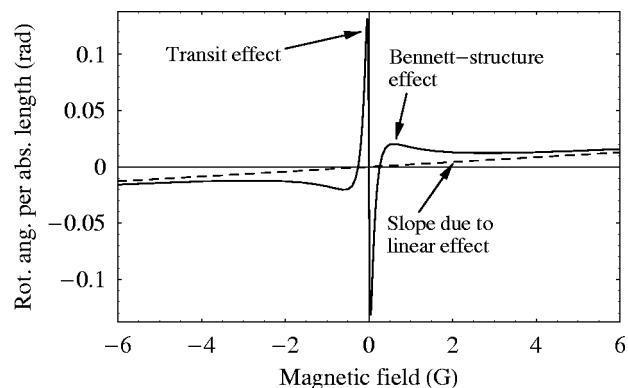
FIG. 10. Density-matrix calculation (Budker, Kimball, *et al.*, 2002a; Sec. VII.B) of light polarization rotation as a function of magnetic field for the case of the samarium 571-nm ($J=1 \rightarrow J'=0$) line, closely reproducing experimental results described by Barkov *et al.* (1989a); see also Zetie *et al.* (1992).

effect on the cesium $D2$ line were performed (Chen *et al.*, 1990; Kanorsky *et al.*, 1993; Weis, Wurster, and Kanorsky, 1993). Because Cs has hyperfine structure and high angular momentum, the situation was somewhat more complicated than for transitions between low-angular-momentum states of the nuclear-spin-less isotopes of Sm (see Sec. VII for a description of the theoretical approaches to NMOE). Nevertheless, excellent quantitative agreement between theory and experiment was obtained.

V. PHYSICAL MECHANISMS OF NONLINEAR MAGNETO-OPTICAL EFFECTS

When a nonlinear magneto-optical effect occurs, the properties of both the medium and the light are affected. Our description of the physical mechanisms that cause NMOE deals with the influence of light on the medium and the influence of the medium on the light separately, first detailing how the populations of and coherences between atomic states are changed (optical pumping) and then how the light polarization is subsequently modified (optical probing). If, as is the case in many of the experiments discussed in Secs. IV, VIII, and XII, a single laser beam is used for both pumping and probing, these processes occur simultaneously and continuously. However, comparison with full density-matrix calculations and experimental results shows that the essential features of NMOE can be understood by considering these processes separately.

As discussed above, we distinguish between two broad classes of mechanisms of NMOE: first, Bennett-structure effects, which involve the perturbation of populations of atomic states during optical pumping, and second, "coherence" effects, which involve the creation and evolution of atomic polarization (although in some cases, with a proper choice of basis, it is possible to describe these effects without explicit use of coherences; see Sec. VII.A).

In the case of nonlinear Faraday rotation, the primary empirical distinction between these two effects is the magnitude of the magnetic field B_{max} at which optical
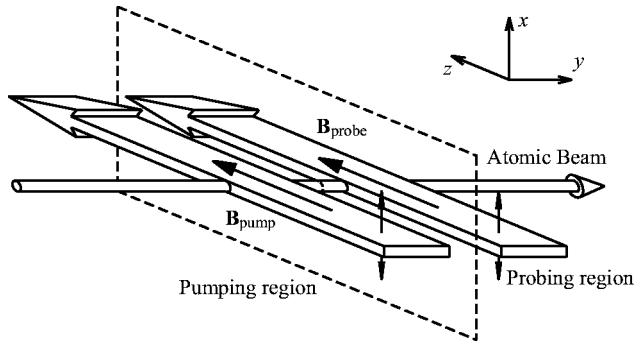
FIG. 11. Conceptual two-region experimental arrangement with separated optical pumping and probing regions used to treat Bennett-structure effects in nonlinear magneto-optical rotation. Pump and probe light beams are initially linearly polarized along x, the atomic beam propagates in the $\hat{\mathbf{y}}$ direction, and the magnetic fields are oriented along the direction of light propagation ($\hat{\mathbf{z}}$).

rotation reaches a maximum. This magnetic-field magnitude is related to a linewidth by the formula [see Eq. (2)]:

$$B_{\max} = \frac{\hbar \Gamma}{2 g \mu}. \tag{14}$$

The smallest achievable linewidth for Bennett-structure-related nonlinear magneto-optical rotation (NMOR) corresponds to the natural width of the atomic transition (typically $2\pi \times 1–10$ MHz for allowed optical electric dipole transitions). In the case of the coherence effects, the linewidth Γ is determined by the rate of atomic depolarization. The smallest NMOR linewidths $\sim 2\pi \times 1$ Hz have been observed by Budker *et al.* (1998a) for atoms in paraffin-coated cells.

A. Bennett-structure effects

We first consider NMOR caused by *Bennett structures*—"holes" and "peaks" in the atomic velocity distributions of the ground-state sublevels resulting from optical pumping (Bennett, 1962). As an example, we discuss a simple case of Bennett-structure-related NMOR in which optical pumping and probing are performed in separate regions (Budker *et al.*, 2002a; Fig. 11). In this example there is $\hat{\mathbf{z}}$-directed magnetic field $\mathbf{B}_{\text{probe}}$ in the probe region ($\mathbf{B}_{\text{pump}}$ is set to zero). In the pumping region, atoms interact with a near-resonant, x-polarized, narrow-band laser beam of saturating intensity [the optical pumping saturation parameter (Sec. III.B) $\kappa = d^2 \mathcal{E}_0^2 / (\hbar^2 \gamma_0 \gamma_t) \gg 1$, where γ_0 is the natural width of the transition, and γ_t is the rate of atoms' transit through the pump laser beam]. In the probing region, a weak ($\kappa \ll 1$) light beam, initially of the same polarization as the pump beam, propagates through the medium. The resultant polarization of the probe beam is then analyzed.

Consider an $F = 1/2 \to F' = 1/2$ transition. This system is especially straightforward because it exhibits no coherence magneto-optical effects with linearly polarized light. Thus NMOR in this system is entirely due to Bennett structures. Suppose that the upper state decays to
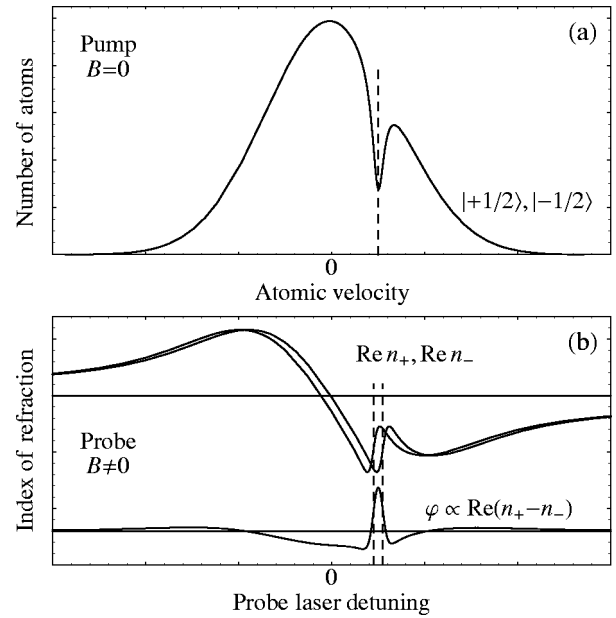
FIG. 12. The Bennett-structure effect on a $1/2 \to 1/2$ transition in which the upper state decays to levels other than the lower state; $\mathbf{B}_{\text{pump}} = 0$, $\mathbf{B}_{\text{probe}} \neq 0$. (a) In the pump region, monochromatic laser light produces Bennett holes in the velocity distributions of atoms in the lower state $|+1/2\rangle$, $|-1/2\rangle$ sublevels. Since there is no magnetic field, the holes occur in the same velocity group (indicated by the dashed line) for each sublevel. (b) In the probe region, a magnetic field is applied, shifting n_+ and n_- relative to each other (upper trace). The real part of the indices of refraction are shown so that the features in plot (a) correspond to dispersive shapes in this plot. The shifted central detunings of the Bennett-structure features are indicated by the dashed lines. Polarization rotation of the probe laser light is proportional to the difference $\text{Re}(n_+ - n_-)$ (lower trace). Features due to the Doppler distribution and the Bennett holes can be seen. Since the Bennett related feature is caused by the removal of atoms from the Doppler distribution, the sign of rotation due to this effect is opposite to that of the linear rotation. From Budker, Kimball, *et al.*, 2002a.

levels other than the ground state. For atoms in the resonant velocity group, the $|M = \pm 1/2\rangle$ lower-state Zeeman sublevels are depopulated by optical pumping, creating "holes" in the atomic velocity distributions of the two states [Fig. 12(a)]. Consequently there are sub-Doppler features (with minimum width γ_0) in the indices of refraction n_- and n_+ for right- and left-circularly polarized (σ^- and σ^+, respectively) light. In the probe region [Fig. 12(b)], a small magnetic field $\mathbf{B}_{\text{probe}} < \hbar \gamma_0 / (2 g \mu)$ is applied. (For simplicity, the Landé factor for the upper state is assumed to be negligible.) The indices of refraction n_- and n_+ are displaced relative to each other due to the Zeeman shift, leading to optical rotation of the probe beam. In the absence of Bennett structures, this gives the linear Faraday effect. When Bennett holes are produced in the pump region, the resultant Faraday rotation can be thought of as rotation produced by the Doppler-distributed atoms without the hole (linear Faraday rotation) minus the rotation that would have been produced by the pumped-out atoms. Thus the rotation

due to Bennett holes has the opposite sign from that due to the linear effect.

As described in detail by Budker *et al.* (2002a), the mechanism of Bennett-structure-related NMOR depends critically on the details of the experimental situation. Depending on whether a magnetic field is present in the pump region, and whether the excited state decays to the ground state or other levels, Bennett-structure-related NMOR can be due to holes (and have one sign), be due to "peaks" generated by spontaneous decay to the ground state (and have the opposite sign), or not be present at all.

Note also that mechanical action of light on atoms could, under certain conditions, lead to redistribution of atoms among velocity groups, thus deforming the Bennett structures and modifying the nonlinear optical properties of the medium (Kazantsev *et al.*, 1986)

B. Coherence effects

Coherence effects can produce even narrower widths than Bennett-structure-related NMOE, thus leading to significantly higher small-field Faraday rotation (Gawlik, 1994; Arimondo, 1996). At low light power, the effect of the pump light can be conceptually separated from that of the magnetic field, so that the coherence effect can be thought of as occurring in three stages. First, atoms are optically pumped into an aligned state, causing the atomic vapor to acquire linear dichroism; second, the atomic alignment precesses in the magnetic field, rotating the axis of dichroism; third, the light polarization is rotated by interaction with the dichroic atomic medium, since the alignment is no longer along the initial light polarization. The third, "probing" step does not require high light intensity, and can be performed either with a weak probe beam or with the same pump light used in the first step.

Consider atoms with total angular momentum $F=1$ that are not aligned initially subject to linearly polarized laser light with frequency corresponding to a transition to a $F'=0$ state (Fig. 2). One can view the atoms as being in an incoherent mixture of the following states: $|M=0\rangle$, $(|M=1\rangle \pm |M=-1\rangle)/\sqrt{2}$. The first of these states can be excited to the $F'=0$ state only by z-polarized radiation; it is decoupled from x- and y-polarized light. Similarly, the other two states (which are coherent superpositions of the Zeeman sublevels) are y- and x-absorbing states, respectively. Suppose the laser light is polarized along the x axis. Optical pumping by this light causes depletion of the x-absorbing state, leaving atoms in the "dark" y- and z-absorbing states.[22] The medium becomes transparent for the x-polarized

---

[22]This process is known as coherent population trapping (Arimondo, 1996) because, as a result of optical pumping by linearly polarized light, atoms in the $|M=\pm1\rangle$ substates are not completely pumped out, as would seem to be the case at first glance (Fig. 2), but largely remain in a dark coherent superposition.
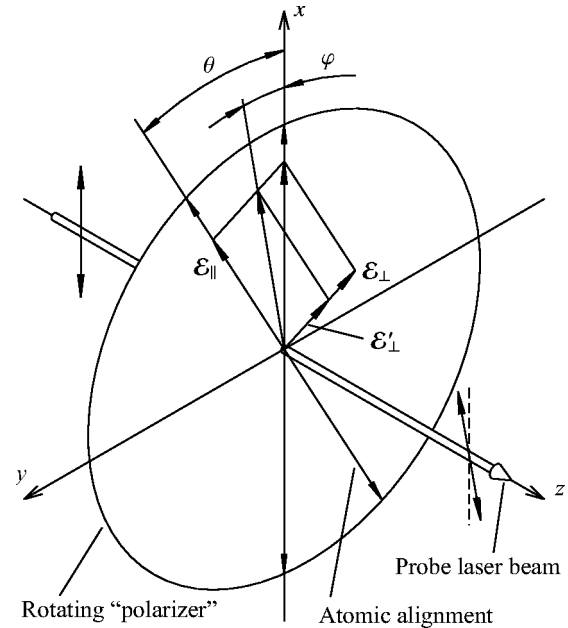
FIG. 13. An optically thin sample of aligned atoms precessing in a magnetic field, which can be thought of as a thin rotating polaroid film that is transparent to light polarized along its axis ($\mathcal{E}_\parallel$) and slightly absorbent for the orthogonal polarization ($\mathcal{E}_\perp$). Here $\mathcal{E}_\parallel$ and $\mathcal{E}_\perp$ are the light electric-field components. The effect of such a "polarizer" is to rotate light polarization by an angle $\varphi \propto \sin 2\theta$). The figure is drawn assuming that a magnetic field is directed along $\hat{\mathbf{z}}$. Adapted from Budker, Orlando, and Yashchuk (1999).

radiation; however, it can still absorb and refract light of an orthogonal polarization. The medium is *aligned*[23] (Appendix B.1) and possesses linear dichroism and birefringence.[24]

In the presence of a magnetic field, the atomic alignment axis precesses around the direction of the field at the Larmor frequency (precession of atomic alignment in a magnetic field is explained in detail in, for example, Corney, 1988, Chap. 15). One can understand the effect of this precession on the light polarization by thinking of the atomic medium as a layer of polarizing material like a polaroid film (Kanorsky *et al.*, 1993; Budker, Orlando, and Yashchuk, 1999). It is easy to show that the rotation of the "polarizer" around the z axis causes the linear output polarization to be rotated by an angle proportional to the optical density of the sample and to $\sin 2\theta$, where θ is the angle between the transmission axis of the rotated "polarizer" and the direction of initial light polarization (Fig. 13). In order to describe optical rotation of cw laser light, one has to sum the effect of atomic

---

[23]In general, alignment can exist for an $F \geq 1$ state even when there is no dark state [i.e., for $F \to F+1$ transitions (Kazantsev *et al.*, 1984)].

[24]The linear birefringence turns out not to be important for the coherence effect because the refractive index is unity on resonance. Note, however, that at high light powers, *circular birefringence* emerges as a dominant effect responsible for nonlinear Faraday rotation (see Sec. V.C).

"polarizers" continually produced by the light, each rotating for a finite time and then relaxing.[25] Using this model, one can show (Kanorsky *et al.*, 1993; Weis, Wurster, and Kanorsky, 1993) that for sufficiently low light power and magnetic field, the rotation due to the coherence effect is once again described by Eq. (2), but now the relevant relaxation rate is that of the ground-state alignment.

Calculations based on the rotating polarizer model reproduce the magnitude and the characteristic details of the low-power line shape of NMOE quite well (Kanorsky *et al.*, 1993), even when complicated by the presence of transverse magnetic fields (Budker, Yashchuk, and Zolotorev, 1998a). To account for transverse fields, the model must include two independent atomic subsamples with alignments corresponding to polarizers with transmission axes directed perpendicular to each other. These subsamples arise due to optical pumping through different hyperfine transitions. For zero transverse field, the NMOE dependences on the longitudinal magnetic field for each of these subsamples have symmetrical dispersive shapes of the same widths, but of different signs and magnitudes. Thus the resulting sum curve has a symmetrical shape. If a transverse field is applied, the features for the two alignments acquire different asymmetrical shapes. This leads to the asymmetrical sum curve seen in the experiments of Budker, Yashchuk, and Zolotorev (1998a).

C. Alignment-to-orientation conversion

In Sec. V.B, the nonlinear magneto-optical coherence effects were described as arising due to Larmor precession of optically induced atomic alignment [Fig. 14(a)]. However, for sufficiently strong light intensities—when the light shifts become comparable to or exceed the ground-state relaxation rate—a more complicated evolution of the atomic polarization state occurs (Budker, Kimball, *et al.*, 2000a). Under these conditions, the combined action of the magnetic and optical electric fields causes atoms to acquire orientation along the direction of the magnetic field, in a process known as alignment-to-orientation conversion (AOC). As discussed in Sec. II.A, an atomic sample oriented along the direction of light propagation causes optical rotation via circular birefringence, since the refractive indices for σ^+ and σ^- light are different.

The evolution of atomic polarization leading to AOC-related NMOR is illustrated for an $F=1 \rightarrow F'=1$ transi-
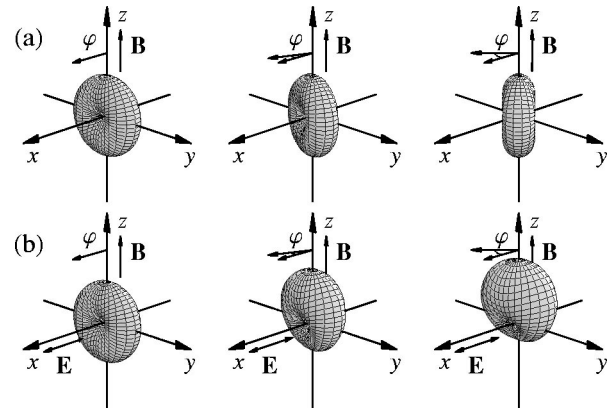

FIG. 14. Sequences showing the evolution of optically pumped ground-state atomic alignment in a longitudinal magnetic field for an $F=1 \rightarrow F'=1$ transition at low and high light powers (time proceeds from left to right). The distance from the surface to the origin represents the probability of finding the projection $M=F$ along the radial direction (Appendix B.2). (a) In the first plot, the atoms have been optically pumped into an aligned state by x-polarized light. The magnetic field along $\hat{\mathbf{z}}$ creates a torque on the polarized atoms, causing the alignment to precess (second and third plots). This rotates the medium's axis of linear dichroism, which is observed as a rotation of the polarization of transmitted light by an angle φ with respect to the initial light polarization. (b) Evolution of the same ground-state atomic alignment in a longitudinal magnetic field for high light power. The light frequency is slightly detuned from resonance to allow for a nonzero light shift. The combined action of the magnetic and light fields produces orientation along the $\hat{\mathbf{z}}$ axis.

tion in Fig. 14(b). In the first plot, the atoms have been optically pumped into an aligned state by x-polarized light (they have been pumped out of the "bright" x-absorbing state into the dark states). If the atomic alignment is parallel to the optical electric field, the light shifts have no effect on the atomic polarization—they merely shift the energies of the bright and dark states relative to each other. However, when the magnetic field along $\hat{\mathbf{z}}$ causes the alignment to precess, the atoms evolve into a superposition of the bright and dark states (which are split by the light shifts), so optical-electric-field-induced quantum beats occur. These quantum beats produce atomic orientation along $\hat{\mathbf{z}}$ (appearing in the second plot and growing in the third plot), causing optical rotation due to circular birefringence.

The atomic orientation produced by AOC is proportional to the torque $\overline{(\mathbf{P} \times \boldsymbol{\mathcal{E}})}$, where $\mathbf{P}$ is the macroscopic induced electric-dipole moment [Eq. (7)], and the bar indicates averaging over a light cycle.[26] The quantity $\overline{(\mathbf{P} \times \boldsymbol{\mathcal{E}})}$ is proportional to the light shift, which has an antisymmetric dependence on detuning of the light from the atomic resonance. Thus (in the Doppler-free case),

---

[25]In the "transit effect," at low light power, this time is the atoms' time of flight between pumping and probing, either within one laser beam (Sec. VIII.A) or between two (Sec. VIII.C). In the "wall-induced Ramsey effect," atoms leave the laser beam after optical pumping and travel about the cell, returning to the beam after colliding with the antirelaxation-coated cell walls (Sec. VIII.E). The relaxation time is thus ultimately determined by collisional relaxation and spin exchange.

---

[26]$\mathbf{P}$ is not collinear with $\boldsymbol{\mathcal{E}}$ due to the presence of the magnetic field. Note also that since $\overline{(\mathbf{P} \times \boldsymbol{\mathcal{E}})}$ is linear in $\mathbf{B}$ (at sufficiently small magnetic fields), it is a T-odd pseudovector, as orientation should be.

net orientation can only be produced when light is detuned from resonance. This is in contrast to NMOR at low light powers, which is maximum when light is tuned to the center of a Doppler-free resonance.

It turns out that in applications to magnetometry (Sec. XII.A), the light power for which optimum magnetometric sensitivity is obtained is sufficient to produce significant AOC, so this effect is important for understanding the properties of an NMOR-based magnetometer. For example, if two atomic species (e.g., Rb and Cs) are employed in an NMOR-based magnetometer, AOC generates a longitudinal spin polarization. Spin-exchange collisions can then couple the polarizations of the two atomic species. [Related AOC-induced coupling of polarization of different ground-state hfs components in ^{85}Rb was studied by Yashchuk, Mikhailov, *et al.* (1999).]

Although the phenomenon of alignment-to-orientation conversion has been studied in a variety of different contexts (Lombardi, 1969; Pinard and Aminoff, 1982; Hilborn *et al.*, 1994; Dovator and Okunevich, 2001; Kuntz *et al.*, 2002), its role in NMOE was only recently recognized by Okunevich (2000) and Budker, Kimball, *et al.* (2000a). However, as is usual with "new" phenomena, a closely related discussion can be found in the classic literature (Cohen-Tannoudji and Dupont-Roc, 1969).

VI. SYMMETRY CONSIDERATIONS IN LINEAR AND NONLINEAR MAGNETO-OPTICAL EFFECTS

The interaction of light with a dielectric medium is characterized by the electric polarizability of the medium, which may be equivalently described by various frequency-dependent complex parameters: the electric susceptibility (χ), the dielectric permittivity (ε), and the index of refraction ($\tilde{n}$). The imaginary parts of these quantities determine light absorption by the medium, while their real parts describe the dispersion, i.e., the phase shifts that a light wave traversing the medium experiences. For isotropic media, the above parameters are scalar quantities and the interaction of the medium with light is independent of the light polarization. In anisotropic media, the interaction parameters are tensors, and the incident optical field and the induced electric polarization are no longer parallel to each other. The induced polarization acts as a source of a new optical field with a polarization (and amplitude) that differs from the incident field and that adds coherently to this field as light propagates through the medium. This leads to macroscopic phenomena such as dichroism and birefringence. Thus linear and nonlinear magneto-optical effects in vapors can be regarded as the result of the symmetry breaking of an initially isotropic medium due to its interaction with an external magnetic field, and for the nonlinear effects, intense polarized light.

An incident-light field propagating along **k** can be written as a superposition of optical eigenmodes (i.e., waves that traverse the medium without changing their state of polarization, experiencing only attenuation and phase shifts) determined by the symmetry properties of the medium. Suppose that the medium is symmetric about **k** and that the light is weak enough so that it does not affect the optical properties of the medium. Then there is no preferred axis orthogonal to **k**, so the optical eigenmodes must be left- and right-circularly polarized waves. If, in addition, the medium has the symmetry of an axial vector directed along **k** (generated, for example, by a magnetic field in the Faraday geometry), the symmetry between the two eigenmodes is broken, and the medium can cause differential dispersion of the eigenmodes (circular birefringence) leading to optical rotation, as well as differential absorption (circular dichroism) causing the light to acquire elliptical polarization (Fig. 1).

If the medium does possess a preferred axis orthogonal to **k** (generated, for example, by a magnetic field in the Voigt geometry), the eigenmodes must be fields linearly polarized along and perpendicular to the preferred axis. There is clearly asymmetry between the two eigenmodes; the medium possesses linear birefringence and dichroism.[27] Since changing the sign of the magnetic field does not reverse the asymmetry between the eigenmodes, there should be no magneto-optical effects that are linear in the applied field. Indeed, the lowest-order Voigt effect is proportional to B^2.

If the light field is strong enough to alter the medium susceptibility, it imposes the symmetry of the optical field onto the medium, i.e., if the light is linearly polarized, the eigenmodes are linearly polarized waves. In the absence of a magnetic field, the input light field is an eigenmode, and no rotation or ellipticity is induced. However, if a weak magnetic field is present (and the light field is not too strong), it effectively rotates the axis of symmetry of the medium, changing the polarization of the eigenmodes. The input light field is no longer an eigenmode, and rotation can occur. At high light powers, the combined optical and magnetic fields cause a more complicated evolution to occur (Sec. V.C).

Consideration of the symmetry of the medium can be used to choose the quantization axis that is most convenient for the theoretical description of a particular effect. The choice of orientation of the quantization axis is in principle arbitrary, but in many situations calculations can be greatly simplified when the quantization axis is chosen along one of the symmetry axes of the system. Thus for the linear Faraday and Voigt effects, a natural choice is to orient $\hat{\mathbf{z}}$ parallel to the magnetic field. For nonlinear effects with low-power linearly polarized light, on the other hand, it may be advantageous to choose the quantization axis along the light polarization direction.

VII. THEORETICAL MODELS

The first theoretical treatment of nonlinear magneto-optical effects was performed by Giraud-Cotton *et al.*

---

[27]The effect of deflection of a linearly polarized light beam by a medium with a transverse axial symmetry was discussed in detail in Sec. II.D.2.

(1980, 1982a, 1982b, 1985a, 1985b), who obtained expressions to lowest order in the Rabi frequency (atom-light coupling) for the nonlinear Faraday effect. In this perturbative approach NMOR is viewed as a $\chi^{(3)}$ process (Sec. III.A), and the NMOR angle is hence proportional to the light intensity. Although the model presented by Giraud-Cotton *et al.* is valid for arbitrary angular momenta, it cannot be directly applied to alkali atoms, because it considers only open systems, i.e., two-level atoms with Zeeman substructure in which the excited states decay to external levels. For alkali atoms under monochromatic excitation, repopulation and hyperfine pumping effects have to be taken into account (only depopulation effects were considered by Giraud-Cotton *et al.*). Chen (1989) and Chen *et al.* (1990) applied the perturbation method developed by Drake (1986; Drake *et al.*, 1988) for $F=1 \rightarrow F'=0$ transitions to the multilevel case of Cs. They extended the results obtained by Giraud-Cotton *et al.* by including repopulation effects, i.e., the transfer of coherences from the excited state into the ground state by fluorescence, allowing the first quantitative comparison of theoretical predictions with experimental data. The agreement was only partially satisfactory, since hyperfine pumping processes were not properly treated—the important role they played was not realized at the time. These processes were later properly included in a calculation by Kanorsky *et al.* (1993; see Sec. VII.A), which turned out to be extremely successful for the description of the coherence NMOE at low light powers.

The steady-state density-matrix equations for a transition subject to light and a static magnetic field (Cohen-Tannoudji, 1975) can be solved nonperturbatively to obtain a theoretical description of the transit, Bennett-structure, and linear effects for arbitrary light power. This was done for systems consisting of two states with low angular momentum ($F,F'=0,1/2,1$) by Davies *et al.* (1987), Schuller *et al.* (1987), Izmailov (1988), Baird *et al.* (1989), Kozlov (1989), Schuller *et al.* (1989), Fomichev (1991), Holmes and Griffith (1995), Schuller *et al.* (1995), and Schuller and Stacey (1999). Good qualitative agreement with experiments in samarium was demonstrated by Davies *et al.* (1987), Baird *et al.* (1989), Kozlov (1989), and Zetie *et al.* (1992). The nonperturbative approach was generalized by Rochester *et al.* (2001) to systems with hyperfine structure for calculation of self-rotation (Sec. XIII.C) in Rb. This method (discussed in Sec. VII.B) was applied to Faraday rotation calculations, and quantitative agreement with experiment was demonstrated (Budker, Kimball, *et al.*, 2000a, 2002a).

A. Kanorsky-Weis approach to low-power nonlinear magneto-optical rotation

Quantitative agreement between theory and experiment for nonlinear magneto-optical effects was achieved by Kanorsky *et al.* (1993), who calculated Faraday rotation assuming both a weak magnetic field and low light power. Under these conditions, the Bennett-structure effects (Sec. V.A) and linear effects (Sec. II.A), as well as saturation effects and alignment-to-orientation conversion (Sec. V.C) are negligible. With these approximations, and with an appropriate choice of quantization axis (Sec. VI), it is possible to perform the calculation making no explicit use of sublevel coherences. Optical pumping rate equations for the sublevel populations are solved, neglecting the effect of the magnetic field, and then precession due to the magnetic field is taken into account. This procedure is a quantitative version of the description of the coherence NMOE as a three-stage process (Sec. V.B).

As described by Kanorsky *et al.* (1993), the complex index of refraction for light of frequency ω and polarization $\hat{\mathbf{e}}$ can be written in terms of level populations:

$$\tilde{n}-1 = \frac{2\pi}{\hbar} \sum_{M,M'} \rho_{FM} \frac{|\langle F'M'|\hat{\mathbf{e}}\cdot\mathbf{d}|FM\rangle|^2}{\Delta - i\gamma_0}, \tag{15}$$

where $\mathbf{d}$ is the electric dipole operator, Δ is the light frequency detuning from resonance, and ρ_{FM} are the ground-state Zeeman-sublevel populations. The rotation angle is given by

$$\varphi = \text{Im}(\tilde{n}_\parallel - \tilde{n}_\perp) \frac{\omega l}{2c} \sin 2\theta, \tag{16}$$

where l is the sample length and θ is the average orientation of the axis of dichroism with respect to the linear polarization. The angle θ is calculated by time-averaging the contributions of individual atoms, each of which precesses in the magnetic field before relaxing at rate γ_t, with the result [cf. Eq. (2)]

$$\varphi = \text{Im}(\tilde{n}_\parallel - \tilde{n}_\perp) \frac{\omega l}{2c} \frac{x}{x^2+1}, \tag{17}$$

where the dimensionless parameter $x = 2g\mu B/(\hbar \gamma_t)$.

B. Density-matrix calculations

This section describes a nonperturbative density-matrix calculation (Budker, Kimball, *et al.*, 2000a, 2002a; Rochester *et al.*, 2001) of NMOE for a transition $\xi J \rightarrow \xi' J'$ in the presence of nuclear spin I. Here J is total electronic angular momentum, and ξ represents additional quantum numbers.

The calculation is carried out in the collision-free approximation and assumes that atoms outside the volume of the laser beam are unpolarized. Thus the calculation is valid for an atomic beam or a cell without antirelaxation wall coating containing a low-density vapor. It is also assumed that light is of a uniform intensity over an effective area and that the passage of atoms through the laser beam can be described by one effective relaxation rate γ_t.

The time evolution of the atomic density matrix ρ is given by the Liouville equation (see discussion by, for example, Stenholm, 1984):

$$\frac{d\rho}{dt} = \frac{1}{i\hbar}[H,\rho] - \frac{1}{2}\{\Gamma_R,\rho\} + \Lambda, \tag{18}$$

where the square brackets denote the commutator and the curly brackets the anticommutator. The total Hamiltonian H is the sum of the light-atom interaction Hamiltonian $H_L = -\mathbf{d} \cdot \boldsymbol{\mathcal{E}}$ (where $\boldsymbol{\mathcal{E}}$ is the electric-field vector, and $\mathbf{d}$ is the electric dipole operator), the magnetic-field–atom interaction Hamiltonian $H_B = -\boldsymbol{\mu} \cdot \mathbf{B}$ (where $\mathbf{B}$ is the magnetic field and $\boldsymbol{\mu}$ is the magnetic moment), and the unperturbed Hamiltonian H_0. The Hamiltonian due to interaction with a static electric field can also be included if necessary. Γ_R is the relaxation matrix (diagonal in the collision-free approximation),

$$\langle \xi J F M | \Gamma_R | \xi J F M \rangle = \gamma_t,$$

$$\langle \xi' J' F' M' | \Gamma_R | \xi' J' F' M' \rangle = \gamma_t + \gamma_0. \quad (19)$$

$\Lambda = \Lambda^0 + \Lambda^{repop}$ is the pumping term, where the diagonal matrix

$$\langle \xi J F M | \Lambda^t | \xi J F M \rangle = \frac{\gamma_t \rho_0}{(2I+1)(2J+1)} \quad (20)$$

describes incoherent ground-state pumping (ρ_0 is the atomic density), and

$$\langle \xi J F M_1 | \Lambda^{repop} | \xi J F M_2 \rangle$$

$$= \gamma_0 \sum_{F'} (2J'+1)(2F+1) \begin{Bmatrix} J & F & I \\ F' & J' & 1 \end{Bmatrix}^2$$

$$\times \sum_{M_1', M_2', q} \langle J, M_1, 1, q | J', M_1' \rangle$$

$$\times \langle J, M_2, 1, q | J', M_2' \rangle \rho_{\xi' J' F' M_1', \xi' J' F' M_2'} \quad (21)$$

describes repopulation due to spontaneous relaxation from the upper level (see, for example, the discussion by Rautian and Shalagin, 1991). Here $\langle \cdots | \cdots \rangle$ are the Clebsch-Gordan coefficients and the curly brackets represent the six-J symbol. A solution for the steady-state density matrix can be found by applying the rotating-wave approximation and setting $d\rho/dt = 0$. For the alkali-atom D lines, one can take advantage of the well-resolved ground-state hyperfine structure by treating transitions arising from different ground-state hyperfine sublevels separately and then summing the results.

The electric-field vector is written (see discussion by, for example, Huard, 1997)

$$\boldsymbol{\mathcal{E}} = \frac{1}{2}[\mathcal{E}_0 e^{i\phi}(\cos\varphi\cos\epsilon - i\sin\varphi\sin\epsilon)e^{i(\omega t - kz)} + \text{c.c.}]\hat{\mathbf{x}}$$

$$+ \frac{1}{2}[\mathcal{E}_0 e^{i\phi}(\sin\varphi\cos\epsilon + i\cos\varphi\sin\epsilon)e^{i(\omega t - kz)} + \text{c.c.}]\hat{\mathbf{y}}, \quad (22)$$

where ω is the light frequency, $k = \omega/c$ is the vacuum wave number, $\mathcal{E}_0$ is the electric-field amplitude, φ is the polarization angle, ϵ is the ellipticity (arc tangent of the ratio of the major and minor axes of the polarization ellipse), and ϕ is the overall phase (the field can also be written in terms of the Stokes parameters; see Appendix A). By substituting Eq. (22) into the wave equation

$$\left(\frac{\omega^2}{c^2} + \frac{d^2}{dz^2}\right)\boldsymbol{\mathcal{E}} = -\frac{4\pi}{c^2}\frac{d^2}{dt^2}\mathbf{P}, \quad (23)$$

where $\mathbf{P} = \mathrm{Tr}\rho\mathbf{d}$ is the polarization of the medium, one can find the rotation, absorption, phase shift, and change of ellipticity per unit distance for an optically thin medium in terms of the density-matrix elements:

$$\frac{d\varphi}{dz} = -\frac{2\pi\omega}{\mathcal{E}_0 c}\sec 2\epsilon[\cos\varphi(P_1\sin\epsilon + P_4\cos\epsilon)$$

$$+ \sin\varphi(-P_2\cos\epsilon + P_3\sin\epsilon)], \quad (24a)$$

$$\frac{d\mathcal{E}_0}{dz} = -\frac{2\pi\omega}{c}[\sin\varphi(-P_1\sin\epsilon + P_4\cos\epsilon)$$

$$+ \cos\varphi(P_2\cos\epsilon + P_3\sin\epsilon)], \quad (24b)$$

$$\frac{d\phi}{dz} = -\frac{2\pi\omega}{\mathcal{E}_0 c}\sec 2\epsilon[\cos\varphi(P_1\cos\epsilon + P_4\sin\epsilon)$$

$$+ \sin\varphi(-P_2\sin\epsilon + P_3\cos\epsilon)], \quad (24c)$$

$$\frac{d\epsilon}{dz} = \frac{2\pi\omega}{\mathcal{E}_0 c}[\sin\varphi(P_1\cos\epsilon + P_4\sin\epsilon)$$

$$+ \cos\varphi(P_2\sin\epsilon - P_3\cos\epsilon)], \quad (24d)$$

where the components of polarization are defined by

$$\mathbf{P} = \frac{1}{2}[(P_1 - iP_2)e^{i(\omega t - kz)} + \text{c.c.}]\hat{\mathbf{x}}$$

$$+ \frac{1}{2}[(P_3 - iP_4)e^{i(\omega t - kz)} + \text{c.c.}]\hat{\mathbf{y}}. \quad (25)$$

Since we neglect collisions between atoms, the solutions for a Doppler-free medium can be generalized to the case of Doppler broadening by simply convolving the calculated spectra with a Gaussian function representing the velocity distribution. In addition, an integration along the light path can be performed to generalize the thin-medium result to media of arbitrary optical thickness.

Results of such calculations have helped to improve understanding of various effects discussed throughout this review (see, for example, Figs. 10 and 15).

VIII. NONLINEAR MAGNETO-OPTICAL EFFECTS IN SPECIFIC SITUATIONS

In the preceding sections, we have outlined the basic nonlinear magneto-optical phenomenology and the methods used for theoretical description of these effects. In this section, we discuss the specific features of NMOE in a wide variety of physical situations.

A. Buffer-gas-free uncoated vapor cells

1. Basic features

There have been numerous studies of nonlinear magneto optical rotation in buffer-gas-free vapor cells without antirelaxation coating (by, for example, Barkov *et al.*, 1989a; Kanorsky *et al.*, 1993; Budker, Kimball,
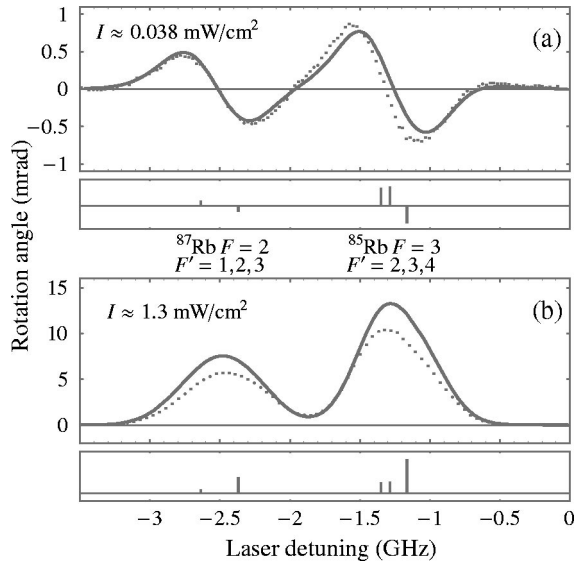
FIG. 15. Comparison of experimental NMOR spectra obtained by Budker *et al.* (2000a) to density-matrix calculations performed in the same work for a natural mixture of Rb isotopes contained in an uncoated buffer-gas-free vapor cell. Solid curves, theory (without free parameters). Offset vertical bars indicate the central frequencies and calculated relative contributions of different hyperfine components ($F \rightarrow F'$) to the overall rotation. Laser detuning is relative to the $D2$ line center. Magnetic field is ~ 0.1 G (at which NMOR is relatively large and coherence effects dominate), laser beam diameter is ~ 3.5 mm, and Rb density is $\sim 10^{10}$ cm^{-3}. Residual discrepancies between data and theory may be due to nonuniform spatial distribution of light intensity. Note that at low light power (a), the sign of rotation for $F \rightarrow F+1$ transitions is opposite to that for $F \rightarrow F-1, F$ transitions, whereas at high light power (b) the sign of rotation is the same for all hyperfine transitions. From Budker, Kimball, *et al.*, 2000a.

et al., 2000a, and references therein). In alkali-atom cells at room temperature, the atomic density is low enough so that the mean free path of the atoms is orders of magnitude larger than the cell dimensions. In addition, because collisions with the walls of the cell destroy atomic polarization, atoms entering the light beam are unpolarized. In such cells, the coherence NMOR (Sec. V.B) is due to the "transit effect"—the pumping, precession, and subsequent probing of atoms during a single pass through the laser beam [Bennett-structure-related NMOR (Sec. V.A) can also be observed in these cells]. Only the region illuminated by the light beam need be considered in a calculation, and the relaxation rate of atomic coherence is determined by the transit time of atoms through the beam. Since velocity-changing collisions rarely occur, the atoms have a constant velocity as they make a single pass through the light beam. Thus when calculating NMOR spectra (Sec. VII), averaging over the atomic velocity distribution is equivalent to averaging over the Doppler-free spectral profiles. At sufficiently low light power, the coherence transit effect is well described by the Kanorsky-Weis model (Sec. VII.A). At higher light powers, where saturation effects and the alignment-to-orientation conversion effect (Sec.

V.C) are important, a density-matrix approach (Sec. VII.B) can be used to describe both the coherence and Bennett-structure effects in uncoated cells.

In addition to being many orders of magnitude greater for small fields, NMOR can have a considerably different spectrum from that of linear magneto-optical rotation (Sec. II). One of the signature features of the low-light-power NMOR transit effect is the dependence of the sign of optical rotation on the nature of the transition (Fig. 15). The sign of optical rotation for $F \rightarrow F-1, F$ transitions is opposite to that for closed $F \rightarrow F+1$ transitions (for ground states with the same Landé factors). This is because linearly polarized light resonant with $F \rightarrow F-1, F$ transitions pumps atoms into an aligned dark state (see Sec. V B), while atoms are pumped on $F \rightarrow F+1$ transitions into a bright state which interacts with the light field more strongly (Kazantsev *et al.*, 1984). Thus, when the magnetic field causes the ground-state alignment to precess, the transmission of light polarized along the initial axis of light polarization decreases for $F \rightarrow F-1, F$ transitions, and increases for $F \rightarrow F+1$ transitions. By considering the "rotating polarizer" model (Fig. 13), one can see that the sign of rotation is opposite in the two cases (for an $F \rightarrow F+1$ transition, the initial "polarizer" is crossed with the light polarization). At higher light powers at which alignment-to-orientation conversion becomes the dominant mechanism for NMOR (Sec. V.C), the sign of optical rotation is the same for all types of transitions.

2. Peculiarities in the magnetic-field dependence

All theories described in the literature predicted the shape of the $\varphi(B)$ dependence of the NMOR transit effect signal to be a dispersive Lorentzian [Eq. (17)], linear near the zero crossing at $B=0$. However, experimental measurement of $\varphi(B)$ for small B by Chen (1989) revealed a slight deviation from this anticipated behavior: the signal had a higher than expected derivative at $B=0$.

This observation was eventually explained as follows. The shape of $\varphi(B)$ was expected to be Lorentzian as a consequence of an assumed exponential relaxation of atomic coherences in time. In room-temperature buffer-gas-free vapor cells, however, the width of the NMOR resonance was determined by the *effective* relaxation due to the finite interaction time of the pumped atoms with the light beam. The nonexponential character of this effective relaxation led to the observed discrepancy. The simplicity of the theoretical model of the NMOR transit effect developed by Kanorsky *et al.* (Sec. VII.A) allowed them to treat these time-of-flight effects quantitatively by averaging over the Gaussian-distributed light beam intensity and the Maxwellian velocity distribution. Their approach produced quasianalytical expressions for $\varphi(B)$ which were beautifully confirmed in an experiment by Pfleghaar *et al.* (1993).

3. Nonlinear magneto-optical effects in optically thick vapors

For a given medium used in studies of near-resonant nonlinear magneto-optical effects, the optimum optical thickness depends on the light power employed; if most of the light is absorbed upon traversal of the medium, there is a loss in statistical sensitivity. At low light power, when the saturation parameter κ (Sec. III.B) is not much greater than unity, it is generally useful to use samples of no more than a few absorption lengths. However, at high light powers, the medium may bleach due to optical pumping, and greater optical thicknesses may be used to enhance the NMOE without unduly compromising statistical sensitivity. Nonlinear Faraday rotation produced by a optically thick vapor of rubidium was studied by Sautenkov *et al.* (2000), Matsko, Novikova, *et al.* (2001), Novikova *et al.* (2001b), and Novikova and Welch (2002). Novikova *et al.* (2001b) used a 5-cm-long vapor cell containing ^{87}Rb and a 2.5-mW, 2-mm-diameter laser beam tuned to the maximum of the NMOR $D1$-line spectrum. They measured maximum polarization rotation φ_{max} (with respect to laser frequency and magnetic field) as a function of atomic density. It was found that φ_{max} increases essentially linearly up to $n \approx 3.5 \times 10^{12}$ cm^{-3}. At higher densities, $d\varphi_{max}/dn$ decreases and eventually becomes negative. The maximum observed rotation, ~ 10 rad, was obtained with magnetic field ~ 0.6 G. (This shows the effect of power broadening on the magnetic-field dependence; at low light power, the maximum rotation would occur at a magnetic field about an order of magnitude smaller.)

A model theory of NMOR in optically thick media, accounting for the change in light power and polarization along the light path and for the high-light-power effects (see Sec. V.C), was developed by several authors (e.g., Matsko, Novikova, and Welch, 2002; Rochester and Budker, 2002, and references therein). However, a complete theoretical description of NMOR in dense media must also consider radiation trapping of photons spontaneously emitted by atoms interacting with the laser light. Matsko, Novikova, *et al.* (2001) and Matsko, Novikova, and Welch (2002) concluded that for densities such that the photon absorption length is comparable to the smallest dimension of the cell, radiation trapping leads to an increase in the effective ground-state relaxation rate.

B. Time-domain experiments

In many nonlinear magneto-optical experiments, the same laser beam serves as both pump and probe light. More complex experiments use separate pump and probe beams that can have different frequencies, spatial positions, directions of propagation, polarizations, and/or temporal structures. A wealth of pump-probe experimental techniques in the time and frequency domains have been developed, including spin nutation, free-induction decay, spin echoes, coherent Raman beats or Raman heterodyne spectroscopy, to name just a few.[28] In this section, we give an example of an experiment in the time domain; in Sec. VIII.C, we discuss frequency domain experiments with spatially separated light fields.

Zibrov *et al.* (2001) and Zibrov and Matsko (2002) applied two light pulses to a ^{87}Rb vapor in sequence, the first strong and linearly polarized and the second weak and circularly polarized. A particular elliptical polarization of the transmitted light from the second pulse was detected. When a longitudinal magnetic field was applied to the cell, the resulting intensity displayed oscillations (within the duration of the probe pulse) at twice the Larmor frequency. The authors interpreted these experiments in terms of Raman scattering of the probe light from atoms with coherent Zeeman-split lower-state sublevels.

Here we point out that the "rotating polarizer" picture of coherence NMOR discussed in Sec. V.B can be used to provide an equivalent description of these experiments. The linearly polarized pump pulse induces alignment and corresponding linear dichroism of the atomic medium, i.e., it prepares a polaroid out of the medium. The polaroid proceeds to rotate at the Larmor frequency in the presence of the magnetic field. Circularly polarized probe light incident on such a rotating polaroid produces linearly polarized light at the output whose polarization plane rotates at the same frequency. This is the same as saying there are two circularly polarized components with a frequency offset.

C. Atomic beams and separated light fields, Faraday-Ramsey spectroscopy

In the coherence effects (Sec. V.B), the resonance width is determined by the relaxation rate of ground-state polarization. In the transit effect, in particular, this relaxation rate is given by the time of flight of atoms between optical pumping and probing. When one laser beam is used for both pumping and probing, this time can be increased, narrowing the resonance, by increasing the diameter of the beam. Another method of increasing the transit time, however, is to use two beams, spatially separating the pump and probe regions. For this technique, the model (Sec. V.B) of the coherence effects in terms of three sequential steps (pumping, precession, probing) becomes an exact description.

As this experimental setup (Fig. 16) bears some similarities to the conventional Ramsey arrangement (see Sec. VIII.C.3), and as the coherence detection in the probe region involves polarimetric detection of polarization rotation, this technique is called *Faraday-Ramsey spectroscopy*.

---

[28]For a detailed discussion, we refer the reader to a comprehensive overview of the underlying mechanisms and applications in Suter (1997).
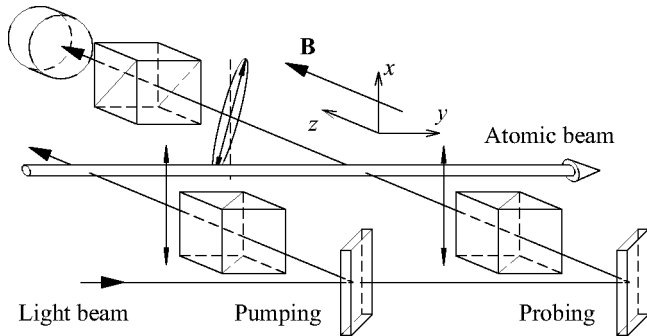
FIG. 16. Faraday rotation technique utilizing separated light beams and an atomic beam. The resonance linewidth is determined by the time of flight between the pump and the probe beams. Variations of this technique include the use of circularly polarized light for both pumping and probing, and the detection of absorption or induced ellipticity instead of polarization rotation.

1. Overview of experiments

Several experiments studying NMOE using spatially separated light fields have been performed, using various detection techniques. The first atomic beam experiment of this sort was performed by Schieder and Walther (1974) with a Na beam using fluorescence detection. Mlynek *et al.* (1988) observed Ramsey fringes in a Sm beam on the 570.68-nm $F=1 \rightarrow F=0$ transition using *Raman heterodyne spectroscopy*, a technique involving application of both light and rf magnetic fields to the atoms (see, for example, Suter, 1997), with light beam separations of up to $L=2.2$ cm. The fringe widths were found to scale as L^{-1} with the beam separation, as anticipated, but signal quality was strongly degraded as L increased (Mlynek *et al.*, 1987).[29]

The first beam experiment with a long (34.5-cm) precession region was done by Theobald *et al.* (1991) using $D2$-line excitation on a Cs beam with fluorescence detection. In similar work, using detection of forward-scattered light rather than fluorescence monitoring, Schuh *et al.* (1993) and Weis, Schuh, *et al.* (1993) applied pump-probe spectroscopy to a Rb beam using $D2$-line excitation. The experiments were performed with interaction lengths of $L=5$ cm (Schuh *et al.*, 1993) and $L=30$ cm (Weis, Schuh, *et al.*, 1993), respectively. Improving the sensitivity by going to longer interaction lengths is difficult because of signal loss due to the finite atomic-

---

[29]Other examples of early work in the field are the work of Bertucceli *et al.* (1986), who used fluorescence detection to observe nonlinear level-crossing Ramsey fringes in a metastable Ca beam, the work of Nakayama *et al.* (1980), who observed Ramsey fringes on the $D1$ line in a Na vapor cell using laser beams separated by up to 10 mm, and an experiment performed by Borghs *et al.* (1984) in the time domain using a monokinetic Ba^+ beam, which showed a large number of higher-order fringes, normally damped in thermal beams due to the large velocity spread. This last experiment determined the ratio of g factors of the $5d\ ^2D_{3/2}$ and $5d\ ^2D_{5/2}$ states of Ba^+.
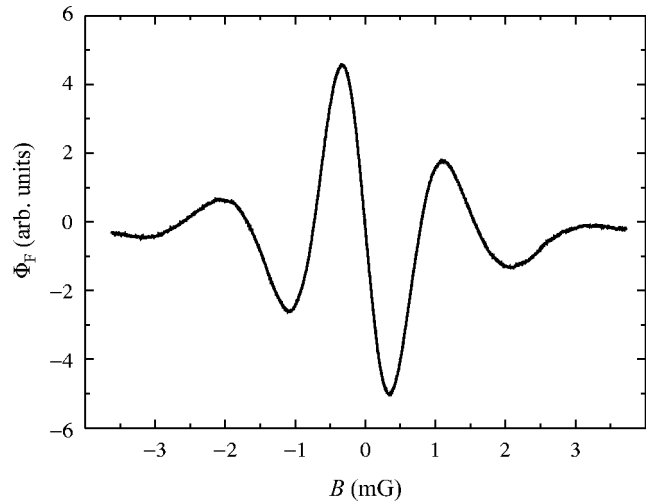
FIG. 17. Experimental Faraday-Ramsey signal from a thermal Cs beam ($T=400$ K) and a precession length of $L=30$ cm. Polarimetric detection of the rotation angle φ of the probe beam is used.

beam divergence. This can be counteracted by laser collimation of the beam (this technique is being used in work towards a 2-m apparatus at the University of Fribourg), or by using atoms that are free-falling from a magneto-optical trap or an atomic fountain (Sec. VIII.H). Hypersonic and laser-slowed beams can also be used to increase the atomic flux and transit time, respectively.

2. Line shape, applications

In Faraday-Ramsey spectroscopy, one measures the magneto-optical rotation angle φ of the linearly polarized probe beam. For a beam with Maxwellian velocity distribution, the magnetic-field dependence of φ is obtained from the three-step model discussed in Sec. V.B in a manner similar to that described in Sec. VII.A:

$$\varphi(B) \propto \int_0^\infty \sin\left(\frac{B}{\mathcal{B}_0^R} \frac{1}{u} + 2\theta_{pp} \right) u^2 e^{-u^2} du, \qquad (26)$$

where θ_{pp} is the relative orientation of the pump and probe polarizations, $u=v/v_0$ is the dimensionless velocity, and v_0 is the most probable velocity in the atomic beam oven, and

$$\mathcal{B}_0^R = \frac{\hbar v_0}{2g\mu L} \qquad (27)$$

is a scaling field (L is the distance between pump and probe beams). The line shape is a damped oscillatory Ramsey fringe pattern centered at $B=0$ (the scaling field $\mathcal{B}_0^R$ is a measure of the fringe width). Figure 17 shows an experimental Faraday-Ramsey spectrum recorded with a thermal Cs beam ($T=400$ K) with a precession region of $L=30$ cm, for which $\mathcal{B}_0^R=170\ \mu$G.

Faraday-Ramsey spectroscopy has proven to be an extremely sensitive tool for investigating spin-coherence

perturbations by magnetic and/or electric[30] fields under collision-free conditions. Any additional external perturbation which affects spin coherence will lead to an additional phase shift in the fringe pattern given by Eq. (26). Faraday-Ramsey spectroscopy has been applied in a variety of situations, including an investigation of the Aharonov-Casher effect in atoms (Sec. XII.C), a precision electric-field calibration (Rasbach *et al.*, 2001), and a measurement of the forbidden electric tensor polarizabilities (Sec. XII.D) of the ground state of Cs (Rasbach *et al.*, 2001; Weis, 2001). Applications of the technique of Faraday-Ramsey spectroscopy with atomic beams to the search for parity- and time-reversal-invariance violation, in particular, for a permanent electric dipole moment (Sec. XII.B), have also been discussed (Schuh *et al.*, 1993; Weis, Schuh, *et al.*, 1993). Note, however, that a competitive electric-dipole-moment experiment would need a very intense optically thick atomic beam, such as the source built for experiments with atomic thallium by DeMille *et al.* (1994).

3. Connection with the Ramsey separated-oscillatory-field method

Faraday-Ramsey spectroscopy is in fact a Ramsey technique (Ramsey, 1990) without oscillating fields. In conventional Ramsey spectroscopy, a spin-polarized beam traverses two identical spatially separated regions in which the particles are exposed to phase-locked radio-frequency magnetic fields $B_1(t)$ oscillating at the same frequency. The whole arrangement is in a homogeneous field B_0. In the first rf region, a $\pi/2$ pulse tips the spins to an orientation perpendicular to B_0. After precessing freely, the spin is projected back onto its original direction in the second region. The rf regions thus play the role of start/stop pulses for the spin precession. The polarization recovered in the second rf region depends on the phase accumulated during the precession. In Faraday-Ramsey spectroscopy, the start pulse is provided by an optical-pumping light pulse (in the atomic frame of reference) which orients the spin so that it can precess, and the weak probe pulse detects the precession angle. In Ramsey spectroscopy, the relative phase ϕ_{rf} of the rf fields determines the symmetry of the fringe pattern (absorptive for $\phi_{rf}=0$, dispersive for $\phi_{rf}=\pi/2$), while in Faraday-Ramsey spectroscopy, this role is played by the relative orientations of the light polarizations θ_{pp}.

D. Experiments with buffer-gas cells

1. Warm buffer gas

Early studies of nonlinear magneto-optical rotation by Davies *et al.* (1987), Baird *et al.* (1989), and Barkov *et al.*

---

[30]Electric interactions do not couple to spin directly; however, they affect the orbital angular momentum. Thus spin coherences are affected by an electric field via spin-orbit and hyperfine interactions.

(1989a) on transitions in Sm showed that nonlinear effects are extremely sensitive to the presence of buffer gas. Bennett-structure-related effects (Sec. V.A) are suppressed when the peaks and holes in the velocity distribution are washed out by velocity-changing collisions. Generally, coherence effects (Sec. V.B) are also easily destroyed by depolarizing buffer-gas collisions. However, a very important exception is effects with atoms with total electronic angular momentum in the ground state $J=1/2$, e.g., the alkali atoms. For such atoms, the cross sections for depolarizing buffer-gas collisions are typically 4–10 orders of magnitude smaller than those for velocity-changing collisions (Walker, 1989; Walker *et al.*, 1997). This suppression allows long-lived ground-state polarization in the presence of buffer gas and also serves to prevent depolarizing wall collisions (Happer, 1972). Recently, coherent dark resonances (Sec. XIII.A) with widths as narrow as 30 Hz were observed by Brandt *et al.* (1997) in Cs and by Erhard *et al.* (2000; Erhard and Helm, 2001) in Rb using neon-buffer-gas vapor cells at room temperature.

Novikova *et al.* (2001a), Zibrov *et al.* (2001), Novikova and Welch (2002), and Zibrov and Matsko (2002) have recently studied NMOE in buffer-gas cells. Spectral line shapes of optical rotation quite different from those seen in buffer-gas-free cells and atomic beams were observed (Novikova *et al.*, 2001a). This effect, discussed in Sec. VIII.E.1, is due to velocity-changing collisions and was previously observed by Budker *et al.* (2000b) in paraffin-coated cells. Novikova *et al.* (2002) proposed the use of the dependence of the NMOR spectral line shape on buffer gas to detect the presence of small amounts of impurities in the resonant medium.

2. Cryogenic buffer gas

Cold-buffer-gas systems are currently under investigation by Hatakeyama *et al.* (2000, 2002), Kimball *et al.* (2001), and Yashchuk, Sushkov, *et al.* (2002) as a method of reducing collisional relaxation. At low temperatures, atomic collisions approach the S-wave scattering regime, in which spin relaxation is suppressed. Theoretical estimates of spin relaxation in spin-rotation interactions by Sushkov (2001), based on the approach of Walker *et al.* (1997), suggest that for the Cs-He case, a reduction of the relaxation cross section from its room-temperature value by a factor of ~ 20–50 may be expected at liquid-nitrogen temperatures. Recently, Hatakeyama *et al.* (2000) showed experimentally that at temperatures below ~ 2 K, the spin relaxation cross section of Rb atoms in collisions with He-buffer-gas atoms is orders of magnitude smaller than its value at room temperature. The results of Hatakeyama *et al.* imply that relaxation times of minutes or even longer (corresponding to resonance widths on the order of 10 mHz) can be obtained. Such narrow resonances may be applied to atomic tests of discrete symmetries (Sec. XII.B) and to very sensitive measurements of magnetic fields (Sec. XII.A).

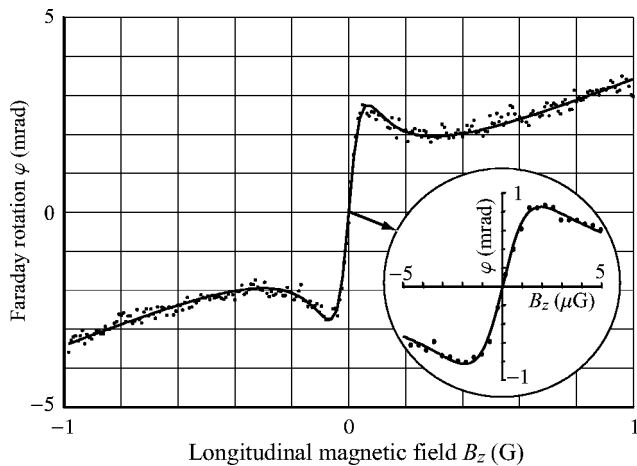The crucial experimental challenge with these systems is creating, in the cold buffer gas, atomic vapor densities

FIG. 18. Longitudinal magnetic-field dependence of optical rotation in a paraffin-coated ^{85}Rb-vapor cell. The background slope is due to the Bennett-structure effect. The dispersionlike structure is due to the transit effect. The inset shows the near-zero B_z-field behavior at a 2×10^5 magnification of the magnetic-field scale. Light intensity is $\sim 100\ \mu W\,cm^2$. The laser is tuned ~ 150 MHz to the high-frequency side of the $F = 3 \rightarrow F'$ absorption peak. From Budker, Yashchuk, and Zolotorev, 1998a.

comparable to those of room-temperature experiments, i.e., on the order of $10^{10}–10^{12}$ cm^{-3}. To accomplish this, Hatakeyama *et al.* use light-induced desorption of alkali atoms from the surface of the liquid He film inside their cell [this is presumably similar to light-induced desorption observed with antirelaxation coatings of siloxane (by, for example, Atutov *et al.*, 1999) and paraffin (Kimball *et al.*, 2001; Alexandrov *et al.*, 2002)]. Hatakeyama *et al.* can successfully[31] inject Rb atoms into the He gas by irradiating the cell with about 200 mW of (750-nm) Ti:sapphire laser radiation for 10 s. Yashchuk, Sushkov, *et al.* (2002) are exploring a significantly different method of injecting atoms into cold He buffer gas—laser evaporation of micron-sized droplets falling through the gas (see also discussion by Kimball *et al.*, 2001).

E. Antirelaxation-coated cells

Antirelaxation-coated cells provide long spin-relaxation times due to the greatly reduced rate of depolarization in wall collisions. Three nonlinear effects can be observed "nested" in the magnetic-field dependence of NMOR produced by such a cell (Fig. 18). The widest feature is due to the Bennett-structure effect (Sec. V.A), followed by the feature due to the transit effect, which also occurs in uncoated cells (Sec. VIII.A). The narrowest feature is due to the wall-induced Ram-

___

[31]It turns out that the injection efficiency decreases with repetitions of the injection cycle. It is found that the efficiency recovers when the cell is heated to room temperature and then cooled again. Hatakeyama *et al.* (2002) report that they cannot inject Cs atoms with their method.

sey effect, a variant of the separated-field transit effect in which atoms leave the light beam after being optically pumped and are later probed after colliding with the cell walls and returning to the beam.

1. Experiments

In their early work on optical pumping, Robinson *et al.* (1958) showed that by coating the walls of a vapor cell with a chemically inert substance such as paraffin (chemical formula C_nH_{2n+2}), the relaxation of atomic polarization due to wall collisions could be significantly reduced.

Recently, working with a paraffin-coated Cs vapor cell, Kanorskii *et al.* (1995) discovered a narrow feature (of width ~ 1 mG) in the magnetic-field dependence of Faraday rotation. Kanorskii *et al.* (1995) described the feature as a Ramsey resonance induced by multiple wall collisions.[32] In antirelaxation-coated cells, the precession stage of the three-step coherence-effect process (Sec. V.B) occurs after the atom is optically pumped and then leaves the light beam. The atom travels about the cell, undergoing many—up to 10^4 [Bouchiat and Brossel (1966); Alexandrov and Bonch-Bruevich (1992); Alexandrov *et al.* (1996)]—velocity-changing wall collisions before it flies through the light beam once more and the probe interaction occurs. Thus the time between pumping and probing can be much longer for the wall-induced Ramsey effect than for the transit effect (Sec. VIII.A), leading to much narrower features in the magnetic-field dependence of NMOR.

Budker, Yashchuk, and Zolotorev (1998a) performed an investigation of the wall-induced Ramsey effect in NMOR using Rb atoms contained in paraffin-coated cells (Alexandrov *et al.*, 1996). The apparatus employed in these investigations is discussed in detail in Sec. XI.A. Budker, Yashchuk, and Zolotorev (1998a) observed ~ 1-μG-width features in the magnetic-field dependence of NMOR (Fig. 18).

Budker *et al.* (2000b) investigated the dependence on atomic density and light frequency and intensity of NMOR due to the wall-induced Ramsey effect. The NMOR spectra for the wall-induced Ramsey effect were found to be quite different from those for the transit effect (Fig. 19). In the wall-induced Ramsey effect, atoms undergo many velocity-changing collisions between pump and probe interactions. When Doppler-broadened hyperfine transitions overlap, it is possible for the light to be resonant with one transition during pumping and another transition during probing. Both the ground-state polarization produced by optical pumping and the effect on the light of the atomic polarization that has evolved in the magnetic field depend on the nature of the tran-

___

[32]It is interesting to note that Ramsey himself (Kleppner, Ramsey, and Fjelstadt, 1958), in order to decrease the resonance widths in experiments with separated oscillatory fields, constructed a "storage box" with Teflon-coated walls in which atoms would bounce around for a period of time before emerging to pass through the second oscillatory field.
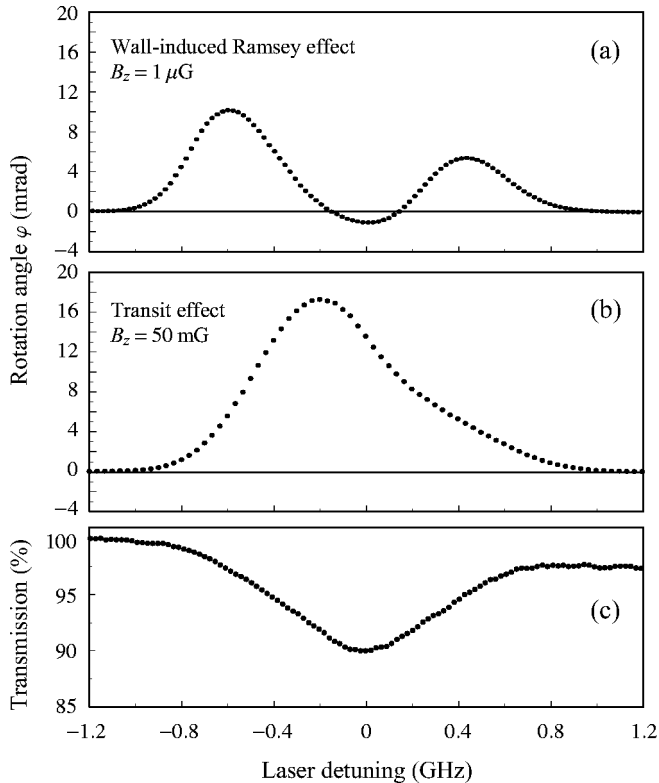
FIG. 19. Comparison of transit effect and wall-induced Ramsey effect spectra: (a) Wall-induced Ramsey rotation spectrum for the $F=3 \rightarrow F'$ component of the $D1$ line of ^{85}Rb obtained by Budker, Kimball, *et al.* (2000b) for light intensity 1.2 mW cm^{-2} and beam diameter ~ 3 mm. (b) Transit effect rotation spectrum, for light intensity 0.6 mW cm^{-2}. (c) Light transmission spectrum for light intensity 1.2 mW cm^2. Background slope in light transmission is due to change in incident laser power during the frequency scan. From Budker, Kimball, *et al.*, 2000b.

sition. For the $F=3 \rightarrow F'=2,3$ component of the ^{85}Rb $D1$ line, the contribution to optical rotation from atoms pumped and probed on different transitions has opposite sign to that from atoms pumped and probed on the same transition. Thus the wall-induced Ramsey NMOR spectrum consists of two peaks, since the contributions to optical rotation nearly cancel at the center of the Doppler profile. In the transit effect for buffer-gas-free cells, in contrast, atoms remain in a particular velocity group during both optical pumping and probing. The transit-effect spectrum has a single peak because for each atom light is resonant with the same transition during both pumping and probing.

Budker *et al.* (2000b) also found that at the light intensity and frequency at which highest magnetometric sensitivity is achieved, the sign of optical rotation is opposite to that obtained for the low-light-power transit effect. Budker *et al.* (2000a) explained this as the effect of alignment-to-orientation conversion (Sec. V.C) due to the combined action of the optical electric field and the magnetic field.

Skalla and Waeckerle (1997) studied the wall-induced Ramsey effect in cells with various geometries (cylindri-

cal, spherical, and toroidal), and used spatially separated pump and probe fields to measure Berry's topological phase (Berry, 1984). Yashchuk, Mikhailov, *et al.* (1999) investigated the possibilities of applying the separated optical field method to improve the sensitivity of NMOR-based magnetometers (Sec. XII.A).

In addition to their application in precision magnetometry, NMOE in paraffin-coated cells were investigated in relation to tests of fundamental symmetries (Sec. XII.B) and the study of light propagation dynamics (Sec. XIII.B).

2. Theoretical analysis

In order to obtain a theoretical description of nonlinear magneto-optic effects in paraffin-coated cells, one must extend the density-matrix calculation of Sec. VII.B to describe both the illuminated and nonilluminated regions of the cell, as well as the effects of velocity mixing and spin exchange. Expressions for the effect of alkali-alkali spin exchange on the density matrix have been obtained by Okunevich (1994, 1995), and Valles and Alvarez (1994, 1996), following work of Grossetete (1965). When atomic orientation is nonzero, the expressions become nonlinear; however, even under conditions in which alignment-to-orientation conversion (Sec. V.C) is important for optical rotation, the total sample orientation can be small enough for linearized spin-exchange equations to be applied. Taking velocity mixing and multiple cell regions into account is straightforward but computationally intensive. A detailed description of such a calculation and comparison with experiment is in preparation by Budker and co-workers.

F. Gas discharge

Gas discharge allows one to study ionized species, refractory materials, and transitions originating from metastable states, and has been extensively used in atomic spectroscopy and polarization studies in particular [see, for example, Lombardi (1969); Aleksandrov and Kulyasov (1972)].

In *optogalvanic spectroscopy* one detects light-induced transitions by measuring the changes in conductivity of a discharge. The optogalvanic method has been applied to the study of nonlinear level crossing and other NMOE (Hannaford and Series, 1981; Stahlberg *et al.*, 1989).

Other examples of NMOE work employing gas discharge include the study of Lowe *et al.* (1987), who used Zeeman quantum beats in transmission (i.e., time-dependent NMOR; see Sec. VIII.B) in a pulsed-pump, cw-probe experiment to determine polarization-relaxation properties of a Sm vapor produced in a cathode sputtering discharge, and that of Alipieva and Karabasheva (1999), who studied the nonlinear Voigt effect in the $2^3P \rightarrow 3^3D$ transition in neutral He.

G. Atoms trapped in solid and liquid helium

A recent (and experimentally demanding) technique for reducing spin relaxation of paramagnetic species is the trapping of the atoms in condensed (superfluid or solid) ^{4}He. Solid-rare-gas-matrix isolation spectroscopy (Coufal, 1984; Dunkin, 1998) has been extensively used by chemists in the past half-century for the investigation of reactive atoms, ions, molecules, and radicals. In all heavy-rare-gas matrices, however, the anisotropy of the local fields at individual atomic trapping sites causes strong perturbation of guest-atom spin polarization via spin-orbit interactions. As a consequence, no high-resolution magneto-optical spectra have been recorded in such matrices. However, the quantum nature (large-amplitude zero-point motion) of a condensed helium matrix makes it extremely compressible, and a single-valence-electron guest atom can impose its symmetry on the local environment via Pauli repulsion. Alkali atoms thus form spherical nanometer-sized cavities (atomic bubbles), whose isotropy, together with the diamagnetism of the surrounding He atoms, allows long-lived spin polarization to be created in the guest atoms via optical pumping. With Cs atoms in the cubic phase of solid He, longitudinal spin-relaxation times T_1 of 1 s were reported by Arndt *et al.* (1995), while transverse relaxation times T_2 are known to be larger than 100 ms (Kanorsky *et al.*, 1996). The T_1 times are presumably limited by quadrupolar zero-point oscillations of the atomic bubble, while the T_2 times are limited by residual magnetic-field inhomogeneities. In superfluid He, the coherence lifetimes are limited by the finite observation time due to convective motion of the paramagnetic atoms in the He matrix (Kinoshita *et al.*, 1994).

Nonlinear magneto-optical level-crossing signals (the longitudinal and transverse ground-state Hanle effects) were observed by Arndt *et al.* (1995) and Weis *et al.* (1995) as rather broad lines due to strong magnetic-field inhomogeneities. In recent years, spin-physics experiments in solid helium have used (radio-frequency/microwave–optical) double-resonance techniques. Optical and magneto-optical studies of defects in condensed helium were reviewed by Kanorsky and Weis (1998).

Applications of spin-polarized atoms in condensed helium include the study of the structure and dynamics of local trapping sites in quantum liquids/solids, and possible use of such samples as a medium in which to search for a permanent atomic electric dipole moment (Weis *et al.*, 1997; Sec. XII.B).

H. Laser-cooled and trapped atoms

Recently, atomic samples with relatively long spin-relaxation times were produced using laser-cooling and trapping techniques. When studying nonlinear magneto-optical effects in trapped atoms, one must take into account the perturbation of Zeeman sublevels by external fields (usually magnetic and/or optical) involved in the trapping technique. Atoms can be released from the trapping potentials before measurements are made in

order to eliminate such perturbations. Another point to consider is that Doppler broadening due to the residual thermal velocities of trapped atoms is smaller than the natural linewidth of the atomic transition. Therefore, in the low-power limit, optical pumping does not lead to formation of Bennett structures (Sec. V.A) narrower than the width of the transition.

There have been several recent studies of the Faraday and Voigt effects using magneto-optical traps (MOT's). Isayama *et al.* (1999) trapped $\sim 10^8$ ^{85}Rb atoms in a MOT and cooled them to about 10 μK. A pump beam was then used to spin-polarize the sample of cold atoms orthogonally to an applied magnetic field of ~ 2 mG. Larmor precession of the atoms was observed by monitoring the time-dependent polarization rotation of a probe beam. The limiting factor in the observation time (~ 11 ms) for this experiment was the loss of atoms from the region of interest due to free fall in the Earth's gravitational field. Labeyrie *et al.* (2001) studied magneto-optical rotation and induced ellipticity in ^{85}Rb atoms trapped and cooled in a MOT that was cycled on and off. The Faraday rotation was measured during the brief time (~ 8 ms) that the trap was off. The time that the MOT was off was sufficiently short so that most of the atoms were recaptured when the MOT was turned back on. Franke-Arnold *et al.* (2001) performed measurements of both the Faraday and Voigt effects (Sec. I) in an ensemble of cold ^{7}Li atoms. Optical rotation of a weak far-detuned probe beam due to interaction with polarized atoms was also used as a technique for nondestructive imaging of Bose-Einstein condensates (as in the work of, for example, Matthews, 1999).

Narducci (2001) has recently begun to explore the possibility of measuring NMOE in cold atomic fountains. The experimental geometry and technique of such an experiment would be similar to the setup for Faraday-Ramsey spectroscopy described in Sec. VIII.C, but the time of flight between the pump and probe regions could be made quite long (a few seconds).

With far-off-resonant blue-detuned optical dipole traps, one can produce alkali vapors with ground-state relaxation rates ~ 0.1 Hz [for example, Davidson *et al.* (1995) observed such relaxation rates for ground-state hyperfine coherences]. Correspondingly narrow features in the magnetic-field dependence of NMOE should be observable. However, we know of no experiments investigating NMOE in far-off-resonant optical dipole traps.

IX. MAGNETO-OPTICAL EFFECTS IN SELECTIVE REFLECTION

1. Linear effects

The standard detection techniques in atomic spectroscopy are the monitoring of the fluorescence light and of the light transmitted through the sample. A complementary, though less often used, technique is monitoring the light reflected from the sample or, more precisely, from the window-sample interface. The reflected light intensity shows resonant features when the light frequency is tuned across an atomic absorption line (Cojan, 1954).

The technique was discovered by Wood (1909) and is called *selective reflection spectroscopy*. A peculiar feature of selective reflection spectroscopy was discovered after the advent of narrow-band tunable lasers: when the light beam is near normal to the interface, the spectral profile of the reflection coefficient shows a narrow absorptive feature of sub-Doppler width superimposed on a Doppler-broadened dispersive pedestal (Woerdman and Schuurmans, 1975). This peculiar line shape is due to the quenching of the optical dipole by atom-window collisions, which breaks the symmetry of the atomic velocity distribution.

A theoretical model of this effect developed by Schuurmans (1976b) for low vapor pressure and low light intensity yields for the resonant modification of the reflection coefficient

$$\delta R\left(y = \frac{\Delta}{\Gamma_D}\right) \propto \mathrm{Re} \int_0^\infty \frac{e^{-x^2}}{(x-y) - i\gamma_0/(2\Gamma_D)} dx, \quad (28)$$

where γ_0 and Γ_D are the homogeneous and Doppler widths of the transition, respectively, and Δ is the light detuning. The expression differs in the lower bound of the integral from the usual Voigt integral of the index of refraction. In the limit of $\Gamma_D \gg \gamma$, the frequency derivative of Eq. (28) is a dispersive Lorentzian of width γ_0, which illustrates the Doppler-free linear nature of the effect. As only atoms in the close vicinity ($\lambda/2\pi$) of the interface contribute significantly to the reflection signal, selective reflection spectroscopy is well suited for experiments in optically thick media and for the study of atom-window van der Waals interactions.

The first theoretical discussion of magnetic-field-induced effects in selective reflection was given by Series (1967). However, that treatment was incorrect, as it did not take into account the above-mentioned sub-Doppler features. The first magneto-optical experiment using selective reflection spectroscopy was performed on mercury vapor by Stanzel (1974b), who studied magnetic-field-induced excited-state level crossings with broadband excitation. The theoretical description of that experiment was given by Schuurmans (1976a), who considered correctly the modifications induced by window collisions. The linear magneto-optical circular dichroism and rotation in the selective reflection spectra from Cs vapor in a weak longitudinal magnetic field were studied by Weis, Sautenkov, and Hänsch (1993), who recorded the spectral profiles of both effects at a fixed magnetic field and provided a theoretical analysis of the observed line shapes. In an experiment of Papageorgiou *et al.* (1994), the narrow spectral lines in selective reflection spectroscopy allowed resolution of Zeeman components in the reflection spectra of σ^+- and σ^--polarized light in fixed (120–280 G) longitudinal magnetic fields. To understand the line shapes observed in both experiments, it proved to be essential to take into account the wave-function mixing discussed in Sec. II.A.

2. Nonlinear effects

To our knowledge the only study to date of NMOE using selective reflection spectroscopy was the observa-

tion by Weis *et al.* (1992) of ground-state Zeeman coherences in a magneto-optical rotation experiment on Cs vapor. In this experiment, the laser light was kept on resonance and the magnetic field was scanned, revealing the familiar narrow dispersive resonance of NMOR. The dependence of the width of this resonance on the light intensity and on the atomic number density was studied under conditions of high optical opacity.

X. LINEAR AND NONLINEAR ELECTRO-OPTICAL EFFECTS

Although linear electro-optical effects in resonant media have been studied since the 1920s (a comprehensive review was written by Bonch-Bruevich and Khodovoi, 1967), there has been relatively little work on nonlinear electro-optical effects. Davies *et al.* (1988) experimentally and theoretically investigated linear and nonlinear light polarization rotation in the vicinity of $F=0 \rightarrow F' = 1$ transitions in atomic samarium, and Fomichev (1995) performed additional theoretical studies of nonlinear electro-optical effects for $0 \rightarrow 1$ and $1 \rightarrow 0$ transitions. There are many similarities between nonlinear electro-optical and nonlinear magneto-optical effects: the shift of Zeeman sublevels due to the applied fields is the fundamental cause of both effects, the nonlinear enhancement in both cases can arise from the formation of Bennett structures in the atomic velocity distribution (Budker, Kimball, *et al.*, 2002a) or the evolution of ground-state atomic polarization, and these mechanisms change the optical properties of the atomic vapor, thereby modifying the polarization properties of the light field.

Consider a Doppler-broadened atomic vapor subject to a dc electric field **E** and light near-resonant with an atomic transition. The light propagates in a direction orthogonal to **E** and is linearly polarized along an axis at 45° to **E**. Due to the Stark shifts Δ_s, the component of the light field along **E** sees a different refractive index than the component of the light field perpendicular to **E**. The difference in the real parts of the refractive indices leads to linear birefringence (causing the light to acquire ellipticity), and the difference in the imaginary parts of the refractive indices leads to linear dichroism (causing optical rotation).

If the light intensity is large enough to form Bennett structures in the atomic velocity distribution, the narrow features (of width $\sim \gamma_0$) in the indices of refraction cause the maximum ellipticity to become proportional to Δ_s/γ_0, rather than Δ_s/Γ_D as in the linear case. Optical rotation is not enhanced by Bennett structures in this case because it is proportional to the difference of bell-shaped features in the imaginary part of the indices of refraction, which is zero for the resonant velocity group (and of opposite signs for velocity groups to either side of the resonance).

There are also coherence effects in nonlinear electro-optical phenomena for electric fields such that $\Delta_s \ll \gamma_{\mathrm{rel}}$ (where γ_{rel} is the ground-state polarization relaxation rate), which result from the evolution of optically pumped ground-state atomic polarization in the electric
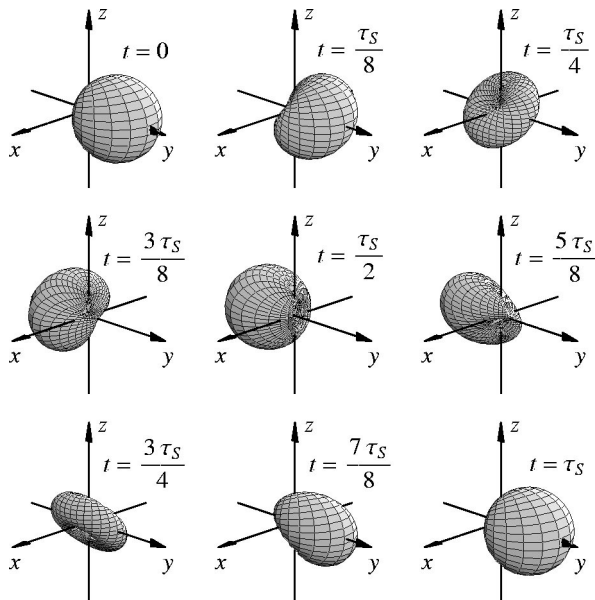
FIG. 20. A sequence of probability surfaces representing evolution of a state with $F=1$. The state is initially stretched along $\hat{\mathbf{y}}$ at $t=0$ and an electric field is applied along $\hat{\mathbf{z}}$, causing Stark beats with period τ_S. See Appendix B for a description of how these probability surfaces are generated.

field (Fig. 20). The maximum ellipticity induced in the light field due to the coherence effect is proportional to $\Delta_s/\gamma_{\mathrm{rel}}$.

While much of the recent work on coherence in non-linear magneto-optics has been done with alkali atoms, these are not necessarily the best choice for the study of electro-optical effects because tensor polarizabilities are suppressed for states with $J=1/2$ as discussed in Sec. XII.D.

Herrmann *et al.* (1986) studied a different kind of nonlinear electro-optical effect in which an electric field is applied to a sample of atoms, and normally forbidden two-photon transitions become allowed due to Stark mixing. The large polarizabilities of Rydberg states make two-photon Stark spectroscopy of transitions involving Rydberg levels an extremely sensitive probe for small electric fields.

XI. EXPERIMENTAL TECHNIQUES

In this section, we give details of some of the experimental techniques that are employed for achieving long ground-state relaxation times (atomic beams with separated light-interaction regions, buffer-gas cells, and cells with antirelaxation wall coating), as well as the techniques used for sensitive detection of nonlinear magneto-optical and electro-optical effects, especially spectropolarimetry (Sec. XI.B).

We begin the discussion by describing a representative experimental setup (Sec. XI.A). Using this example, we formulate some general requirements for experimental apparatus of this sort [for example, laser frequency tun-
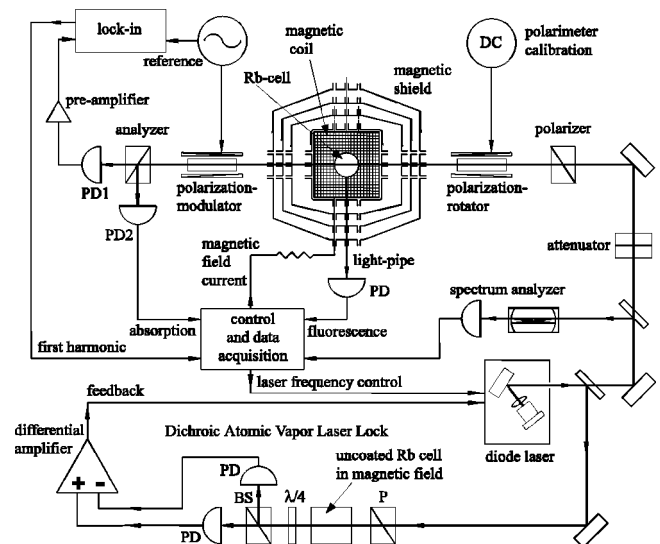

FIG. 21. Schematic diagram of the modulation polarimetry-based experimental setup used by Budker, Yashchuk, and Zolotorev (1998a) to investigate nonlinear magneto-optical effects in paraffin-coated alkali-metal-vapor cells. From Budker, Yashchuk, and Zolotorev, 1998a.

ability and stability (Sec. XI.E) and magnetic shielding (Sec. XI.D)], and outline how these requirements have been met in practice.

A. A typical nonlinear magneto-optical experiment

Here we give an overview of the Berkeley nonlinear magneto-optical apparatus, which has been used to investigate various aspects of the physics and applications of narrow [$\sim 2\pi \times 1$-Hz (Budker, Yashchuk, and Zolotorev, 1998a)] resonances, such as alignment-to-orientation conversion (Budker, Kimball, *et al.*, 2000a), self-rotation (Rochester *et al.*, 2001), and reduced group velocity of light (Budker, Kimball, *et al.*, 1999). The setup has also been used to investigate electro-optical effects and to conduct exploratory experiments whose ultimate goal is testing fundamental symmetries (Yaschuk, Budker, and Zolotorev, 1999; Kimball *et al.*, 2001). Due to the large enhancement of small-field optical rotation produced by the narrow resonance, this setup is a sensitive low-field magnetometer (Budker, Kimball, *et al.*, 2000b). With a few modifications, this apparatus can also be applied to extremely high-sensitivity magnetometry within the range of typical geomagnetic fields (Budker, Kimball, *et al.*, 2002b).

The Berkeley apparatus is shown in Fig. 21. Rubidium and/or cesium atoms are contained in a vapor cell with paraffin coating (Alexandrov *et al.*, 1996), used to suppress relaxation of atomic ground-state polarization in wall collisions (Sec. VIII.E). The experiments are performed on the $D1$ and $D2$ resonance lines. A tunable extended-cavity diode laser is used as the light source. The laser frequency is actively stabilized and can be locked to an arbitrary point on the resonance line using the dichroic-atomic-vapor laser-lock technique (Sec. XI.E). The laser linewidth, measured with a Fabry-Perot

spectrum analyzer, is ≤ 7 MHz. Optical rotation is detected with a conventional spectropolarimeter using a polarization-modulation technique (Sec. XI.B). The polarimeter incorporates a crossed Glan prism polarizer and polarizing beam splitter used as an analyzer. A Faraday glass element modulates the direction of the linear polarization of the light at a frequency $\omega_m \simeq 2\pi \times 1$ kHz with an amplitude $\varphi_m \simeq 5 \times 10^{-3}$ rad. The first harmonic of the signal from the photodiode in the darker channel of the analyzer is detected with a lock-in amplifier. It is proportional to the angle of the optical rotation φ_s caused by the atoms in the cell (Sec. XI.B). This signal, normalized to the transmitted light power detected in the brighter channel of the analyzer, is a measure of the optical rotation in the vapor cell.

A coated 10-cm-diameter cell containing the alkali vapor is placed inside a four-layer magnetic shield and surrounded with three mutually perpendicular magnetic coils (Yashchuk, Budker, *et al.*, 2002). The three outer layers of the shield are nearly spherical in shape, while the innermost shield is a cube (this facilitates application of uniform fields to the cell). The shield provides nearly isotropic shielding of external dc fields by a factor of $\sim 10^6$ (Yashchuk, Budker, *et al.*, 2002). Although a very primitive degaussing procedure is used (Sec. XI.D), the residual magnetic fields averaged over the volume of the vapor cell are typically found to be at a level of a few tens of microgauss before compensation with the magnetic coils, and a few tenths of a microgauss after such compensation.

B. Polarimetry

Successful application of the NMOE-based experimental methods (Sec. XII) depends on one's ability to perform precision polarimetry or, more specifically, laser spectropolarimetry.

In a "balanced polarimeter" (Huard, 1997), a sample is placed between a polarizer and a polarizing beam splitter (analyzer) whose transmission axes are oriented at $45°$ to one another. The optical rotation φ due to the optical activity of the sample can be found from a simple expression valid for $\varphi \ll 1$,

$$\varphi = \frac{I_1 - I_2}{2(I_1 + I_2)}, \tag{29}$$

where I_1 and I_1 are the light intensities detected in the two output channels of the analyzer. In order to measure the ellipticity ϵ of the transmitted light, a $\lambda/4$ plate is placed in front of the analyzer, oriented at $45°$ to its axis, to form a circular analyzer (Huard, 1997; see also Sec. XI.E).

Another method of polarimetry employs a crossed polarizer and analyzer (Fig. 1 and Sec. II.B) and polarization modulation. A polarization modulator using a Faraday-glass element is shown in Fig. 21. The signal in the "dark" (crossed) channel of the analyzer is given by

$$I_s(t) \simeq \chi I_0 \left(r_e + \frac{1}{2} \alpha_m^2 + \varphi^2 \right) + 2\chi I_0 \alpha_m \varphi \sin \omega_m t$$

$$- \frac{1}{2} \chi I_0 \alpha_m^2 \cos 2\omega_m t. \tag{30}$$

Here χ is the coefficient defined by absorption and scattering of light by the atomic vapor cell, I_0 is the total photon flux of the linearly polarized light (in photons per unit time) transmitted through the polarizer, r_e is the polarizer/analyzer extinction ratio, and α_m and ω_m are the polarization modulation amplitude and frequency, respectively. The amplitude of the first harmonic of the signal Eq. (30) is a measure of the polarization rotation caused by the sample. The first-harmonic amplitude is also proportional to the modulation amplitude α_m. Typically, with a Faraday modulator with a high-Verdet-constant glass (such as Hoya FR-5), the modulation α_m is $\sim 10^{-2}$ rad (Wolfenden *et al.*, 1990, 1991) at modulation frequencies ~ 1 kHz. (High-frequency modulation is often limited by the inductance of the Faraday modulator solenoid.) Resonant photoelastic modulators can also be used for polarimetry (as in the work of, for example, Oakberg, 1995; Wang and Oakberg, 1999), allowing for larger polarization modulation and higher modulation frequencies (several tens of kilohertz).

From Eq. (30), one can obtain the sensitivity of the polarimeter with data accumulation time T for shot-noise-limited detection of the first-harmonic signal in the case of an "ideal polarimeter" ($\alpha_m^2 \gg r_e + \varphi^2$):

$$\delta\varphi_s \simeq \frac{1}{2\sqrt{\chi I_0 T}}. \tag{31}$$

For a 1-mW visible-light beam and $\chi \simeq 0.5$, this corresponds to $\sim 2 \times 10^{-8}$ rad Hz$^{-1/2}$. Similar shot-noise-limited sensitivity can be achieved with a balanced polarimeter (Birich *et al.*, 1994).

Various modifications of the spectropolarimetry techniques have been developed to meet specific experimental requirements, with the common challenge of realizing the shot-noise limit of Eq. (31). A review of magneto-optics and polarimetry of condensed matter was given by Zapasskii and Feofilov (1975). Birich *et al.* (1994) considered in detail experimental approaches to the measurement of small optical rotation and their limiting factors.

C. Nonlinear magneto-optical rotation with frequency-modulated light

Budker, Kimball, *et al.* (2000b) showed that nonlinear magneto-optical rotation can be used for measurements of sub-microgauss magnetic fields with sensitivity potentially exceeding 10^{-11} G Hz$^{-1/2}$ (Sec. VIII.E). However, for many applications (such as geophysics, magnetic prospecting, and navigation), it is necessary to have a magnetometer with dynamic range ~ 1 G. Budker, Kimball, *et al.* (2002b) recently demonstrated that if frequency-modulated light is used to induce and detect

nonlinear magneto-optical rotation, the ultranarrow features in the magnetic-field dependence of optical rotation normally centered at $B=0$ can be translated to much larger magnetic fields. In this setup, light polarization modulation (Fig. 21) is replaced by frequency modulation of the laser, and the time-dependent optical rotation is measured at a harmonic of the light modulation frequency Ω_m. The frequency modulation affects both optical pumping and probing of atomic polarization. This technique should extend the dynamic range of an NMOR-based magnetometer to beyond the range of the Earth's magnetic field.

For sufficiently low light intensities (so that the optical pumping saturation parameter does not exceed unity), frequency-modulated NMOR can be understood as a three-stage (pump, precession, probe) process (Sec. V.B). Due to the frequency modulation of the laser light, the optical pumping and probing acquire a periodic time dependence. When the pumping rate is synchronized with the precession of atomic polarization, a resonance occurs and the atomic medium is pumped into an aligned state whose axis rotates at the Larmor frequency Ω_L. The optical properties of the medium are modulated at $2\Omega_L$, due to the symmetry of atomic alignment. This periodic change of the optical properties of the atomic vapor modulates the angle of the light polarization, leading to high-field NMOR resonances. If the time-dependent optical rotation is measured at the first harmonic of Ω_m, a resonance occurs when Ω_m coincides with $2\Omega_L$. Additional resonances can be observed at higher harmonics.

It should be noted that this technique is closely related to the work of Bell and Bloom (1961), in which the intensity of pump light was modulated in order to optically pump the atomic medium into a polarized state which precessed with the Larmor frequency. Also related is the work on ^{4}He optical pumping magnetometers with light frequency and intensity modulation and transmission monitoring [Gilles *et al.* (2001) and references therein].

D. Magnetic shielding

Nonlinear magneto-optical effects are generally very sensitive to magnetic-field magnitude, direction, and gradients. For ground-state spin-relaxation times of $\lesssim 1$ s, NMOE are maximum at sub-microgauss magnetic fields [Eq. (2)], necessitating their control at this level.[33] This control can be achieved with ferromagnetic shielding in spite of the fact that residual fields due to imperfections of the shield material are usually ~ 10–$50\ \mu$G (Kozlov *et al.*, 1982). With a carefully designed four-layer magnetic shield and three-dimensional coil system inside the shield (see Fig. 21), it is possible to achieve

long-term magnetic-field stability inside the innermost shield at the level of 0.1 μG (Budker, Yashchuk, and Zolotorev, 1988a; Yashchuk, Budker, and Zolotorev, 1999; Yashchuk, Budker, *et al.*, 2002).

Closed ferromagnetic shells shield external fields of different frequencies via different physical mechanisms. For static and very-low-frequency external fields, the most important mechanism is flux shunting due to the high permeability of the material. At high frequencies, the skin effect becomes the most important mechanism. A review of early work on the shielding problem, a theoretical treatment, and a survey of practical realizations was given by Sumner *et al.* (1987); see also Rikitake (1987) and Khriplovich and Lamoreaux (1997).

For static fields, the dependence of the shielding ratio on the shape and size of n shielding layers is given by an approximate formula:

$$S_{\text{tot}} \equiv \frac{B_{in}}{B_0} \simeq S_n \prod_{i=1}^{n-1} S_i \left[1 - \left(\frac{X_{i+1}}{X_i} \right)^k \right]^{-1}, \qquad (32)$$

where

$$S_i \simeq \frac{X_i}{\mu_i t_i}.$$

Here B_0 is the magnetic field applied to the shield, B_{in} is the field inside the shield, S_i is the shielding factor of the ith layer, X_i is the layer's radius or length (depending on the relative orientation of the magnetic field and the layer), and t_i and μ_i are the thickness and magnetic permeability of each layer, respectively. We assume $X_i > X_{i+1}$ and $\mu_i \gg X_i/t_i$. The power k depends on the geometry of the shield: $k \simeq 3$ for a spherical shield; $k \simeq 2$ for the transverse and $k \simeq 1$ for the axial shielding factor of a cylindrical shield with flat lids. Thus, for shields of comparable dimensions, spherical shells provide the best shielding. In the design of the three outer layers of the four-layer shield shown in Fig. 21, an approximation to a spherical shape, simpler to manufacture than a true sphere, is used. The overall shielding ratio is measured to be $\sim 10^{-6}$, roughly the same in all directions. The innermost shield is in the shape of a cube with rounded edges. This allows compensation of the residual magnetic field and its gradients as well as application of relatively homogeneous fields with a simple system of nested 3D coils of cubic shape (Yashchuk, Budker, *et al.*, 2002). The field homogeneity is increased by image currents, due to the boundary conditions at the interface of the high-permeability material, which make the short coils into effectively infinite solenoidal windings.

An important characteristic of a magnetic shield, in addition to the shielding factor and the residual fields and gradients within the shielded volume, is the residual magnetic noise. One source of such noise is Johnson thermal currents (Nenonen *et al.*, 1996; Lamoreaux, 1999; Allred *et al.*, 2002) in the shield itself.

Superconducting shielding [Cabrera and Hamilton (1973); Cabrera (1988), and references therein] yields the highest field stability. The shielding properties of superconductors originate in the Meissner effect, i.e., the

---

[33]There are specific magnetic shielding requirements for the work with atoms in a cryogenic-buffer-gas environment discussed in Sec. VIII.D.2, in which relaxation times of up to minutes are expected.

exclusion, due to persistent currents, of magnetic flux from the bulk of a superconductor. Hamilton (1970) and Taber *et al.* (1993) developed a technique for reducing the magnetic field inside a superconducting shield by expanding the shield. When the dimensions of the superconducting enclosure increase, the enclosed magnetic field decreases due to conservation of magnetic flux "frozen" into the superconductor. In one experiment, expansion of a folded lead-foil (100-μm-thick) balloon was used; an ultralow residual magnetic field ($\sim 0.06 \, \mu$G) was achieved over a liter-sized volume (Cabrera and Hamilton, 1973). With expanded lead bags as superconducting shields and a surrounding conventional ferromagnetic shield, a magnetic field of $<0.1 \, \mu$G in the flight Dewar of the Gravity Probe B Relativity Mission was maintained in a volume of 1.3 m by 0.25 m diameter enclosing a gyroscope (Mester *et al.*, 2000), giving a shielding ratio of about 5×10^{-9}. Some limitations of superconducting shields were discussed by Dietzfelbinger *et al.* (1990).

An essential difference between superconducting and ferromagnetic shields is their opposite boundary conditions. Since a superconductor is an ideal diamagnetic material, magnetic field lines cannot penetrate into it, and so image currents are of opposite sign to those in ferromagnetic material. This is important for determining the shield geometry that provides the best field homogeneity.

E. Laser-frequency stabilization using magneto-optical effects

The development of frequency-stabilized diode laser systems has led to recent progress in experimental atomic and molecular physics in general, and the study of nonlinear magneto-optical effects in particular. Conversely, some of the simplest and most effective methods of laser-frequency stabilization are based on linear and nonlinear magneto-optics.

A simple laser-locking system that uses no electronics is based on the linear Macaluso-Corbino effect, employing a cell in a longitudinal magnetic field and a polarizer placed inside the laser cavity and forming a frequency-selective element (Lukomskii and Polishchuk, 1986; Wanninger *et al.*, 1992, and references therein). A similar method based on narrow (Doppler-free) peaks in the spectrum of the nonlinear magneto-optical activity for laser-frequency stabilization was suggested by Cyr and Tetu (1991) and adopted for laser stabilization by, for example, Lee and Campbell (1992); Lee *et al.* (1993); Kitching *et al.* (1994, 1995); Wąsik *et al.* (2002).

A method based on magnetic-field-induced circular dichroism of an atomic vapor was developed by Cheron *et al.* (1994) for frequency stabilization of single-frequency solid-state $La_x Nd_{1-x} MgAl_{11} O_{19}$ (LNA) lasers. This technique was subsequently adapted to diode lasers by Corwin *et al.* (1998), who coined the term dichroic-atomic-vapor laser lock (DAVLL).

Figure 21 shows an example of DAVLL application (Budker, Yashchuk, and Zolotorev, 1998a). The optical scheme incorporates a polarizer (P), an uncoated Rb-vapor cell placed in a static longitudinal magnetic field, a $\lambda/4$ plate, and a polarizing beam splitter (BS). With the fast axis of the $\lambda/4$ plate oriented at 45° to the axis of the polarizing beam splitter, as was originally suggested by Cheron *et al.* (1994), the scheme realizes a circular analyzer sensitive to the outgoing light ellipticity induced by the circular dichroism of the atomic vapor. The output signal from the differential amplifier has dispersionlike frequency dependence corresponding to the difference between absorption spectra for left and right circular components of the light. The differential signal is used to frequency lock an external-cavity diode laser to the center of the absorption line by feeding back voltage to a piezoelectric transducer which adjusts a diffraction grating in the laser cavity [Patrick and Wieman (1991); Wieman and Hollberg (1991); Fox *et al.* (1997)]. This setup is shown schematically in Fig. 21. Frequency tuning in the vicinity of the line center can be achieved by adjusting the angle of the $\lambda/4$ plate, or by applying an appropriate bias in the electronic feedback circuit.

Various modifications of the DAVLL technique were devised to meet specific experimental requirements. Yashchuk *et al.* (2000) showed that a simple readjustment of the respective angles of optical elements allowed one to extend the DAVLL frequency tuning range to the wings of a resonance line. The DAVLL system of Yashchuk *et al.* was developed for use in the vicinity of equipment sensitive to magnetic fields. The cell-magnet system, the core component of the device, was designed to suppress the magnetic-field spillage from the ~ 200-G magnetic field that is applied over the Rb-cell volume. Beverini *et al.* (2001) developed a DAVLL device with fast response in which the optical length of the laser cavity is adjusted with an intracavity electro-optical modulator instead of the much slower mechanical motion of the grating. Clifford *et al.* (2000) showed that the zero crossing of the DAVLL signal (and thus the laser locking frequency) is dependent on the magnitude of the magnetic field applied to the Rb- or Cs-vapor cell; they used this feature for tuning the locked laser by varying the applied magnetic field.

Zeeman shifts of resonances in linear (discussed by, for example, Rikukawa *et al.*, 1991) and nonlinear spectroscopy [Weis and Derler (1988); Ikegami *et al.* (1989); Dinneen *et al.* (1992); Lecomte *et al.* (2000)] can be used for laser-frequency locking and tuning. Using nonlinear saturation spectroscopy, laser output is locked to a saturated absorption line whose frequency is modulated and shifted by a combination of ac and dc magnetic fields. With this method, a line width of 15 kHz and long-term stability of 10 kHz can be achieved. By changing the dc magnetic field applied to the atomic cell, one can tune the frequency of the laser almost linearly in the range of hundreds of megahertz without modulation of laser intensity or frequency.

XII. APPLICATIONS

A. Magnetometry

In Sec. IV.A, we mentioned that Cohen-Tannoudji *et al.* (1969), Dupont-Roc *et al.* (1969), and Dupont-Roc

(1970) performed ultrasensitive ($\sim 10^{-9}$ G Hz$^{-1/2}$) magnetometry using the ground-state Hanle effect. Since then, the technology of optical-pumping magnetometers has been further refined (by, for example, Aleksandrov *et al.*, 1987), and such magnetometers, typically employing the rf-optical double-resonance method, are now used in a variety of applications (by, for example, Alexandrov and Bonch-Bruevich, 1992), particularly for measuring geomagnetic fields.

The sensitivity of nonlinear magneto-optical rotation to small magnetic fields naturally suggests it as a magnetometry technique (Barkov *et al.*, 1989a). In this section, we discuss the limits of the sensitivity and recent experimental work on NMOR magnetometry.

1. Quantum noise limits

The shot-noise-limited sensitivity of a magnetic field measurement performed for a time T with an ensemble of N particles with spin-coherence time τ is

$$\delta B \simeq \frac{1}{g\mu} \frac{\hbar}{\sqrt{N\tau T}}. \tag{33}$$

In this expression, we have neglected factors of order unity that depend on particulars of the system (for example, the value of F and the relative contributions of different Zeeman sublevels). When light is used to interrogate the state of the spins, as in NMOR, one also needs to consider the photon shot noise [Eq. (31)].[34] Depending on the details of a particular measurement, either the spin noise [Eq. (33)] or the photon noise [Eq. (31)] may dominate. If a measurement is optimized for statistical sensitivity, the two contributions to the noise are found to be comparable (Budker, Kimball, *et al.*, 2000b).

Fleischhauer *et al.* (2000) considered an additional source of noise in polarimetric spin measurements. When the input light is off-resonant, independent quantum fluctuations in intensity of the two oppositely circularly polarized components of the light couple to the atomic Zeeman sublevels via ac Stark shifts and cause excess noise in the direction of the atomic spins. Fleischhauer *et al.* (2000) concluded that this source of noise, while negligible at low light power, actually dominates over the photon shot noise above a certain critical power. Estimates based on the formulas derived by Fleischhauer *et al.* show that, for the optimal conditions found by Budker, Kimball, *et al.* (2000b), this effect could contribute to the overall noise at a level comparable to the photon shot noise. However, the effect of the ac Stark shifts can, in certain cases, be minimized by tuning the light frequency so that the shifts due to different off-resonance levels compensate each other (No-

---

[34]We do not consider the use of the so-called spin-squeezed quantum states (discussed, for example, by Ulam-Orgikh and Kitagawa, 2001, and references therein) or squeezed states of light (Grangier *et al.*, 1987), which can allow sensitivity beyond the standard quantum limit.

vikova *et al.*, 2001a). Some other possibilities for minimizing the additional noise may include compensation of the effect by different atomic isotopes (Novikova *et al.*, 2001a), or the use, instead of a polarization rotation measurement, of another combination of the Stokes parameters (Appendix A) chosen to maximize the signal-to-noise ratio.

2. Experiments

One approach to using nonlinear magneto-optical rotation for precision magnetometry is to take advantage of the ultranarrow (width ~ 1 μG) resonance widths obtainable in paraffin-coated cells (Sec. VIII.E). Using the experimental setup described in Sec. XI.A, Budker, Kimball, *et al.* (2000b) optimized the sensitivity of an NMOR-based magnetometer to submicrogauss magnetic fields with respect to atomic density, light intensity, and light frequency near the $D1$ and $D2$ lines of ^{85}Rb. They found that a shot-noise-limited magnetometric sensitivity of $\sim 3 \times 10^{-12}$ G Hz$^{-1/2}$ was achievable in this system. This sensitivity was close to the shot-noise limit for an ideal measurement [Eq. (33)] with the given number of atoms in the vapor cell ($\sim 10^{12}$ at 20 °C) and rate of ground-state relaxation (~ 1 Hz), indicating that, in principle, NMOR is a nearly optimal technique for measuring the precession of polarized atoms in external fields. If limitations due to technical sources of noise can be overcome, the sensitivity of an NMOR-based magnetometer may surpass that of current optical pumping (Alexandrov *et al.*, 1996) and SQUID (superconducting quantum interference device) magnetometers (Clarke, 1996), both of which operate near their shot-noise limit, by an order of magnitude. Even higher sensitivities, up to 2×10^{-14} G Hz$^{-1/2}$, may be achievable with an ingenious magnetometric setup of Allred *et al.* (2002) in which K vapor at a density of 10^{14} cm^{-3} is used and the effect of spin-exchange relaxation is reduced by "locking" the precession of the two ground-state hyperfine components together via the spin-exchange collisions themselves (Happer and Tang, 1973).

The magnetic-field dependence of NMOR is strongly affected by the magnitude and direction of transverse magnetic fields (Budker, Yashchuk, and Zolotorev, 1998a, 1998b). At low light powers, the transverse-field dependence can be quantitatively understood using a straightforward extension of the Kanorsky-Weis model discussed in Sec. VII.A, which opens the possibility of sensitive three-dimensional magnetic-field measurements.

As discussed in detail in Sec. XI.C, if frequency-modulated light is used to induce and detect NMOR, the dynamic range of an NMOR-based magnetometer may be increased beyond the microgauss range to >1 G without appreciable loss of sensitivity.

Novikova *et al.* (2001a; Novikova and Welch, 2002), using buffer-gas-free uncoated cells, investigated the application of NMOR in optically thick media to magnetometry (Sec. VIII.A.3). Although the ultimate sensitivity that may be obtained with this method appears to be

some two orders of magnitude inferior to that obtained with paraffin-coated cells,[35] this method does provide a broad dynamic range, so that Earth-field (~ 0.4 G) values could be measured with a standard polarimeter.

Rochester and Budker (2002) theoretically analyzed the magnetometric sensitivity of thick-medium NMOR measurements optimized with respect to light intensity in the case of negligible Doppler broadening and of large Doppler broadening. In the former case, the sensitivity improves as the square root of optical density, while in the latter it improves linearly—a result which can be obtained from standard quantum-limit considerations (Sec. XII.A.1).

Cold atoms prepared by laser trapping and cooling were also recently used for NMOR-based magnetometry. Isayama *et al.* (1999) employed a pump/probe geometry with $\sim 10^8$ cold ^{85}Rb atoms that were trapped in a MOT and then released (Sec. VIII.H) for measurement of an applied magnetic field of ~ 2 mG. The observation time for a single measurement was limited to about 10 ms due to the free fall of the atoms in the Earth's gravitational field; after 30 such measurements, Isayama *et al.* (1999) obtained a precision of 0.18 μG in the determination of the applied magnetic field. It is expected that by using atomic fountains (Narducci, 2001) or far-off-resonant optical dipole traps (Davidson *et al.*, 1995), the observation time and overall sensitivity to magnetic fields can be considerably improved.

B. Electric-dipole-moment searches

The existence of a permanent electric dipole moment (reviewed by, for example, Khriplovich and Lamoreaux, 1997) of an elementary or composite particle such as an atom would violate parity- (P) and time-reversal (T) invariance. The nonrelativistic Hamiltonian H_{EDM} describing the interaction of an electric dipole moment **d** with an electric field **E** is given by

$$H_{\mathrm{EDM}} = -\mathbf{d}\cdot\mathbf{E} \propto \mathbf{F}\cdot\mathbf{E}. \tag{34}$$

Under the parity operator $\hat{P}$ (the space-inversion operator that transforms $\mathbf{r}\rightarrow -\mathbf{r}$), the axial vector **F** does not change sign, whereas the polar vector **E** does. Therefore H_{EDM} is P odd, i.e., violates parity. Under the time-reversal operator $\hat{T}$, **E** is invariant and **F** changes sign, so H_{EDM} is also T odd.

Ever since the discovery in 1964 of CP violation in the neutral kaon system (C is charge-conjugation), there has been considerable interest in the search for electric dipole moments of elementary particles (CP violation implies T violation if the combined CPT symmetry is valid, as is generally believed). Many theoretical attempts to explain CP violation in the neutral kaon system, such as supersymmetry, predict electric dipole mo-

ments of the electron and neutron that are near the current experimental sensitivities (see discussion by Khriplovich and Lamoreaux, 1997). Measurements of the electric dipole moment of paramagnetic atoms and molecules (that have unpaired electrons) are primarily sensitive to the electron electric dipole moment d_e. It is important to note that, due to relativistic effects in heavy atoms, the atomic electric dipole moment can be several orders of magnitude larger than d_e.

If an atom has an electric dipole moment, its Zeeman sublevels will experience linear electric-field-induced splitting much like the usual Zeeman effect. Most methods of searching for an electric dipole moment have thus been based on detection (using magnetic-resonance methods or light absorption) of changes in the Larmor precession frequency of polarized atoms when a strong electric field is applied, for example, parallel or antiparallel to a magnetic field.

Another (related) way of searching for electric dipole moments is to use induced optical activity. As was pointed out by Baranova *et al.* (1977) and Sushkov and Flambaum (1978), a vapor of electric-dipole-moment-possessing atoms subject to an electric field will cause rotation of the polarization plane of light propagating along the direction of the electric field—the analog of Faraday rotation. Barkov *et al.* (1988a) demonstrated that, just as in magneto-optics, nonlinear optical rotation is significantly more sensitive than linear optical rotation to the electric dipole moment of an atom or molecule (see also discussion by Hunter, 1991; Schuh *et al.*, 1993; Weis, Schuh, *et al.*, 1993).

Yashchuk, Budker, and Zolotorev (1999) and Kimball *et al.* (2001) recently investigated the possibility of performing a search for the electron electric dipole moment d_e using nonlinear optical rotation in a paraffin-coated Cs-vapor cell subjected to a longitudinal electric field. In addition to Cs, which has an enhancement factor for the electron electric dipole moment of ~ 120, the cell would also contain Rb, which has a much smaller enhancement factor and would be used as a "co-magnetometer." The estimated shot-noise-limited sensitivity to d_e for such an experiment is $\sim 10^{-26}e$ cm Hz$^{-1/2}$ (for a 10 kV cm^{-1} electric field). This statistical sensitivity should enable a NMOR-based electric dipole moment search to compete with the best present limits on d_e from measurements in Tl (Regan *et al.*, 2002), which has an enhancement factor of ~ 600, and Cs (Murthy *et al.*, 1989). However, in order to reach this projected sensitivity, there are several problems that must be overcome. The first is a significant change in the atomic density when electric fields are applied to the cell. The second is a coupling of the atomic polarizations of Cs and Rb via spin-exchange collisions, which would prevent Rb from functioning as an independent co-magnetometer. These issues are discussed in more detail by Kimball *et al.* (2001).

There are also molecular (YbF) beam experiments (Sauer *et al.*, 2001) searching for an electron electric dipole moment using a separated light pump and probe technique that is a variant of the Faraday-Ramsey spectroscopic method (Sec. VIII.C).

---

[35]The limitation in practical realizations of thick-medium magnetometry may come from the effects of radiation trapping (Matsko, Novikova, *et al.*, 2001; Matsko, Novikova, and Welch, 2002; Novikova and Welch, 2002).
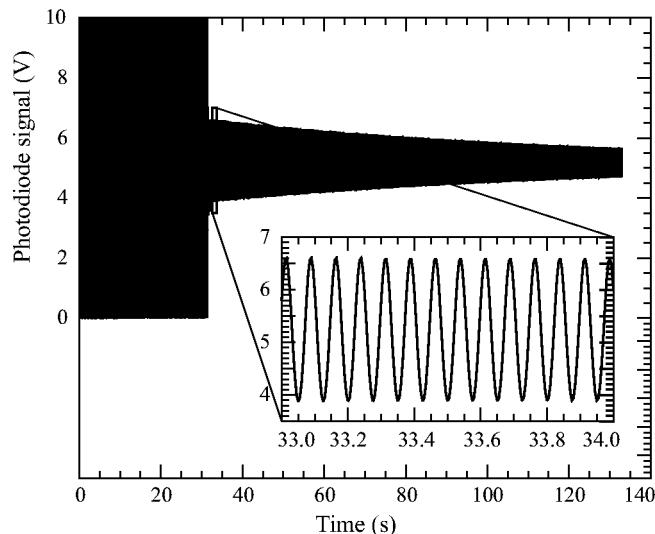
FIG. 22. Experimental optical rotation signal obtained by Romalis *et al.* (2001b) produced by Hg atomic polarization in a magnetic field of 17 mG. The inset shows a one-second segment of the data. From Romalis *et al.*, 2001b.

In another class of experiments, one searches for electric dipole moments of diamagnetic atoms and molecules. Such experiments are less sensitive to the electric dipole moment of the electron than those employing paramagnetic atoms and molecules. However, they probe CP-violating interactions within nuclei and are sensitive to electric dipole moments of the nucleons. Romalis *et al.* (2001a, 2001b) have conducted the most sensitive experiment of this kind in ^{199}Hg. A cylindrical quartz vapor cell at room temperature (vapor concentration $\sim 5 \times 10^{13}$ cm^{-3}) is subjected to an electric field of up to 10 kV cm^{-1}, applied via conductive SnO$_2$ electrodes deposited on the inner surfaces of the flat top and bottom quartz plates. The entire inner surface of the cell including the electrodes is coated with paraffin. The cell is filled with a N$_2$/CO buffer-gas mixture at a total pressure of several hundred Torr. The buffer gas is used to maintain high breakdown voltage and to quench metastable states of mercury that are populated by the UV light employed. The nuclear-spin-relaxation time ($I = 1/2$ for ^{199}Hg) is ~ 100–200 s. The experiment utilizes the $6\,^1S_0 \rightarrow 6\,^3P_1$ transition at 253.7 nm, excited with light from a homemade cw laser system. A magnetic field of 17 mG and the electric field are applied to the cell, and circularly polarized resonant light, chopped at the Larmor frequency, illuminates the cell in a direction perpendicular to that of the fields. After the atoms are pumped for ~ 30 s with 70 μW of light power to establish transverse circular polarization, optical rotation of linearly polarized probe light, detuned from resonance by 20 GHz, is detected (Fig. 22).[36] The spin-precession frequency is measured in two identical cells with oppo-

site directions of the electric field with respect to the magnetic field. This device has a sensitivity to energy level shifts of ~ 0.3 μHz/Hz$^{1/2}$ over a measurement time of a hundred seconds, better than any other existing device (see Sec. XII.A). With several months of data taking, it has set a limit on the atomic electric dipole moment of $|d(^{199}\text{Hg})| < 2.1 \times 10^{-28}$ e cm (95% confidence).

C. The Aharonov-Casher phase shift

An atom moving in an electric field **E** with velocity **v** experiences a magnetic field $\mathbf{B} = \mathbf{E} \times \mathbf{v}/c$. This "motional" magnetic field induces phase shifts of the atomic magnetic sublevels and thus affects nonlinear magneto-optical signals. The $\mathbf{E} \times \mathbf{v}$ effect is a linear Stark effect that represents a severe systematic problem in many electric-dipole-moment experiments. The induced phase shift is given by the Aharonov-Casher (1984) phase

$$\phi_{AC} = \frac{1}{\hbar c} \int_{(c)} \boldsymbol{\mu} \times \mathbf{E}(\mathbf{s}) \cdot d\mathbf{s} \tag{35}$$

acquired by a magnetic moment $\boldsymbol{\mu}$ carried on a path (c).[37] The phase [Eq. (35)] is independent of the shape of the trajectory (c) and is thus referred to as a "topological phase."

The Aharonov-Casher effect was studied interferometrically with neutrons (Cimmino *et al.*, 1989) and with the fluorine nucleus in the TlF molecule (Sangster *et al.*, 1993, 1995) using conventional Ramsey molecular-beam spectroscopy. Faraday-Ramsey spectroscopy (Sec. VIII.C) is a convenient method for measuring the Aharonov-Casher effect with atoms. Gorlitz *et al.* (1995) performed such an experiment with Rb atoms and found agreement with the theoretical prediction at the level of 1.4%. They verified the linear dependence of the phase shift on the strength of the electric field as well as its nondispersive nature (independence of velocity). An atomic Aharonov-Casher effect was also measured by Zeiske *et al.* (1995) using an atomic interferometer.

In Faraday-Ramsey geometry, the phase shift accumulated in a homogeneous static electric field between $\Delta M = 2$ sublevels of an aligned atom is given by

$$\phi_{AC} = \frac{2g\mu}{\hbar c} \int E \, dL, \tag{37}$$

where the field integral extends over the flight region between the two optical interaction regions. This phase shift enters directly in the Faraday-Ramsey line-shape function given by Eq. (26). When using atoms with a well-known g factor, one can thus use the measurement

---

[36]A previous (several times less sensitive) version of this experiment (Jacobs *et al.*, 1995) used the same light beam for both pumping and probing.

---

[37]Equation (35) can be easily derived by considering a particle with magnetic moment $\boldsymbol{\mu}$ moving along a trajectory whose element is given by $d\mathbf{s} = \mathbf{v} dt$. The particle acquires a differential phase shift

$$d\phi = \frac{\boldsymbol{\mu} \cdot \mathbf{B}}{\hbar} dt = \frac{\boldsymbol{\mu} \cdot \mathbf{E} \times \mathbf{v}}{\hbar c} dt = \frac{\boldsymbol{\mu} \cdot \mathbf{E} \times d\mathbf{s}}{\hbar c}, \tag{36}$$

which gives Eq. (35) upon integration.

of ϕ_{AC} to determine experimentally the electric-field integral (Rasbach *et al.*, 2001).

D. Measurement of tensor electric polarizabilities

The quadratic Stark effect in a Zeeman manifold $|F,M\rangle$ in a homogeneous static electric field E can be parametrized by

$$\Delta_s(F,M) = -\frac{1}{2}\alpha E^2, \tag{38}$$

where the static electric polarizability α can be decomposed into scalar (α_0) and tensor (α_2) parts according to Angel and Sandars (1968):

$$\alpha = \alpha_0 + \frac{3M^2 - F(F+1)}{F(2F-1)}\alpha_2. \tag{39}$$

States with $J = 1/2$, such as the alkali ground states, can have only tensor properties due to nonzero nuclear spin. Tensor polarizabilities of such states are suppressed compared to the scalar polarizabilities by the ratio of the hyperfine splitting to the energy separation between the state of interest and electric-dipole-coupled states of opposite parity. For the alkali ground states, the suppression is $\sim 10^6 - 10^7$.

When combined with the magnetic shifts of Zeeman sublevels, the tensor electric shifts lead to complex signals in level-crossing experiments (Sec. II.D.1) when the magnetic field is scanned. This technique has been used for several decades to measure excited-state tensor polarizabilities. The combination of electric and magnetic shifts is also responsible for the alignment-to-orientation conversion processes (Sec. V.C).

Measurements of ground-state tensor polarizabilities in the alkalis were performed in the 1960s using conventional atomic beam Ramsey resonance spectroscopy [Sandars and Lipworth, 1964; Carrico *et al.*, 1968; Gould *et al.*, 1969]. Weis and co-workers are currently using the effect of the electric-field-dependent energy shifts on the nonlinear magneto-optical properties of the atomic medium to remeasure these polarizabilities (Rasbach, 2001; Rasbach *et al.*, 2001; Weis, 2001). The technique is an extension of Faraday-Ramsey spectroscopy (Sec. VIII.C) to electric interactions in the precession region. The renewed interest in the tensor polarizabilities is related to a discrepancy between previous experimental and theoretical values, and it is believed that increased precision in both (at the sub-1% level) will provide a valuable test of atomic structure calculations.

E. Electromagnetic-field tomography

Various techniques involving nonlinear magneto-optical and electro-optical effects can be used to perform spatially resolved measurements of magnetic and electric fields (electromagnetic field tomography). Skalla *et al.* (1997b) used NMOR to measure the precession of spin-polarized ^{85}Rb atoms contained in a cell filled with dense N_2 buffer gas to ensure sufficiently long diffusion times for Rb atoms. The Rb atoms were spin polarized with a set of spatially separated, pulsed pump beams and subjected to a magnetic field with a gradient. Since the precession frequency of the Rb atoms depended on the position of the atoms within the cell, the spatial distribution of the magnetic field within the cell could be determined from the detected Larmor precession frequencies. Skalla *et al.* (1997a) and Giel *et al.* (2000) used similar techniques to measure the diffusion of spin-polarized alkali atoms in buffer-gas-filled cells. Allred *et al.* (2002) have investigated the possibility of biomagnetic imaging applications of NMOE.

It is possible to localize regions of interest by intersecting pump and probe light beams at an angle. Analysis of the polarization properties of the probe beam could, in principle, allow the reconstruction of the electric and magnetic fields inside the volume where the pump and probe beams overlap. This reconstruction would be aided by the fact that magneto-optic effects enhance optical rotation while electro-optical effects enhance induced ellipticity. Scanning the region of intersection would allow one to create a three-dimensional map of the fields.

F. Parity violation in atoms

We have discussed applications of linear magneto-optics to the study of parity violation in Sec. II.C.6.

In work related to a study of parity violation, Bouchiat *et al.* (1995) studied both theoretically and experimentally magnetic-field-induced modification of polarization of light propagating through Cs vapor whose frequency was tuned near a resonance between two excited states. The population of the upper state of the transition was created by subjecting atoms to a pump laser pulse connecting this state to the ground state [in the work of Bouchiat *et al.* (1995), this is a nominally forbidden $M1$ transition which has a parity-violating $E1$ contribution, as well as an $E1$ contribution induced by by an applied electric field]. A particular feature incorporated in the design of this experiment is that there is probe-beam amplification rather than absorption.

Kozlov and Porsev (1990) considered theoretically the possibility of applying an effect directly analogous to Bennett-structure-related NMOR (Sec. V.A) to the measurement of parity violation (of the P-odd, T-even rotational invariant $\mathbf{k}\cdot\mathbf{B}$) in the vicinity of atomic transitions with unsuppressed $M1$ amplitude. They found that, while the maximum effect is not enhanced compared to the linear case, the magnitude of the field B at which the maximum occurs is reduced in the nonlinear case by the ratio γ_0/Γ_D of the homogenous width to the Doppler width of the transition.

Cronin *et al.* (1998) attempted to use electromagnetically induced transparency (Sec. XIII.A) to address the problems of the traditional optical-rotation parity-violation experiments, namely, the problem of detailed understanding of a complicated spectral line shape, and the absence of reversals that would help distinguish a true P-violating rotation from systematics. In addition to

a probe beam tuned to an $M1$ transition, there is a second, counter-propagating pump laser beam present whose frequency is tuned to an adjacent, fully allowed transition. The presence of this pump beam modifies the effective refractive index "seen" by the probe beam in a drastic way. The main advantages of using this scheme for a parity-violation measurement are that the optical rotation line shapes are now Doppler-free and can be turned on and off by modulating the pump beam intensity.

Other applications of nonlinear spectroscopic methods to the study of P violation were reviewed by Budker (1999).

XIII. CLOSELY RELATED PHENOMENA AND TECHNIQUES

A. Dark and bright resonances

Zero-field level-crossing phenomena involving linearly polarized light such as those occurring in the nonlinear Faraday effect or the ground-state Hanle effect (Sec. II.B) can be interpreted in terms of *dark resonances*, or *lambda resonances*. Such resonances occur when a light field consisting of two phase-coherent components of frequency ω_1 and ω_2 is near resonance with an atomic Λ system [a three-level system having two close-lying lower levels[38] and one excited level; see Fig. 23(a)]. When the difference frequency $\Delta\omega_{\text{light}} = \omega_1 - \omega_2$ is equal to the frequency splitting $\Delta\omega_{ab}$ of the two lower levels (the Raman resonance condition), the system is pumped into a coherent superposition of the two lower states which no longer absorbs the bichromatic field. Due to the decrease of fluorescence at the Raman resonance, this situation is called a "dark resonance" (see, for example, the review of Arimondo, 1996).[39] The creation of a nonabsorbing coherent superposition of the lower states is also referred to as "coherent population trapping." When one frequency component of the light

———————

[38]In many dark-resonance experiments, the lower-state splitting is the ground-state hyperfine splitting (for example, as with the $F = I \pm 1/2$ states in alkali atoms). As the coherent superposition of hyperfine levels can be very long lived, the lambda resonances can have correspondingly small linewidths. In Cs and Rb, linewidths below 50 Hz have been observed (Brandt *et al.*, 1997; Erhard *et al.*, 2000; Erhard and Helm, 2001). In a magnetic field, the dark resonance of an alkali atom splits into $4I + 1$ components; the outermost components correspond to $\Delta M = \pm 2I$ coherences which have a Zeeman shift of $\sim \pm 4\mu BI/(2I+1)$ (Wynands *et al.*, 1998). For cesium ($I = 7/2$) this yields a sevenfold enhanced sensitivity to magnetic fields relative to experiments detecting $\Delta M = \pm 1$ coherences. A magnetometer based on dark resonances with a sensitivity of $120\,\text{nG}\,\text{Hz}^{-1/2}$ has recently been demonstrated by Stahler *et al.* (2001).

[39]As discussed in Sec. VIII.A, optical pumping in the case of a closed $F \rightarrow F+1$ transition leads to an increased absorption of the medium, rather than transparency (Kazantsev *et al.*, 1984; Lezama *et al.*, 1999; Renzoni *et al.*, 2001), which leads to *bright resonances*.
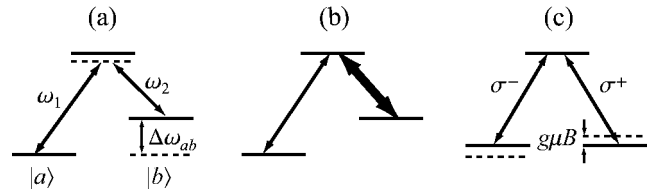

FIG. 23. Illustration of the connection between lambda resonances, electromagnetically induced transparency, and nonlinear magneto-optical effects: (a) Lambda resonance in a three-level system. Two phase-coherent optical fields at frequencies ω_1 and ω_2 pump the system into a "dark" state in which absorption and fluorescence are suppressed. (b) Electromagnetically induced transparency in the Λ configuration. In this case, one component of the light field is much stronger than the other. In the absence of the coupling field, absorption on the probe transition is large. When the coupling field is applied, a dip, with width given by the relaxation rate of the coherence between the two lower states, appears in the absorption profile. (c) Nonlinear magneto-optical effects in the Λ configuration. In this case, the two light fields have the same intensity and frequency and the two transitions have the same strength. Here the frequency splitting of the transitions—rather than that of the light components—is tuned, using a magnetic field.

field is much stronger than the other [Fig. 23(b)], it is referred to as a "coupling" or "drive" field, and the reduction of the absorption of the weaker probe field is called "electromagnetically induced transparency" (see, for example, the review[40] by Harris, 1997).

An analogous situation occurs in nonlinear magneto-optical experiments with linearly polarized light resonant with, for example, an $F = 1 \rightarrow F' = 0$ transition [Fig. 23(c)]. The σ^+ and σ^- components of the linear polarization can be viewed as two phase-coherent fields which happen to have the same frequency and intensity. A resonance occurs when the atomic levels, tuned via the Zeeman effect, become degenerate. Even though here it is the level splitting rather than the light frequency that is tuned, the origin of the resonance is the same.[41]

Other closely related topics discussed in the literature include "lasing without inversion" (see, for example, discussion by Kocharovskaya, 1992) and phase-coherent atomic ensembles, or "phaseonium" (Scully, 1992).

B. "Slow" and "fast" light

When a pulse of weak probe light propagates through a nonlinear medium in the presence of a strong field, various peculiar phenomena can be observed in the propagation dynamics. Under certain conditions, the light pulse is transmitted without much distortion, and the apparent group velocity can be very slow ($\sim 1\,\text{m s}^{-1}$ in some experiments), faster than c, or nega-

———————

[40]A list of earlier references dating back to the 1950s can be found in the review of Matsko, Kocharovskaya, *et al.* (2001).

[41]Although the connection between various nonlinear effects discussed here and NMOE is straightforward, it has not been widely recognized until very recently.

tive (see recent comprehensive reviews by Matsko, Kocharovskaya, *et al.*, 2001; Boyd and Gauthier, 2002). From the point of view of an observer detecting the probe pulse shape and timing at the input and the output, the system appears to be an effectively *linear* optical medium, but with unusually large magnitude of dispersion. The "slow" and "fast" light effects, as well as similar effects in linear optics, are due to different amplification or absorption of the leading and trailing edges of the pulse ("pulse reshaping"; see, for example, discussion by Chiao, 1996).

The connection between NMOE and "fast" and "slow" light was established by Budker, Kimball, *et al.* (1999) in an investigation of the dynamics of resonant light propagation in Rb vapor in a cell with antirelaxation wall coating. They modulated the direction of the input light polarization and measured the time dependence of the polarization after the cell. The light propagation dynamics that they observed, including negative "group delays" associated with electromagnetically induced opacity (Akulshin *et al.*, 1998; Lezama *et al.*, 1999), were analogous to those in electromagnetically induced transparency experiments. The spectral dependence of light pulse delays was measured to be similar to that of NMOR, confirming a theoretical prediction. In addition, magnetic fields of a few microgauss were used to control the apparent group velocity. Further studies of magnetic-field control of light propagation dynamics were carried out by Novikova *et al.* (1999) and Mair *et al.* (2002).

Recently, Shvets and Wurtele (2002) pointed out that electromagnetically induced transparency and "slow" light phenomena can also occur in magnetized plasma.[42] They observed that in such a medium, EIT, commonly described as a quantum interference effect (Sec. XIII.A), can be completely described by classical physics.

C. Self-rotation

If the light used to study nonlinear magneto-optical rotation is elliptically polarized, additional optical rotation (present in the absence of a magnetic field) can occur due to nonlinear self-rotation. Self-rotation arises when the elliptically polarized light field causes the atomic medium to acquire circular birefringence and linear dichroism, causing optical rotation. There are several physical mechanisms that can lead to self-rotation in atomic media.[43] These are discussed in detail by Rochester *et al.* (2001). Optical rotation can be caused by circular birefringence, created by either a difference in the populations (due to optical pumping; Davis *et al.*, 1992)

or the energies (due to ac Stark shifts) of the $\pm M$ Zeeman sublevels. At high power, orientation-to-alignment conversion can generate atomic alignment not along the axes of light polarization, leading to optical rotation due to linear dichroism. In general, the spectra of self-rotation and NMOR are different, and thus both the magnetic field and the light frequency dependences can be used to distinguish NMOR and self-rotation.

Self-rotation can play an important role in the output polarization of gas lasers (Alekseev and Galitskii, 1969) and in high-resolution polarization spectroscopy (Saikan, 1978; Agarwal, 1984; Adonts *et al.*, 1986; Alekseev, 1988). Self-rotation was theoretically considered in relation to NMOR by Giraud-Cotton *et al.* (1985b) and Fomichev (1995) and as a systematic effect in the study of atomic parity nonconservation by Kosulin and Tumaikin (1986). Self-rotation in alkali vapors has been studied experimentally by Bonch-Bruevich *et al.* (1973), Bakhramov *et al.* (1989), Davis *et al.* (1992), and Rochester *et al.* (2001).

Recently, it was found that if linearly polarized light propagates through a medium in which elliptically polarized light would undergo self-rotation, squeezed vacuum is produced in the orthogonal polarization (Tanás and Kielich, 1983; Boivin and Haus, 1996; Margalit *et al.*, 1998; Matsko, Novikova, Welch, *et al.*, 2002). It may be possible to use this effect to perform sub-shot-noise polarimetry (Grangier *et al.*, 1987) in the detection of NMOR.

XIV. CONCLUSION

In this review, we have described the history and recent developments in the study and application of resonant nonlinear magneto-optical effects. We have discussed the connections and parallels between this and other subfields of modern spectroscopy, and pointed out open questions and directions for future work. Numerous and diverse applications of NMOE include precision magnetometry, very-high-resolution measurements of atomic parameters, and investigations of the fundamental symmetries of nature. We hope that this article has succeeded in conveying the authors' excitement about working in this field.

ACKNOWLEDGMENTS

---

[42]Earlier studies of electromagnetically induced transparency phenomena in plasma were conducted by Harris (1996); Matsko and Rostovtsev (1998); Gordon *et al.* (2000a, 2000b).

[43]Self-rotation was first observed in molecular liquids (Maker *et al.*, 1964). The alignment of anisotropic molecules in the light field can lead to self-rotation (Chiao and Godine, 1969).

search KBN (Grants Nos. 2P03B06418 and PBZ/KBN/ 043/PO3/2001) and the National Laboratory of AMO Physics in Torun, Poland.

APPENDIX A: DESCRIPTION OF LIGHT POLARIZATION IN TERMS OF THE STOKES PARAMETERS

In Eq. (22) for the electric field of light propagating in the $\hat{\mathbf{z}}$ direction, the polarization state of the light is given in terms of the parameters $\mathcal{E}_0$, φ, ϵ, ϕ—the light field amplitude, polarization angle, ellipticity, and phase, respectively. Another parametrization of the polarization state is that given by the *Stokes parameters* (see, for example, the book by Huard, 1997), which are useful because they are defined in terms of directly measurable intensities:

$$
\begin{aligned}
S_0 &= I_x + I_y = I_0, \\
S_1 &= I_x - I_y, \\
S_2 &= I_{+\pi/4} - I_{-\pi/4}, \\
S_3 &= I_+ - I_-,
\end{aligned}
\tag{A1}
$$

where I_x and I_y are the intensities of the components along the x and y axes, $I_{\pm\pi/4}$ are the intensities of the components at $\pm\pi/4$ to the x and y axes, and I_+ and I_- are the intensities of the left- and right-circularly polarized components, respectively.

The Stokes parameters for fully polarized light can also be written in a normalized form that is easily related to the polarization angle and ellipticity:

$$
\begin{aligned}
S_1' &= S_1/S_0 = \cos 2\epsilon \cos 2\varphi, \\
S_2' &= S_2/S_0 = \cos 2\epsilon \sin 2\varphi, \\
S_3' &= S_3/S_0 = \sin 2\epsilon.
\end{aligned}
\tag{A2}
$$

APPENDIX B: DESCRIPTION OF ATOMIC POLARIZATION

1. State multipoles

The density matrix of an ensemble of atoms in a state with angular momentum F has $(2F+1)\times(2F+1)$ components $\rho_{M,M'}$. Since magneto-optical effects involve spin rotation (Larmor precession) and other more complex forms of atomic polarization evolution, it is often useful to work with the irreducible components of ρ, i.e, the components $\rho_q^{(\kappa)}$ with $q=-\kappa,\ldots,\kappa$ and $\kappa=0,\ldots,2F$, which transform among themselves under rotations (see, for example, Omont, 1977 and Varshalovich *et al.*, 1988). The $\rho_q^{(\kappa)}$ are related to the $\rho_{M,M'}$ by

$$
\rho_q^{(\kappa)} = \sum_{M,M'=-F}^{F} (-1)^{F-M'} \langle F,M,F,-M'|\kappa,q\rangle \rho_{M,M'},
\tag{B1}
$$

where $\langle\cdots|\cdots\rangle$ indicate the Clebsch-Gordan coefficients. The density matrix for atoms in a state with angular momentum F can be decomposed into irreducible multipole components according to

$$
\rho = \sum_{\kappa=0}^{2F} \sum_{q=-\kappa}^{\kappa} \rho_q^{(\kappa)} T_q^{(\kappa)},
\tag{B2}
$$

where the $T_q^{(k)}$ are components of the irreducible tensors $T^{(\kappa)}$ obtained from coupling **F** with **F**:

$$
F \otimes F = T^{(0)} \oplus T^{(1)} \oplus \cdots \oplus T^{(2F)}.
\tag{B3}
$$

The components $\rho_q^{(\kappa)}$ are called *state multipoles*. The following terminology is used for the different multipoles: $\rho^{(0)}$, monopole moment or *population*; $\rho^{(1)}$, vector moment or *orientation*; $\rho^{(2)}$, quadrupole moment or *alignment*; $\rho^{(3)}$, octupole moment; and $\rho^{(4)}$, hexadecapole moment.[44] Each of the moments $\rho^{(\kappa)}$ has $2\kappa+1$ components.

The term *polarization* is used for the general case of an ensemble that has any moment higher than population. When the Zeeman sublevels are not equally populated, $\rho_0^{(\kappa)} \neq 0$ for some $\kappa > 0$, and the medium is said to have *longitudinal polarization*. When there are coherences between the sublevels, $\rho_q^{(\kappa)} \neq 0$ for some $q \neq 0$, and the medium is said to have *transverse polarization*. If ρ is represented in the basis $|F,M\rangle$, longitudinal orientation and longitudinal alignment are given by

$$
\begin{aligned}
P_z &\propto \rho_0^{(1)} \propto \langle F_z \rangle, \\
A_{zz} &\propto \rho_0^{(2)} \propto \langle 3F_z^2 - \mathbf{F}^2 \rangle,
\end{aligned}
\tag{B4}
$$

respectively.

Note also that optical pumping with circularly polarized light (in the absence of other external fields) creates multipoles of all orders ($\kappa \leq 2F$), while pumping with linearly polarized light creates only even-ordered multipoles. This latter fact is a consequence of a symmetry that is most clearly seen when the quantization axis is along the light polarization direction.

2. Visualization of atomic polarization

In this section, we outline a technique for visualizing atomic polarization by drawing a surface in three dimensions representing the probability distribution of the angular momentum, as presented in more detail by Rochester and Budker (2001a). A similar approach has been used to describe molecular polarization and its evolution (Auzinsh and Ferber, 1995; Auzinsh, 1997), and more recently to analyze anisotropy induced in atoms and molecules by elliptically polarized light (Milner and Prior, 1999; Milner *et al.*, 1999).

In order to visualize the angular momentum state of atoms with total angular momentum F, we draw a surface whose distance r from the origin is equal to the probability of finding the projection $M = F$ along the radial direction. To find the radius in a direction given by

---

[44]There are other definitions of the terms "orientation" and "alignment" in the literature. For example, in Zare (1988), alignment designates even moments in atomic polarization (quadrupole, hexadecapole, etc.), while orientation designates the odd moments (dipole, octupole, etc.).

polar angles θ and φ, we rotate the density matrix ρ so that the quantization axis is along this direction and then take the $\rho_{F,F}$ element:

$$r(\theta,\varphi) = \langle M = F | \mathbf{R}_{\varphi,\theta,0}^{-1} \rho \mathbf{R}_{\varphi,\theta,0} | M = F \rangle. \qquad \text{(B5)}$$

Here $\mathbf{R}_{\alpha,\beta,\gamma}$ is the quantum-mechanical rotation matrix (see, for example, discussion by Edmonds, 1996).

Consider, for example, atoms prepared at $t=0$ in the $|F=1, M=1\rangle$ ("stretched") state with the quantization axis chosen along $\hat{\mathbf{y}}$. An electric field $\mathbf{E}$ is applied along $\hat{\mathbf{z}}$, causing the evolution depicted in Fig. 20. We see that the state originally stretched along $\hat{\mathbf{y}}$ oscillates between this state and the one stretched along $-\hat{\mathbf{y}}$. In between, the system evolves through states with no orientation, but which are aligned along the $\hat{\mathbf{z}} \pm \hat{\mathbf{x}}$ directions. Since the stretched states have orientation, this evolution is an example of orientation-to-alignment and alignment-to-orientation conversion (see, for example, discussion by Blum, 1996).

REFERENCES

Adonts, G. G., D. G. Akopyan, and K. V. Arutunyan, 1986, J. Phys. B **19**, 4113.

Agarwal, G. P., 1984, Phys. Rev. A **29**, 994.

Agarwal, G. S., P. Anantha Lakshmi, J. P. Connerade, and S. West, 1997, J. Phys. B **30**, 5971.

Aharonov, Y., and A. Casher, 1984, Phys. Rev. Lett. **53**, 319.

Ahmad, I., U. Griesmann, I. Martin, W. Dussa, M. A. Baig, and J. Hormes, 1996, J. Phys. B **29**, 2963.

Akulshin, A. M., S. Barreiro, and A. Lezama, 1998, Phys. Rev. A **57**, 2996.

Aleksandrov, E. B., 1965, Opt. Spectrosk. **19**, 455 [Opt. Spectrosc. **19**, 254 (1965)].

Aleksandrov, E. B., M. V. Balabas, and V. A. Bonch-Bruevich, 1987, Pis'ma Zh. Tekh. Fiz. **13**, 749 [Sov. Tech. Phys. Lett. **13**, 312 (1987)].

Aleksandrov, E. B., and V. N. Kulyasov, 1972, Opt. Spectrosk. **33**, 1010 [Opt. Spectrosc. **33**, 557 (1972)].

Alekseev, A. I., 1988, Zh. Éksp. Teor. Fiz. **94**, 130 [Sov. Phys. JETP **67**, 1370 (1988)].

Alekseev, A. I., and V. M. Galitskii, 1969, Zh. Éksp. Teor. Fiz. **57**, 1002 [Sov. Phys. JETP **30**, 548 (1970)].

Alexandrov, E. B., M. V. Balabas, D. Budker, D. S. English, D. F. Kimball, C. H. Li, and V. Yashchuk, 2002, Phys. Rev. A **66**, 042903.

Alexandrov, E. B., M. V. Balabas, A. S. Pasgalev, A. K. Vershovskii, and N. N. Yakobson, 1996, Laser Phys. **6**, 244.

Alexandrov, E. B., and V. A. Bonch-Bruevich, 1992, Opt. Eng. (Bellingham) **31**, 711.

Alexandrov, E. B., M. Chaika, and G. Khvostenko, 1993, *Interference of Atomic States* (Springer, New York).

Alipieva, E. A., and S. I. Karabasheva, 1999, Eur. Phys. J. D **6**, 291.

Allen, L., and J. H. Eberly, 1987, *Optical Resonance and Two-Level Atoms* (Dover, New York).

Allred, J., R. Lyman, T. Kornack, and M. Romalis, 2002, Phys. Rev. Lett. **89**, 130801.

Angel, J. R. P., and P. G. H. Sandars, 1968, Proc. R. Soc. London, Ser. A **305**, 125.

Arimondo, E., 1996, in *Progess in Optics XXXV*, edited by E. Wolf (Elsevier Science, New York), p. 259.

Arndt, M., S. I. Kanorsky, A. Weis, and T. W. Hänsch, 1995, Phys. Rev. Lett. **74**, 1359.

Attwood, D. T., 2000, *Soft X-rays and Extreme Ultraviolet Radiation: Principles and Applications* (Cambridge University, Cambridge, England).

Atutov, S. N., V. Biancalana, P. Bicchi, C. Marinelli, E. Mariotti, M. Meucci, A. Nagel, K. A. Nasyrov, S. Rachini, and L. Moi, 1999, Phys. Rev. A **60**, 4693.

Aubel, J., and C. Hause, 1966, J. Chem. Phys. **44**, 2659.

Auzinsh, M., 1997, Can. J. Phys. **75**, 853.

Auzinsh, M., and R. Ferber, 1995, *Optical Polarization of Molecules*, Cambridge Monographs on Atomic, Molecular, and Chemical Physics No. 4 (Cambridge University, Cambridge, England).

Badalyan, A. M., V. I. Kovalevskii, M. K. Mararov, E. G. Saprykin, G. I. Smirnov, and V. A. Sorokin, 1984, Kvant. Elektron. **11**, 1802 [Sov. J. Quantum Electron. **14**, 1206 (1984)].

Baird, P. E. G., M. Irie, and T. D. Wolfenden, 1989, J. Phys. B **22**, 1733.

Bakhramov, S. A., A. T. Berdikulov, A. M. Kokharov, and V. V. Tikhonenko, 1989, Phys. Lett. A **141**, 31.

Baranova, N. B., Y. V. Bogdanov, and B. Y. Zel'dovich, 1977, Usp. Fiz. Nauk **123**, 349 [Sov. Phys. Usp. **20**, 870 (1977)].

Baranova, N. B., and B. Y. Zel'dovich, 1979, Proc. R. Soc. London, Ser. A **368**, 591.

Barkov, L. M., D. A. Melik-Pashayev, and M. S. Zolotorev, 1989a, Opt. Commun. **70**, 467.

Barkov, L. M., and M. S. Zolotorev, 1980, Zh. Éksp. Teor. Fiz. **79**, 713 [Sov. Phys. JETP **52**, 360 (1980)].

Barkov, L. M., M. S. Zolotarev, and D. A. Melik-Pashayev, 1989b, Opt. Spectrosk. **66**, 495 [Opt. Spectrosc. **66**, 288 (1989)].

Barkov, L. M., M. S. Zolotorev, and D. A. Melik-Pashaev, 1987, Opt. Spectrosk. **62**, 243 [Opt. Spectrosc. **62**, 144 (1987)].

Barkov, L. M., M. Zolotorev, and D. A. Melik-Pashaev, 1988a, Pis'ma Zh. Éksp. Teor. Fiz. **48**, 144 [JETP Lett. **48**, 144 (1988)].

Barkov, L. M., M. S. Zolotorev, and D. A. Melik-Pashaev, 1988b, Kvant. Elektron. (Moscow) **15**, 1106 [Sov. J. Quantum Electron. **18**, 710 (1988)].

Barrat, J., 1959, J. Phys. Radium **20**, 657.

Barrat, J. P., and C. Cohen-Tannoudji, 1961, J. Phys. Radium **22**, 329.

Bell, W., and A. Bloom, 1957, Phys. Rev. **107**, 1559.

Bell, W., and A. Bloom, 1961, Phys. Rev. Lett. **6**, 280.

Bennett, W., 1962, Phys. Rev. **126**, 580.

Berry, M. V., 1984, Proc. R. Soc. London, Ser. A **392**, 45.

Bertucceli, G., N. Beverini, M. Galli, M. Inguscio, and F. Strumia, 1986, Opt. Lett. **11**, 351.

Beverini, N., E. Maccioni, P. Marsili, A. Ruffini, and F. Sorrentino, 2001, Appl. Phys. B: Lasers Opt. **B73**, 133.

Birich, G. N., Y. V. Bogdanov, S. I. Kanorskii, I. I. Sobelman, V. N. Sorokin, I. I. Struk, and E. A. Yukov, 1994, J. Russ. Laser Res. **15**, 455.

Blasberg, T., and D. Suter, 1992, Phys. Rev. Lett. **69**, 2507.

Blum, K., 1996, *Density Matrix Theory and Applications, Physics of Atoms and Molecules*, 2nd ed. (Plenum, New York).

Bogdanov, Y. V., and S. I. Kanorskii, 1987, Acta Phys. Hung. **61**, 13.

Bogdanov, Y. V., S. I. Kanorskii, I. I. Sobelman, V. N. Sorokin, I. I. Struk, and E. A. Yukov, 1986, Opt. Spectrosk. **61**, 446 [Opt. Spectrosc. **61**, 281 (1986)].

Bogdanov, Y. V., S. I. Kanorskii, I. I. Sobelman, V. A. Sorokin, I. I. Struk, and E. A. Yukov, 1988, in *Spectral Line Shapes*, edited by J. Szudy (North-Holland, Torun, Poland), Vol. 5, p. 459.

Bohr, N., 1924, Naturwissenschaften **12**, 1115.

Boivin, L., and H. A. Haus, 1996, Opt. Lett. **21**, 146.

Bonch-Bruevich, A., and V. Khodovoi, 1967, Usp. Fiz. Nauk **93**, 71 [Sov. Phys. Usp. **10**, 637 (1968)].

Bonch-Bruevich, A. M., V. A. Khodovoi, and V. V. Khromov, 1973, Opt. Spektrosk. **34**, 195 [Opt. Spectrosc. **34**, 109 (1973)].

Borghs, G., P. De Bisschop, M. Van Hove, and R. E. Silverans, 1984, Phys. Rev. Lett. **52**, 2030.

Bouchiat, M. A., and C. Bouchiat, 1997, Rep. Prog. Phys. **60**, 1351.

Bouchiat, M. A., and J. Brossel, 1966, Phys. Rev. **147**, 41.

Bouchiat, M. A., and F. Grossetete, 1966, J. Phys. (Paris) **27**, 353.

Bouchiat, M. A., J. Guena, P. Jacquier, M. Lintz, and M. D. Plimmer, 1995, Z. Phys. D: At., Mol. Clusters **33**, 89.

Boyd, R. W., 1992, *Nonlinear Optics* (Academic, Boston).

Boyd, R. W., and D. J. Gauthier, 2002, in *Progress in Optics*, edited by E. Wolf (Elsevier, Amsterdam), Vol. 43, p. 497.

Brandt, S., A. Nagel, R. Wynands, and D. Meschede, 1997, Phys. Rev. A **56**, R1063.

Breit, G., 1932, Rev. Mod. Phys. **4**, 504.

Breit, G., 1933, Rev. Mod. Phys. **5**, 91.

Bretenaker, F., L. Dutriaux, J. C. Cotteverte, B. Lepine, and A. Le Floch, 1995, in *3eme Colloque sur les Lasers et l'Optique Quantique* (3rd Colloquium on Lasers and Quantum Optics. Horizons of Optics) Limoges, France, 6–8 Sept. 1993, Ann. Phys. (Paris), Vol. 20, p. 21.

Bretenaker, F., B. Lepine, J. C. Cotteverte, and A. Le Floch, 1992, Phys. Rev. Lett. **69**, 909.

Budker, D., 1999, in *Physics Beyond the Standard Model, Proceedings of the Fifth International WEIN Symposium*, edited by P. Herczeg, C. M. Hoffman, and H. V. Klapdor-Kleingrothaus (World Scientific, Singapore), p. 418.

Budker, D., D. F. Kimball, S. M. Rochester, and V. V. Yashchuk, 1999, Phys. Rev. Lett. **83**, 1767.

Budker, D., D. F. Kimball, S. M. Rochester, and V. V. Yashchuk, 2000a, Phys. Rev. Lett. **85**, 2088.

Budker, D., D. F. Kimball, S. M. Rochester, and V. V. Yashchuk, 2002a, Phys. Rev. A **65**, 033401.

Budker, D., D. F. Kimball, S. M. Rochester, V. V. Yashchuk, and M. Zolotorev, 2000b, Phys. Rev. A **62**, 043403/1.

Budker, D., D. F. Kimball, V. V. Yashchuk, and M. Zolotorev, 2002b, Phys. Rev. A **65**, 055403.

Budker, D., D. J. Orlando, and V. Yashchuk, 1999, Am. J. Phys. **67**, 584.

Budker, D., V. Yashchuk, and M. Zolotorev, 1998a, Phys. Rev. Lett. **81**, 5788.

Budker, D., V. Yashchuk, and M. Zolotorev, 1998b, in *ICAP XVI* (Windsor, Ontario, Canada), Abstracts of contributed papers, p. 356.

Buevich, O. E., I. S. Grigor'ev, A. F. Semerok, and V. A. Firsov, 1987, Pis'ma Zh. Éksp. Teor. Fiz. **45**, 322 [JETP Lett. **45**, 407 (1987)].

Cabrera, B., 1988, in *Near Zero: New Frontiers of Physics*, edited by J. D. Fairbank, B. S. J. Deaver, C. W. F. Everitt, and P. F. Michelson (Freeman, New York), p. 312.

Cabrera, B., and W. O. Hamilton, 1973, in *The Science and Technology of Superconductivity*, edited by W. D. Gregory, W. N. Matthews, Jr., and E. A. Edelsack (Plenum, New York), Vol. 2, p. 587.

Carrico, J. P., A. Adler, M. R. Baker, S. Legowski, E. Lipworth, P. G. H. Sandars, T. S. Stein, and M. C. Weisskopf, 1968, Phys. Rev. **170**, 64.

Chen, X., 1989, "Experimental and theoretical studies of the linear and non-linear Faraday effect at the resonance D2 line in Caesium vapour," Ph.D. thesis (ETH Zurich).

Chen, X., V. L. Telegdi, and A. Weis, 1987, J. Phys. B **20**, 5653.

Chen, X., V. L. Telegdi, and A. Weis, 1990, Opt. Commun. **74**, 301.

Cheron, B., H. Gilles, J. Hamel, O. Moreau, and H. Sorel, 1994, J. Phys. III **4**, 401.

Chiao, R. Y., 1996, in *Amazing Light: A Volume Dedicated to Charles Hard Townes on his 80th Birthday*, edited by R. Y. Chiao (Springer, New York), p. 91.

Chiao, R. Y., and J. Godine, 1969, Phys. Rev. **185**, 430.

Church, D. A., and T. Hadeishi, 1973, Phys. Rev. A **8**, 1864.

Church, D. A., and T. Hadeishi, 1974, Appl. Phys. Lett. **24**, 185.

Cimmino, A., G. I. Opat, A. G. Klein, H. Kaiser, S. A. Werner, M. Arif, and R. Clothier, 1989, Phys. Rev. Lett. **63**, 380.

Clarke, J., 1996, in *SQUID Sensors: Fundamentals, Fabrication, and Applications*, edited by H. Weinstock (Kluwer Academic, The Netherlands), p. 1.

Clifford, M. A., G. P. T. Lancaster, R. S. Conroy, and K. Dholakia, 2000, J. Mod. Opt. **47**, 1933.

Cohen-Tannoudji, C., 1968, in *Cargèse Lectures in Physics*, edited by M. Lévy (Gordon and Breach, New York), Vol. 2, p. 347 [reprinted in *Atoms in Electromagnetic Fields*, edited by C. Cohen-Tannoudji (World Scientific, Singapore, 1994), p. 119].

Cohen-Tannoudji, C., 1975, in *Atomic Physics IV*, edited by A. W. G. zu Putlitz (Plenum, New York), p. 589.

Cohen-Tannoudji, C., and J. Dupont-Roc, 1969, Opt. Commun. **1**, 184.

Cohen-Tannoudji, C., J. DuPont-Roc, S. Haroche, and F. Laloë, 1969, Phys. Rev. Lett. **22**, 758.

Cojan, J. L., 1954, Ann. Phys. (Paris) **9**, 385.

Colegrove, F., P. Franken, R. Lewis, and R. Sands, 1959, Phys. Rev. Lett. **3**, 420.

Connerade, J. P., 1983, J. Phys. B **16**, 399.

Connerade, J. P., W. A. Farooq, and M. Nawaz, 1992, J. Phys. B **25**, L175.

Connerade, J. P., and A. M. Lane, 1988, Rep. Prog. Phys. **51**, 1439.

Corney, A., 1988, *Atomic and Laser Spectroscopy* (Clarendon, Oxford).

Corney, A., B. Kibble, and G. W. Series, 1966, Proc. R. Soc. London, Ser. A **293**, 70.

Corwin, K. L., L. Zheng-Tian, C. F. Hand, R. J. Epstein, and C. E. Wieman, 1998, Appl. Opt. **37**, 3295.

Cotton, A., and H. Mouton, 1907, C. R. Hebd. Seances Acad. Sci. **145**, 870.

Cotton, A., and H. Mouton, 1911, J. Phys. (Paris) **1**, 5.

Coufal, H., 1984, *Rare Gas Solids*, Springer Tracts in Modern Physics Vol. 103 (Springer, Berlin).

Cronin, A. D., R. B. Warrington, S. K. Lamoreaux, and E. N. Fortson, 1998, Phys. Rev. Lett. **80**, 3719.

Culshaw, W., and J. Kannelaud, 1964a, Phys. Rev. **133**, A691.

Culshaw, W., and J. Kannelaud, 1964b, Phys. Rev. **135**, A316.

Culshaw, W., and J. Kannelaud, 1964c, Phys. Rev. **136**, A1209.

Cyr, N., and M. Tetu, 1991, Opt. Lett. **16**, 946.

Davidson, N., L. Heun Jin, C. S. Adams, M. Kasevich, and S. Chu, 1995, Phys. Rev. Lett. **74**, 1311.

Davies, I. O. G., P. E. G. Baird, and J. L. Nicol, 1987, J. Phys. B **20**, 5371.

Davies, I. O. G., P. E. G. Baird, and J. L. Nicol, 1988, J. Phys. B **21**, 3857.

Davis, W. V., A. L. Gaeta, and R. W. Boyd, 1992, Opt. Lett. **17**, 1304.

Decomps, B., M. Dumont, and M. Ducloy, 1976, in *Laser Spectroscopy of Atoms and Molecules*, edited by H. Walther (Springer, Berlin), p. 283.

Dehmelt, H., 1957, Phys. Rev. **105**, 1924.

DeMille, D., D. Budker, and E. D. Commins, 1994, Phys. Rev. A **50**, 4657.

Demtröder, W., 1996, *Laser Spectroscopy: Basic Concepts and Instrumentation*, 2nd ed. (Springer, Berlin).

Dietzfelbinger, S. H., M. G. Richards, and K. Machin, 1990, Cryogenics **30**, 693.

Dinneen, T. P., C. D. Wallace, and P. L. Gould, 1992, Opt. Commun. **92**, 277.

Dodd, J. N., and G. W. Series, 1978, in *Progress in Atomic Spectroscopy*, edited by W. Hanle and H. Kleinpoppen (Plenum, New York), p. 639.

Dovator, N. A., and A. I. Okunevich, 2001, Opt. Spektrosk. **90**, 23 [Opt. Spectrosc. **90**, 18 (2001)].

Drake, K., 1986, "Nichtlinearer Faraday-Effekt und nichtlinearer Voigt-Effekt am Beispiel eines $(J=1-J=0)$-bergangs im Samarium," Ph.D. thesis (Universität Hannover).

Drake, K. H., W. Lange, and J. Mlynek, 1988, Opt. Commun. **66**, 315.

Ducloy, M., 1973, Phys. Rev. A **8**, 1844.

Dumont, M., 1972, J. Phys. (Paris) **23**, 971.

Dumont, M., and G. Durand, 1964, Phys. Lett. **8**, 100.

Dunkin, I. R., 1998, *Matrix-Isolation Techniques: A Practical Approach*, The Practical Approach in Chemistry Series (Oxford University, Oxford).

Dupont-Roc, J., 1970, Rev. Phys. Appl. **5**, 853.

Dupont-Roc, J., S. Haroche, and C. Cohen-Tannoudji, 1969, Phys. Lett. **28A**, 638.

Durrant, A. V., 1972, J. Phys. B **5**, 1456.

Durrant, A. V., and B. Landheer, 1971, J. Phys. B **4**, 1200.

Dyakonov, M. I., and V. Perel, 1966, Opt. Spektrosk. **20**, 472 [Opt. Spectrosc. **20**, 257 (1966)].

Edmonds, A. R., 1996, *Angular Momentum in Quantum Mechanics*, Princeton Landmarks in Mathematics and Physics (Princeton University, Princeton, N.J.).

Erhard, M., and H. Helm, 2001, Phys. Rev. A **63**, 043813.

Erhard, M., S. Nussmann, and H. Helm, 2000, Phys. Rev. A **62**, 061802.

Faraday, M., 1846a, Philos. Trans. R. Soc. London **XIX**, 1.

Faraday, M., 1846b, Philos. Mag. **28**, 294.

Faraday, M., 1855, *Experimental Researches in Electricity*, Vol. III (Taylor, London).

Fischer, A., and I. V. Hertel, 1982, Z. Phys. A **304**, 103.

Fleischhauer, M., A. B. Matsko, and M. O. Scully, 2000, Phys. Rev. A **62**, 013808.

Fomichev, S. V., 1987, Technical Report IAE-4431/12, Kurchatov Institute of Atomic Energy.

Fomichev, S. V., 1991, J. Phys. B **24**, 4695.

Fomichev, S. V., 1995, J. Phys. B **28**, 3763.

Fork, R., and L. Bradley III, 1964, Appl. Opt. **3**, 137.

Fork, R., L. Hargrove, and M. A. Pollack, 1964, Phys. Rev. Lett. **12**, 705.

Fox, R. W., A. S. Zibrov, and L. Hollberg, 1997, in *Atomic, Molecular and Optical Physics Experimental Methods in the Physical Sciences No. 29c*, edited by F. B. Dunning and R. G. Hulet (Academic Press, New York), p. 77.

Franke-Arnold, S., M. Arndt, and A. Zeilinger, 2001, J. Phys. B **34**, 2527.

Franken, P., 1961, Phys. Rev. **121**, 508.

Garton, W. R. S., J. P. Connerade, M. A. Baig, J. Hormes, and B. Alexa, 1983, J. Phys. B **16**, 389.

Gawlik, W., 1975, "On the forward scattering of resonance radiation on sodium atoms," Ph.D. thesis (Jagiellonian University).

Gawlik, W., 1977, in *IX Conference of the European Group for Atomic Spectroscopy (EGAS)*, Kraków (Jagiellonian University, Kraków), p. 147.

Gawlik, W., 1982, Phys. Lett. **89A**, 278.

Gawlik, W., 1994, in *Modern Nonlinear Optics*, edited by M. Evans and S. Kielich, Advances in Chemical Physics No. 85 (Wiley, New York), p. 733.

Gawlik, W., J. Kowalski, R. Neumann, and F. Träger, 1974a, Opt. Commun. **12**, 400.

Gawlik, W., J. Kowalski, R. Neumann, and F. Träger, 1974b, Phys. Lett. **48A**, 283.

Gawlik, W., J. Kowalski, R. Neumann, H. B. Wiegemann, and K. Winkler, 1979, J. Phys. B **12**, 3873.

Gibbs, H. M., G. G. Churchill, and G. J. Salamo, 1974, Opt. Commun. **12**, 396.

Giel, D., G. Hinz, D. Nettels, and A. Wies, 2000, Opt. Express **6**, 251.

Gilles, H., J. Hamel, and B. Cheron, 2001, Rev. Sci. Instrum. **72**, 2253.

Giraud-Cotton, S., M. Giraud, and L. Klein, 1975, Chem. Phys. Lett. **32**, 317.

Giraud-Cotton, S., V. P. Kaftandjian, and L. Klein, 1982a, Phys. Lett. **88A**, 453.

Giraud-Cotton, S., V. P. Kaftandjian, and L. Klein, 1982b, Phys. Lett. **90A**, 393.

Giraud-Cotton, S., V. P. Kaftandjian, and L. Klein, 1985a, Phys. Rev. A **32**, 2211.

Giraud-Cotton, S., V. P. Kaftandjian, and L. Klein, 1985b, Phys. Rev. A **32**, 2223.

Giraud-Cotton, S., V. P. Kaftandjian, and B. Talin, 1980, J. Phys. (Paris) **41**, 591.

Gordon, D. F., W. B. Mori, and C. Joshi, 2000a, Phys. Plasmas **7**, 3156.

Gordon, D. F., W. B. Mori, and C. Joshi, 2000b, Phys. Plasmas **7**, 3145.

Gorlitz, A., B. Schuh, and A. Weis, 1995, Phys. Rev. A **51**, R4305.

Gould, H., E. Lipworth, and M. C. Weisskopf, 1969, Phys. Rev. **188**, 24.

Gozzini, A., 1962, C. R. Hebd. Seances Acad. Sci. **255**, 1905.

Grangier, P., R. E. Slusher, B. Yurke, and A. LaPorta, 1987, Phys. Rev. Lett. **59**, 2153.

Grossetete, F., 1965, J. Phys. (Paris) **26**, 26.

Guichon, M. A., J. E. Blamont, and J. Brossel, 1957, J. Phys. Radium **18**, 99.

Guillaume, C., and L. Poincaré, 1900, Eds., *Congres International de Physique Réuni* (Gauthier-Villars, Paris).

Hackett, R. Q., and G. W. Series, 1970, Opt. Commun. **2**, 93.

Hamilton, W. O., 1970, Rev. Phys. Appl. **5**, 41.

Hanle, W., 1924, Z. Phys. **30**, 93.

Hanle, W., 1926, Z. Phys. **35**, 346.

Hannaford, P., and G. W. Series, 1981, J. Phys. B **14**, L661.

Happer, W., 1971, *Progress in Quantum Electronics* (Pergamon, New York), Vol. 1 (part 2), p. 51.

Happer, W., 1972, Rev. Mod. Phys. **44**, 169.

Happer, W., and H. Tang, 1973, Phys. Rev. Lett. **31**, 273.

Haroche, S., 1976, in *High-Resolution Laser Spectroscopy*, edited by K. Shimoda (Springer, Berlin), p. 256.

Harris, S. E., 1996, Phys. Rev. Lett. **77**, 5357.

Harris, S. E., 1997, Phys. Today **50**(7), 36.

Hatakeyama, A., K. Enomoto, N. Sugimoto, and T. Yabuzaki, 2002, Phys. Rev. A **65**, 022904.

Hatakeyama, A., K. Oe, K. Ota, S. Hara, J. Arai, T. Yabuzaki, and A. R. Young, 2000, Phys. Rev. Lett. **84**, 1407.

Heisenberg, W., 1925, Z. Phys. **31**, 617.

Hellwig, O., J. B. Kortright, K. Takano, and E. E. Fullerton, 2000, Phys. Rev. B **62**, 11694.

Hermann, G., G. Lasnitschka, and A. Scharmann, 1977, Z. Phys. A **282**, 253.

Hermann, G., and A. Scharmann, 1967, Phys. Lett. **24A**, 606.

Hermann, G., and A. Scharmann, 1968, Z. Phys. **208**, 367.

Hermann, G., and A. Scharmann, 1972, Z. Phys. **254**, 46.

Herrmann, P. P., J. Hoffnagle, N. Schlumpf, V. L. Telegdi, and A. Weis, 1986, J. Phys. B **19**, 1271.

Herzberg, G., 1989, *Spectra of Diatomic Molecules* (Krieger, Malabar, FL).

Hilborn, R., L. Hunter, K. Johnson, S. Peck, A. Spencer, and J. Watson, 1994, Phys. Rev. A **50**, 2467.

Hinz, A., J. Pfeiffer, W. Bohle, and W. Urban, 1982, Mol. Phys. **45**, 1131.

Holmes, B. W., and J. A. R. Griffith, 1995, J. Phys. B **28**, 2829.

Huard, S., 1997, *Polarization of Light* (Wiley, New York).

Hunter, L., 1991, Science **252**, 73.

Ikegami, T., S. Ohshima, and M. Ohtsu, 1989, Jpn. J. Appl. Phys., Part 2 **28**, L1839.

Isayama, T., Y. Takahashi, N. Tanaka, K. Toyoda, K. Ishikawa, and T. Yabuzaki, 1999, Phys. Rev. A **59**, 4836.

Ito, M., S. Murayama, K. Kayama, and M. Yamamoto, 1977, Spectrochim. Acta, Part B **32B**, 327.

Izmailov, A. C., 1988, Kvant. Elektron. (Moscow) **15**, 517 [Sov. J. Quantum Electron. **18**, 328 (1988)].

Jacobs, J. P., W. M. Klipstein, S. K. Lamoreaux, B. R. Heckel, and E. N. Fortson, 1995, Phys. Rev. A **52**, 3521.

Jones, R. V., 1976, Proc. R. Soc. London, Ser. A **349**, 423.

Jungner, P., T. Fellman, B. Stahlberg, and M. Lindberg, 1989, Opt. Commun. **73**, 38.

Kanorsky, S. I., S. Lang, S. Lucke, S. B. Ross, T. W. Hänsch, and A. Weis, 1996, Phys. Rev. A **54**, R1010.

Kanorsky, S. I., and A. Weis, 1998, in *Advances in Atomic, Molecular, and Optical Physics*, edited by B. Bederson and H. Walther (Academic, San Diego), Vol. 38, p. 87.

Kanorskii, S. I., A. Weis, and J. Skalla, 1995, Appl. Phys. B: Lasers Opt. **60**, S165.

Kanorsky, S. I., A. Weis, J. Wurster, and T. W. Hänsch, 1993, Phys. Rev. A **47**, 1220.

Kastler, A., 1950, J. Phys. Radium **11**, 225.

Kazantsev, A., V. Smirnov, A. Tumaikin, and I. Yagofarov, 1984, Opt. Spectrosk. **57**, 189 [Opt. Spectrosc. **57**, 116 (1984)].

Kazantsev, A. P., G. I. Surdutovich, and V. P. Yakovlev, 1986, Pis'ma Zh. Éksp. Teor. Fiz. **43**, 222 [JETP Lett. **43**, 281 (1986)].

Khriplovich, I. B., 1991, *Parity Nonconservation in Atomic Phenomena* (Gordon and Breach, Philadelphia).

Khriplovich, I. B., and S. K. Lamoreaux, 1997, *CP Violation Without Strangeness: Electric Dipole Moments of Particles, Atoms, and Molecules*, Texts and Monographs in Physics (Springer, Berlin).

Kimball, D. F., D. Budker, D. S. English, C. H. Li, A.-T. Nguyen, S. M. Rochester, A. O. Sushkov, V. V. Yashchuk, and M. Zolotorev, 2001, in *Art and Symmetry in Experimental Physics: Festschrift for Eugene D. Commins*, edited by D. Budker, S. J. Freedman, and P. Bucksbaum, AIP Conf. Proc. No. 596 (AIP, Melville, NY), p. 84.

Kinoshita, T., Y. Takahashi, and T. Yabuzaki, 1994, Phys. Rev. B **49**, 3648.

Kitching, J., R. Boyd, A. Yariv, and Y. Shevy, 1994, Opt. Lett. **19**, 1331.

Kitching, J., A. Yariv, and Y. Shevy, 1995, Phys. Rev. Lett. **74**, 3372.

Kleppner, D., N. F. Ramsey, and P. Fjelstadt, 1958, Phys. Rev. Lett. **1**, 232.

Kocharovskaya, O., 1992, *XXth Solvay Conference on Physics Phys. Rep. (The Netherlands)* (Brussels, Belgium), p. 175.

Korff, S. A., and G. Breit, 1932, Rev. Mod. Phys. **4**, 471.

Kortright, J. B., and S. K. Kim, 2000, Phys. Rev. B **62**, 12216.

Kortright, J. B., S. K. Kim, T. Warwick, and N. V. Smith, 1997, Appl. Phys. Lett. **71**, 1446.

Kortright, J. B., and M. Rice, 1995, in *Magnetic Ultrathin Films, Multilayers and Surfaces*, edited by A. Fert, H. Fujimori, G. Guntherodt, B. Heinrich, W. F. J. Egelhoff, Jr., E. E. Marinero, and R. L. White, MRS Symp. Proc. No. 384 (Materials Research Society, Pittsburgh), p. 461.

Kortright, J. B., M. Rice, S. K. Kim, C. C. Walton, and T. Warwick, 1999, J. Magn. Magn. Mater. **191**, 79.

Kosulin, N. L., and A. M. Tumaikin, 1986, Opt. Commun. **59**, 188.

Kozlov, A. N., Y. V. Nikitenkio, and Y. V. Taran, 1982, Nucl. Instrum. Methods Phys. Res. **192**, 379.

Kozlov, M. G., 1989, Opt. Spektrosk. **67**, 1342 [Opt. Spectrosc. **67**, 789 (1989)].

Kozlov, M. G., and S. P. Porsev, 1990, Éksp. Teor. Fiz. **97**, 154 [Sov. Phys. JETP **70**, 85 (1990)].

Kristensen, M., F. Blok, M. v. Eijkelenborg, G. Nienhuis, and J. Woerdman, 1994, Phys. Rev. A **51**, 1085.

Królas, I., and W. Winiarczyk, 1972, Acta Phys. Pol. A **A41**, 785.

Krupennikova, T., and M. Chaika, 1966, Opt. Spektrosk. **20**, 1088 [Opt. Spectrosc. **20**, 604 (1966)].

Kuntz, M. C., R. Hilborn, and A. M. Spencer, 2002, Phys. Rev. A **65**, 023411.

Labeyrie, G., C. Miniatura, and R. Kaiser, 2001, Phys. Rev. A **64**, 033402.

Lamoreaux, S. K., 1999, Phys. Rev. A **60**, 1717.

Landau, L. D., E. M. Lifshits, and L. P. Pitaevskii, 1995, *Electrodynamics of Continuous Media*, Teoreticheskaia fizika (Izd. 2-e). Vol. 8. 2nd rev. and enl. edition (Butterworth-Heinemann, Oxford, England).

Lange, W., K. H. Drake, and J. Mlynek, 1986, *XIV Internation Conference on Quantum Electronics* (Digest of Technical Papers, San Francisco, California), paper number MDD4.

Le Floch, A., and R. Le Naour, 1971, Phys. Rev. A **4**, 290.

Le Floch, A., and G. Stephan, 1972, Phys. Rev. A **6**, 845.

Lecomte, S., E. Fretel, G. Mileti, and P. Thomann, 2000, Appl. Opt. **39**, 1426.

Lee, W. D., and J. C. Campbell, 1992, Appl. Phys. Lett. **60**, 1544.

Lee, W. D., J. J. Heuring, and J. C. Campbell, 1993, *Frequency-Stabilized Lasers and their Applications Proceedings of the SPIE-International Society of Optical Engineers* (Boston, MA), p. 34.

Lezama, A., S. Barreiro, and A. M. Akulshin, 1999, Phys. Rev. A **59**, 4732.

Litfin, G., C. R. Pollock, J. Curl, R. F. , and F. K. Tittel, 1980, J. Chem. Phys. **72**, 6602.

Lobodziński, B., and W. Gawlik, 1996, Phys. Rev. A **54**, 2238.

Lobodziński, B., and W. Gawlik, 1997, Phys. Scr. **T70**, 138.

Lombardi, M., 1969, J. Phys. (Paris) **30**, 631.

Lowe, R. M., D. S. Gough, R. J. McLean, and P. Hannaford, 1987, Phys. Rev. A **36**, 5490.

Lukomskii, N. G., and V. A. Polishchuk, 1986, Zh. Prikl. Spektrosk. **45**, 382 [J. Appl. Spectrosc. **45**, 911 (1986)].

Macaluso, D., and O. M. Corbino, 1898a, C. R. Hebd. Seances Acad. Sci. **127**, 548.

Macaluso, D., and O. M. Corbino, 1898b, Nuovo Cimento **8**, 257.

Macaluso, D., and O. M. Corbino, 1899, Nuovo Cimento **9**, 384.

Mair, A., J. Hager, D. F. Phillips, R. L. Walsworth, and M. D. Lukin, 2002, Phys. Rev. A **65**, 031802.

Majumder, P. K., and L. L. Tsai, 1999, Phys. Rev. A **60**, 267.

Maker, P., R. Terhune, and C. Savage, 1964, Phys. Rev. Lett. **12**, 507.

Margalit, M., C. X. Yu, E. P. Ippen, and H. A. Haus, 1998, Opt. Express **2**, 72.

Matsko, A. B., O. A. Kocharovskaya, Y. Rostovtsev, G. R. Welch, A. S. Zibrov, and M. O. Scully, 2001, in *Advances in Atomic, Molecular, and Optical Physics*, edited by B. Bederson (Academic Press, New York), Vol. 46, p. 191.

Matsko, A. B., I. Novikova, M. O. Scully, and G. R. Welch, 2001, Phys. Rev. Lett. **87**, 133601.

Matsko, A. B., I. Novikova, and G. R. Welch, 2002, J. Mod. Opt. **49**, 367.

Matsko, A. B., I. Novikova, G. R. Welch, D. Budker, D. F. Kimball, and S. M. Rochester, 2002, "Vacuum squeezing in atomic media via self-rotation," Phys. Rev. A **66**, 043815.

Matsko, A. B., and Y. V. Rostovtsev, 1998, Phys. Rev. E **58**, 7846.

Matthews, M. R., 1999, "Two-Component Bose-Einstein Condensation," Ph.D. thesis (University of Colorado).

McCall, S. L., and E. L. Hahn, 1969, Phys. Rev. **183**, 457.

McLean, R. J., R. J. Ballagh, and D. M. Warrington, 1986, J. Phys. B **19**, 3477.

Meekhof, D. M., P. A. Vetter, P. K. Majumder, S. K. Lamoreaux, and E. N. Fortson, 1995, Phys. Rev. A **52**, 1895.

Menzies, R. T., 1973, Phys. Lett. **43A**, 209.

Mester, J. C., J. M. Lockhart, B. Muhlfelder, D. O. Murray, and M. A. Taber, 2000, Adv. Space Res. **25**, 1185.

Milner, V., B. M. Chernobrod, and Y. Prior, 1999, Phys. Rev. A **60**, 1293.

Milner, V., and Y. Prior, 1999, Phys. Rev. A **59**, R1738.

Mitchell, A. C. G., and M. W. Zemansky, 1971, *Resonance Radiation and Excited Atoms* (Cambridge University, Cambridge, England).

Mlynek, J., R. Grimm, E. Buhr, and V. Jordan, 1987, in *Fundamentals of Quantum Optics II*, edited by F. Ehlotzy (Springer, Berlin), p. 249.

Mlynek, J., R. Grimm, E. Buhr, and V. Jordan, 1988, Appl. Phys. B: Photophys. Laser Chem. **B45**, 77.

Moruzzi, G., and F. Strumia, 1991, *The Hanle Effect and Level-Crossing Spectroscopy*, Physics of Atoms and Molecules (Plenum, New York).

Murthy, S. A., D. J. Krause, Z. L. Li, and L. R. Hunter, 1989, Phys. Rev. Lett. **63**, 965.

Nakayama, S., G. W. Series, and W. Gawlik, 1980, Opt. Commun. **34**, 389.

Narducci, F., 2001, private communication.

Nenonen, J., J. Montonen, and T. Katila, 1996, Rev. Sci. Instrum. **67**, 2397.

Nienhuis, G., and S. Kryszewski, 1994, Phys. Rev. A **50**, 5051.

Nienhuis, G., J. P. Woerdman, and I. Kuscer, 1992, Phys. Rev. A **46**, 7079.

Novikov, V. N., O. P. Sushkov, and I. B. Khriplovich, 1977, Opt. Spectrosk. **43**, 621 [Opt. Spectrosc. **43**, 370 (1977)].

Novikova, I., A. B. Matsko, V. L. Velichansky, M. O. Scully, and G. R. Welch, 2001a, Phys. Rev. A **63**, 063802/1.

Novikova, I., A. B. Matsko, and G. R. Welch, 2001b, Opt. Lett. **26**, 1016.

Novikova, I., A. B. Matsko, and G. R. Welch, 2002, Appl. Phys. Lett. **81**, 193.

Novikova, I., V. A. Sautenkov, G. R. Welch, and M. O. Scully, 1999, preprint, "Reduction of the group velocity in nonlinear magneto-optic experiment in dense coherent media," unpublished.

Novikova, I., and G. R. Welch, 2002, J. Mod. Opt. **49**, 349.

Oakberg, T. C., 1995, Opt. Eng. (Bellingham) **34**, 1545.

Okunevich, A. I., 1994, Opt. Spectrosk. **77**, 178 [Opt. Spectrosc. **77**, 160 (1994)].

Okunevich, A. I., 1995, Opt. Spectrosk. **79**, 12 [Opt. Spectrosc. **79**, 8 (1995)].

Okunevich, A. I., 2000, private communication.

Omont, A., 1977, Prog. Quantum Electron. **5**, 70.

Oppenheimer, R., 1927, Z. Phys. **43**, 27.

Pancharatnam, S., 1966, J. Opt. Soc. Am. **56**, 1636.

Papageorgiou, N., A. Weis, V. A. Sautenkov, D. Bloch, and M. Ducloy, 1994, Appl. Phys. B: Lasers Opt. **B59**, 123.

Patrick, H., and C. E. Wieman, 1991, Rev. Sci. Instrum. **62**, 2593.

Pfleghaar, E., J. Wurster, S. I. Kanorsky, and A. Weis, 1993, Opt. Commun. **99**, 303.

Pinard, M., and C. Aminoff, 1982, J. Phys. (Paris) **43**, 1327.

Ramsey, N. F., 1990, Rev. Mod. Phys. **62**, 541.

Rasbach, U., 2001, "Magneto-optische Effekte und Messung der elektrischen Tensorpolarisierbarkeit an einem Csium-Atomstrahl," Ph.D. thesis (University of Fribourg).

Rasbach, U., C. Ospelkaus, and A. Weis, 2001, *International Conference on Coherent and Nonlinear Optics 2001* [SPIE, Minsk (Belarus)] (in press).

Rautian, S. M., and A. M. Shalagin, 1991, *Kinetic Problems of Non-linear Spectroscopy* (North-Holland, Amsterdam).

Regan, B. C., E. D. Commins, C. J. Schmidt, and D. DeMille, 2002, Phys. Rev. Lett. **88**, 071805.

Renzoni, F., S. Cartaleva, G. Alzetta, and E. Arimondo, 2001, Phys. Rev. A **63**, 065401.

Rikitake, T., 1987, *Magnetic and Electromagnetic Shielding* (Reidel, Tokyo).

Rikken, G. L. J. A., and B. A. van Tiggelen, 1996, Nature (London) **381**, 54.

Rikken, G. L. J. A., and B. A. van Tiggelen, 1997, Phys. Rev. Lett. **78**, 847.

Rikukawa, H., T. Sato, M. Nakagawa, and M. Shimba, 1991, Electron. Commun. Jpn., Part 2: Electron. **74**, 41.

Roberts, G. J., P. E. G. Baird, M. W. S. M. Brimicombe, P. G. H. Sandars, D. R. Selby, and D. N. Stacey, 1980, J. Phys. B **13**, 1389.

Robinson, H., E. Ensberg, and H. Dehment, 1958, Bull. Am. Phys. Soc. **3**, 9.

Rochester, S. M., and D. Budker, 2001a, Am. J. Phys. **69**, 450.

Rochester, S. M., and D. Budker, 2001b, unpublished.

Rochester, S. M., and D. Budker, 2002, J. Mod. Opt. (in press).

Rochester, S. M., D. S. Hsiung, D. Budker, R. Y. Chiao, D. F. Kimball, and V. V. Yashchuk, 2001, Phys. Rev. A **63**, 043814.

Romalis, M. V., W. C. Griffith, J. P. Jacobs, and E. N. Fortson, 2001a, Phys. Rev. Lett. **86**, 2505.

Romalis, M. V., W. C. Griffith, J. P. Jacobs, and E. N. Fortson, 2001b, in *Art and Symmetry in Experimental Physics: Festschrift for Eugene D. Commins*, edited by D. Budker, S. J. Freedman, and P. Bucksbaum, AIP Conf. Proc. No. 596 (AIP, Melville, NY), p. 47.

Rubinowicz, A., 1918, Phys. Z. **19**, 441 and 465.

Saikan, S., 1978, J. Opt. Soc. Am. **68**, 1184.

Sandars, P. G. H., and E. Lipworth, 1964, Phys. Rev. Lett. **13**, 718.

Sangster, K., E. A. Hinds, S. M. Barnett, and E. Riis, 1993, Phys. Rev. Lett. **71**, 3641.

Sangster, K., E. A. Hinds, S. M. Barnett, E. Riis, and A. G. Sinclair, 1995, Phys. Rev. A **51**, 1776.

Sargent, M. I., W. Lamb, and R. Fork, 1967, Phys. Rev. **164**, 436, 450.

Sauer, B. E., J. J. Hudson, M. R. Tarbutt, and E. A. Hinds, 2001, in *Art and Symmetry in Experimental Physics: Festschrift for Eugene D. Commins*, edited by D. Budker, S. J. Freedman, and P. Bucksbaum, AIP Conf. Proc. No. 596 (AIP, Melville, NY), p. 62.

Sautenkov, V. A., M. D. Lukin, C. J. Bednar, I. Novikova, E. Mikhailov, M. Fleischhauer, V. L. Velichansky, G. R. Welch, and M. O. Scully, 2000, Phys. Rev. A **62**, 023810.

Schieder, R., and H. Walther, 1974, Z. Phys. **270**, 55.

Schlesser, R., and A. Weis, 1992, Opt. Lett. **17**, 1015.

Schlossberg, H. R., and A. Javan, 1966, Phys. Rev. Lett. **17**, 1242.

Schmieder, R. W., A. Lurio, W. Happer, and A. Khadjavi, 1970, Phys. Rev. A **2**, 1216.

Schuh, B., S. I. Kanorsky, A. Weis, and T. W. Hänsch, 1993, Opt. Commun. **100**, 451.

Schuller, F., M. J. D. Macpherson, and D. N. Stacey, 1987, Physica B & C **147C**, 321.

Schuller, F., M. J. D. Macpherson, and D. N. Stacey, 1989, Opt. Commun. **71**, 61.

Schuller, F., and D. N. Stacey, 1999, Phys. Rev. A **60**, 973.

Schuller, F., D. N. Stacey, R. B. Warrington, and K. P. Zetie, 1995, J. Phys. B **28**, 3783.

Schuurmans, M. F. H., 1976a, Z. Phys. A **279**, 243.

Schuurmans, M. F. H., 1976b, J. Phys. (Paris) **37**, 469.

Scully, M. O., 1992, Phys. Rep. **209**, 191.

Series, G. W., 1967, Proc. Phys. Soc. London **91**, 432.

Shen, Y. R., 1984, *The Principles of Nonlinear Optics* (Wiley, New York).

Shvets, G., and J. S. Wurtele, 2002, Phys. Rev. Lett. **89**, 115003.

Siegmund, W., and A. Scharmann, 1976, Z. Phys. A **276**, 19.

Skalla, J., and G. Waeckerle, 1997, Appl. Phys. B: Lasers Opt. **B64**, 459.

Skalla, J., G. Waeckerle, and M. Mehring, 1997a, Opt. Commun. **143**, 209.

Skalla, J., G. Waeckerle, M. Mehring, and A. Pines, 1997b, Phys. Lett. A **226**, 69.

Stahlberg, B., P. Jungner, and T. Fellman, 1989, Opt. Commun. **70**, 329.

Stahlberg, B., P. Jungner, T. Fellman, and A. Lindberg, 1990, Appl. Phys. B: Photophys. Laser Chem. **B50**, 547.

Stahlberg, B., M. Lindberg, and P. Jungner, 1985, J. Phys. B **18**, 627.

Stahler, M., S. Knappe, C. Affolderbach, W. Kemp, and R. Wynands, 2001, Europhys. Lett. **54**, 323.

Stanzel, G., 1974a, Phys. Lett. **47A**, 283.

Stanzel, G., 1974b, Z. Phys. **270**, 361.

Stenholm, S., 1984, *Foundations of Laser Spectroscopy*, Wiley Series in Pure and Applied Optics (Wiley, New York).

Stephens, P., 1989, Prog. Anal. Spectrosc. **12**, 277.

Sumner, T. J., J. M. Pendlebury, and K. F. Smith, 1987, J. Phys. D **20**, 1095.

Sushkov, A. O., 2001, unpublished.

Sushkov, O. P., and V. V. Flambaum, 1978, Zh. Éksp. Teor. Fiz. **75**, 1208 [Sov. Phys. JETP **48**, 608 (1978)].

Suter, D., 1997, *The Physics of Laser-Atom Interactions* (Cambridge University, Cambridge, England).

Taber, M. A., D. O. Murray, J. M. Lockhart, D. J. Frank, and D. Donegan, 1993, in *Cryogenic Engineering Conference*, edited by P. Kittel (Plenum, Albuquerque, New Mexico), Vol. 39, p. 161.

Tanás, R., and S. Kielich, 1983, Opt. Commun. **45**, 351.

Theobald, G., V. Giordano, N. Dimarcq, and P. Cerez, 1991, J. Phys. B **24**, 2957.

Thiel, C. W., H. Cruguel, H. Wu, Y. Sun, G. J. Lapeyre, R. L. Cone, R. W. Equall, and R. M. Macfarlane, 2001, Phys. Rev. B **64**, 085107.

Tomlinson, W., and R. Fork, 1967, Phys. Rev. **164**, 466.

Tregidgo, K. M. J., P. E. G. Baird, M. J. D. Macpherson, C. W. P. Palmer, P. G. H. Sandars, D. N. Stacey, and R. C. Thompson, 1986, J. Phys. B **19**, 1143.

Ulam-Orgikh, D., and M. Kitagawa, 2001, Phys. Rev. A **64**, 052106.

Valles, J. A., and J. M. Alvarez, 1994, Phys. Rev. A **50**, 2490.

Valles, J. A., and J. M. Alvarez, 1996, Phys. Rev. A **54**, 977.

van Haeringen, W., 1967, Phys. Rev. **158**, 256.

Varshalovich, D. A., A. N. Moskalev, and V. K. Khersonskii, 1988, *Quantum Theory of Angular Momentum: Irreducible Tensors, Spherical Harmonics, Vector Coupling Coefficients, 3nj Symbols* (World Scientific, Singapore).

Vasilenko, L. S., L. N. Gus'kov, and A. V. Shishaev, 1978, Kvant. Elektron. (Moscow) **5**, 1746 [Sov. J. Quantum Electron. **8**, 980 (1978)].

Vedenin, V. D., V. N. Kulyasov, A. L. Kurbatov, N. V. Rodin, and M. V. Shubin, 1986, Opt. Spectrosk. **60**, 239 [Opt. Spectrosc. **60**, 146 (1986)].

Vedenin, V. D., V. N. Kulyasov, A. L. Kurbatov, N. V. Rodin, and M. V. Shubin, 1987, Opt. Spectrosk. **62**, 737 [Opt. Spectrosc. **62**, 439 (1987)].

Vetter, P. A., D. M. Meekhof, P. K. Majumder, S. K. Lamoreaux, and E. N. Fortson, 1995, Phys. Rev. Lett. **74**, 2658.

Vliegen, E., S. Kadlecek, L. W. Anderson, T. G. Walker, C. J. Erickson, and W. Happer, 2001, Nucl. Instrum. Methods Phys. Res. A **460**, 444.

Voigt, W., 1898a, Kgl. Ges. Wiss. Nachr., Math.-Phys. Kl. **1898**, 329.

Voigt, W., 1898b, Kgl. Ges. Wiss. Nachr., Math.-Phys. Kl. **1898**, 355.

Voigt, W., 1901, Ann. Phys. (Leipzig) **4**, 197.

Voytovich, A. P., 1984, *Magneto-optics of Gas Lasers* (Nauka i Tekhnika, Minsk).

Walker, T. G., 1989, Phys. Rev. A **40**, 4959.

Walker, T. G., J. H. Thywissen, and W. Happer, 1997, Phys. Rev. A **56**, 2090.

Wang, B., and T. C. Oakberg, 1999, Rev. Sci. Instrum. **70**, 3847.

Wanninger, P., E. C. Valdez, and T. M. Shay, 1992, IEEE Photonics Technol. Lett. **4**, 94.

Warry, A. J., D. J. Heading, and J. P. Connerade, 1994, J. Phys. B **27**, 2229.

Wąsik, G., W. Gawlik, J. Zachorowski, and W. Zawadzki, 2002 Appl. Phys. B: Lasers Opt. (in press).

Weingeroff, M., 1931, Z. Phys. **67**, 679.

Weis, A., 2001, in *Laser Physics at the Limits*, edited by H. Figger, D. Meschede, C. Zimmermann, and J. F. Rodrigues (Springer, New York), p. 123.

Weis, A., and S. Derler, 1988, Appl. Opt. **27**, 2662.

Weis, A., S. Kanorsky, M. Arndt, and T. W. Hänsch, 1995, Z. Phys. B: Condens. Matter **98**, 359.

Weis, A., S. Kanorsky, S. Lang, and T. W. Hänsch, 1997, in *Atomic Physics Methods in Modern Research*, Lecture Notes in Physics Vol. 499, edited by K. Jungmann, J. Kowalski, I. Reinhard, and F. Träger (Springer, Berlin), p. 57.

Weis, A., V. A. Sautenkov, and T. W. Hänsch, 1992, Phys. Rev. A **45**, 7991.

Weis, A., V. A. Sautenkov, and T. W. Hänsch, 1993, J. Phys. II **3**, 263.

Weis, A., B. Schuh, S. I. Kanorsky, and T. Hänsch, 1993, in *EQEC'93*, Vol. II, Technical Digest, edited by P. d. Natale, R. Meucci, and S. Pelli (EPS, Firenze), p. 854.

Weis, A., J. Wurster, and S. I. Kanorsky, 1993, J. Opt. Soc. Am. B **10**, 716.

Weisskopf, V., 1931, Ann. Phys. (Leipzig) **9**, 23.

Wieman, C. E., and L. Hollberg, 1991, Rev. Sci. Instrum. **62**, 1.

Winiarczyk, W., 1977, Acta Phys. Pol. A **A52**, 157.

Woerdman, J. P., G. Nienhuis, and I. Kuscer, 1992, Opt. Commun. **93**, 135.

Woerdman, J. P., and M. F. H. Schuurmans, 1975, Opt. Commun. **14**, 248.

Wolfenden, T. D., P. E. G. Baird, J. A. Deeny, and M. Irie, 1990, Meas. Sci. Technol. **1**, 1060.

Wolfenden, T. D., P. E. G. Baird, and P. G. H. Sandars, 1991, Europhys. Lett. **15**, 731.

Wood, R. W., 1909, Philos. Mag. **18**, 187.

Wood, R. W., 1922, Philos. Mag. **44**, 1109.

Wood, R. W., and A. Ellett, 1923, Proc. R. Soc. London, Ser. A **103**, 396.

Wood, R. W., and A. Ellett, 1924, Phys. Rev. **24**, 243.

Wynands, R., A. Nagel, S. Brandt, D. Meschede, and A. Weis, 1998, Phys. Rev. A **58**, 196.

Yamamoto, M., J. Hanari, and Y. Takubo, 1986, J. Opt. Soc. Am. B **3**, 1245.

Yashchuk, V., D. Budker, and M. Zolotorev, 1999, in *Trapped Charged Particles and Fundamental Physics*, edited by D. H. E. Dubin and D. Schneider, AIP Conf. Proc. No. 457 (AIP, Woodbury, NY), p. 177.

Yashchuk, V. V., D. Budker, and J. R. Davis, 2000, Rev. Sci. Instrum. **71**, 341.

Yashchuk, V. V., D. Budker, D. F. Kimball, and M. Zolotorev, 2002, unpublished.

Yashchuk, V. V., E. Mikhailov, I. Novikova, and D. Budker, 1999, "Nonlinear magneto-optical rotation with separated light fields in ^{85}Rb vapor contained in an antirelaxation coated cell," Technical Report LBNL-44762, Lawrence Berkeley National Laboratory.

Yashchuk, V. V., A. O. Sushkov, D. Budker, E. R. Lee, I. T. Lee, and M. L. Perl, 2002, Rev. Sci. Instrum. **73**, 2331.

Zapasskii, V. S., and P. P. Feofilov, 1975, Usp. Fiz. Nauk **116**, 41 [Sov. Phys. Usp. **18**, 323 (1975)].

Zare, E., 1988, *Angular Momentum: Understanding Spatial Aspects in Chemistry and Physics* (Wiley, New York).

Zeiske, K., G. Zinner, F. Riehle, and J. Helmcke, 1995, Appl. Phys. B: Lasers Opt. **60**, 205.

Zetie, K. P., R. B. Warrington, M. J. D. Macpherson, D. N. Stacey, and F. Schuller, 1992, Opt. Commun. **91**, 210.

Zibrov, A. S., and A. B. Matsko, 2002, Phys. Rev. A **65**, 013814.

Zibrov, A. S., I. Novikova, and A. B. Matsko, 2001, Opt. Lett. **26**, 1311.